International Conference on Engineering and Agro-industrial Technology

Sustainable Agro-industrial and Food Engineering Systems (SAFE Systems): Current Trends, Challenges and Opportunities

iCEAT2022

PROCEEDINGS

23-24 · February · 2022

iceat.uplb@up.edu.ph

International Conference on Engineering and Agro-industrial Technology (iCEAT 2022)

Sustainable Agro-industrial and Food Engineering (SAFE) Systems: Current Trends, Challenges and Opportunities

23-24 February 2022

Los Baños, Laguna, Philippines

A Virtual Conference organized by the
University of the Philippines Los Baños
College of Engineering and Agro-industrial Technology

Edited by the
International Conference on Engineering and Agro-industrial Technology

Published by the
University of the Philippines Los Baños
College of Engineering and Agro-industrial Technology

About iCEAT 2022

The College of Engineering and Agro-Industrial Technology (CEAT) traces its roots to the former Department of Agricultural Engineering created in 1912 as one of the departments of the UP College of Agriculture. In 1976, the department was elevated to the Institute of Agricultural Engineering and Technology (INSAET). On February 24, 1983, the CEAT was established with the approval of the UP Board of Regents in its 958th meeting. Since then, CEAT has been hailed as one of the best engineering colleges inthe country. It has continuously produced quality graduates, developed and generated technologies and knowledge products in service of the Filipino people.

On its 110th Founding Anniversary, CEAT is holding for the 1st time the iCEAT 2022 as a major part of its celebration. Through iCEAT 2022, UP through UPLB and CEAT can reiterate its role as a National University, who is responsible in promoting research and development, dissemination and application of SAFE Systems. Anchored on its vision toward an interdisciplinary, scientific research and innovation, the iCEAT 2022 aims to provide a virtual avenue for discussion and recommendations among leading scientists, policy makers, researchers, and educators on the latest issues, trends, solutions, and best practices for the field of engineering and agro-industrial technology. It is envisioned that this conference will be held annually to keep abreast of the dynamic landscape of SAFE Systems.

The 2-day conference aims to delve into the multifarious world of agro- industrial and food engineering – as it will discuss the following topics among others:

- Food Systems
- Bioprocess Engineering
- Agricultural and Fisheries Mechanization
- Land and Water Resources Engineering
- Biomass and Biofuels - Renewable Energy
- Environmental Engineering and Waste Management
- Information and Communications Technology for SAFE Systems

- Materials Engineering
- Electrical Engineering
- Infrastructure and Civil Engineering
- Industrial Engineering
- Engineering and Social Science

The iCEAT 2022 envisions working collaboratively with various stakeholders for a universal call to take action towards sustainable development goals (SDGs) as set forth by the United Nations (UN). This includes no poverty, zero hunger, clean water and sanitation, affordable and clean energy, industry, innovation and infrastructure, sustainable cities and communities, responsible consumption and production, and climate action.

General Programme

DAY 1: Wednesday, 23 February 2022		
TIME	**ACTIVITIES**	
OPENING SESSION		
8:30 AM	***Zoom Opens -- CEAT AVP -- UPLB AVP -- House Rules***	
8:55 AM - 9:00 AM	National Anthem	
9:01 AM - 9:05 AM	Introduction of participants	**Dr. Arthur L. Fajardo** Chair, iCEAT Organizing Committee
9:06 AM - 9:10AM	Welcome remarks	**Dr. Rossana Marie C. Amongo** CEAT Dean
9:11 AM - 9:20AM	Opening remarks	**Dr. Jose V. Camacho, Jr.** UPLB Chancellor
	KEYNOTE SPEAKERS:	
9:21 AM - 9:40 AM	**Atty. Danilo L. Concepcion** President, University of the Philippines	
9:41 AM - 10:00 AM	**Hon. Fortunato T. dela Peña** Secretary, Department of Science and Technology (DOST)	
10:01AM - 10:20 AM	**Hon. William D. Dar** Secretary, Department of Agriculture (DA)	
Awarding of certificates of appreciation **Photo Opportunity/Health Break**		
PLENARY SESSION 1		
10:30AM - 10:50AM	*"Advances at the interface of environmental microbiology and water/sanitation infrastructure"*	**Dr. Francis L. de los Reyes III** Professor, University Faculty Scholar, Department of Civil, Construction, and Environmental Engineering, North Carolina State University
10:51AM – 10:55AM	***Open Forum***	
10:56AM – 11:15AM	*"Accelerating the Application of Conservation Agriculture Production Systems in the Philippines"*	**Dr. Manuel R. Reyes** Research Professor, Kansas State University

11:16AM – 11:20AM	***Open Forum***	
11:21AM – 11:40AM	*"Sustainable Food and Bioenergy Systems Research and Commercialization for a Circular Economy"*	**Dr. Sergio C. Capareda** Professor, Biological & Agricultural Engineering Department College of Agriculture and Life Sciences Texas A&M University
11:41AM – 11:45AM	***Open Forum***	
11:46AM – 12:05PM	*"Integrated Quality, Productivity, Reliability & Safety Management Systems: Continuing Improvement Strategies for Sustainable Philippine Agro-Industrial"*	**Dr. Isagani Sarmiento** QPRS Consultant and Continuing Improvement Advocate
12:06PM – 12:10PM	***Open Forum***	
12:11PM - 12:15PM	Awarding of certificates of appreciation	
Lunch Break		
PARALLEL SESSIONS		
1:30PM - 4:30PM	Technical paper presentations (15 mins)	
	Food Systems, Bio Process Engineering, Agricultural and Fisheries Mechanization	Asst. Prof. Rina A. Bawar
	Land and Water Resources Engineering, Biomass and Biofuels - Renewable Energy	Dr. Maurice A. Duka
4:30PM - 4:45PM	Synthesis for Day 1	
4:45PM - 5:00PM	Awarding of winners	

DAY 2: Thursday, 24 February 2022

TIME	ACTIVITIES	
PLENARY SESSION 2		
8:30 AM	***Zoom Opens -- CEAT AVP -- UPLB AVP -- House Rules***	
9:00AM - 9:20AM	"From Vertical Farming to Alternative Protein: Transformative On-Demand New Food Systems for Both Earth and Extraterrestrial Applications"	**Dr. Joel Cuello** Professor of Biosystems Engineering, The University of Arizona
9:21AM - 9:25AM	Open Forum	
9:26AM - 9:45AM	"Digital crop protection using artificial intelligence and the internet of things"	**Dr. Siti Khairunniza Bejo** Associate Professor, Department of Biological and Agricultural Engineering, Universiti Putra Malaysia
9:46AM - 9:50AM	***Open Forum***	
9:51AM - 10:10AM	**"**Development of the Selective "Smart" Technology for Accelerating Sustainable Agriculture in Indonesia"	**Dr. Lilik Soetiarso** Professor - Agricultural System and Machinery, Department of Agricultural & Bio-systems Engineering, Universitas Gadjah Mada
10:11AM - 10:15AM	***Open Forum***	
10:16AM - 10:35AM	"Empowering the Agriculture Industry through Education and Research in Engineering of Renewable Materials and Resources"	**Dr. Leslie Joy Diaz** Professor, Department of Mining, Metallurgical and Materials Engineering, University of the Philippines – Diliman
10:36AM - 10:40AM	***Open Forum***	
10:41PM - 10:45PM	Awarding of certificates of appreciation	
Lunch Break		
PARALLEL SESSIONS		
1:30PM - 4:30PM	Technical paper presentations (15 mins)	
	Environmental Engineering and Waste Management	Dr. Ramon Christian P. Eusebio

	Information and Communication Technology for SAFE Systems	
	Industrial Engineering, Engineering & Social Sciences	
	Materials Engineering, Electrical Engineering, Infrastructure and Civil Engineering	Asst. Prof. Jedidiah Joel C. Aguirre
4:30PM - 4:45PM	Synthesis for Day 2	
4:45PM - 5:00PM	Awarding of winners	
	Closing Remarks	

Keynote Speakers

Dr. Jose V. Camacho, Jr. is the 10th chancellor of UPLB. He was elected by the Board of Regents at its 1354th meeting on Sept. 24 and started his three-year term on 01 November 2020.

Dr. Camacho was the dean of the Graduate School (GS) from February 2012 to October 31 2020, and a professor of economics at the College of Economics and Management (CEM).

His vision-mission statement is entitled "Future-Proofing UPLB."

Dr. Camacho specified the need to future-proof UPLB's human resources, lifelong learning and instruction system, research and innovation system, commitment to public good and social welfare, and global engagement.

Dr. Camacho first served as the associate dean and chair of academic programs and curriculum of CEM (2007-2012), and chair of the Department of Economics (2001-2004).

He also serves as the chair of the Technical Working Group (TWG) on Graduate Education, and co-chair of the TWG for the Expanded Tertiary Education Equivalency and Accreditation Program, both of the Commission on Higher Education.

Dr. Camacho finished in 2007 his Doctor of Economics, with specialization in Economics of Education, Labor, and Human Resource Economics at Kyoto University, Japan.

He holds a Master of Arts in Economics from Erasmus University International Institute of Social Studies in The Hague, Netherlands, and a Bachelor of Science in Economics from UPLB.

President Danilo Lardizabal Concepción is the 21st President of the University of the Philippines. His six-year term started in February 2017, serving after former President Alfredo E. Pascual.
He is a member of the UP College of Law faculty where he served as Dean (2011-2017), as Associate Dean (2002-2006), and as Head of the UP Law Center (2002-2006). He also served briefly as the Vice President for Legal Affairs and the UP Bonifacio Global City Campus' Executive Director in former President Pascual's term.

President Concepcion was also appointed as President of the Dela Salle-Araneta University from 2000-2002 before returning to UP to teach at the College of Law. He also served in various capacities for the government including his appointment as Associate Commissioner of the Securities and Exchange Commission (1996-2000), Chief-of-Staff of the Chief Presidential Legal Counsel (1996), among others.

Presently, he continues his work in the Philippine Judicial Academy's Civil Code Committee, the MCLE Governing Board, the Supreme Court's Committee on Bar Matter and Continuing Legal Education, the Pamantasan ng Lungsod ng Valenzuela's Board of Regents, and the Philippine Association of Law Schools. His civic activities include his governorship at the Philippine Red Cross; Knight Grand Order of Rizal for the Order of the Knights of Rizal, fellowship with the Upsilon Sigma Phi Fraternity, and membership in the Phi Kappa Phi International Honor Society among many others.

He graduated from Dela Salle-Araneta University with a Bachelor of Science in Agricultural Engineering (*summa cum laude*) and was a topnotcher for the Agricultural Engineers' State Board Examination in 1979. He then took his Bachelor of Laws (LLB) at the UP College of Law where he graduated in 1983 as *cum laude*, also belonging to the top passers of the Bar Examination in the same year. He received his Master of Laws (LLM) from the University of London, Queen Mary College in 1986, attending as a Chevening Scholar. He also underwent the Finance for Senior Executives program at the Asian Institute of Management (AIM) in 2000 where he received recognition as the Best Financial Strategist.

Fortunato T. de la Peña started his professional career at the then ESSO Standard Eastern as a cost and operations engineer in 1969 after graduating with a BS Chemical Engineering degree from the University of the Philippines (UP) that year. He then took up graduate studies in Industrial Engineering at the same university and earned an MS degree in Industrial Engineering. He joined the UP College of Engineering faculty as an Instructor in 1973 and rose to become Full Professor in 1988. He served UP in various capacities: as Chairman of the Department of Industrial Engineering & Operations Research, as Assistant to the Executive Director of the National Engineering Center, as Director of the Institute for Small Scale Industries and as System Vice President for Planning & Development. He taught Industrial Engineering and Operations Research at the University of the Philippines for 43 years from 1973 to 2016.

He was seconded to the National Science & Technology Authority (NSTA) which later became the Department of Science & Technology (DOST) three times: as Head of its Planning Service, as Director of its Technology Application & Promotion Institute and as Undersecretary for Scientific & Technical Services after which he retired in 2014. In 2016 he was appointed DOST Secretary.

He led a number of professional organizations as its President. These are the Philippine Institute of Chemical Engineers, the Association of Management & Industrial Engineers of the Philippines, the National Research Council of the Philippines and the Philippine Association for the Advancement of Science & Technology. He also served as Chair of the UN Commission on Science & Technology for Development. The awards he received include the Dangal ng Bayan Award from the Civil Service Commission, the Outstanding Career Executive Officer Award from the Career Executive Service Board, the Outstanding Professional Award from the Professional Regulations Commission, the UP Alumni Association Award for Public Service, the UP Alumni Engineers Most Distinguished Alumnus Award, the UP Alumni Association Lifetime Distinguished Achievement Award and The Ateneo Government Service Award. The University of the Philippines conferred on him the degree of Doctor of Laws, honoris causa in 2018.

William Dollente Dar serves for the second time as the Secretary of the Department of Agriculture. His first stint as agri chief was in 1998-1999 under the administration of President Joseph Ejercito Estrada.

To date, he is the only Filipino who led a global agricultural research institute, the International Crops Research Institute for the Semi-Arid Tropics, headquartered in India. He served for three consecutive five-year terms, from 2000 to 2014.

His extensive research and professional experience include crop management, farming systems development, and technology sharing and upscaling.

Dr. Dar earned his BS in Agricultural Education in 1969 and MS in Agronomy in 1976 at Mountain State Agricultural College, now known as Benguet State University (BSU), in La Trinidad, Benguet. At BSU, he started as a researcher and instructor in 1979 and rose to become Professor VI and Vice President for R&D support services in 1985. In between those years, he pursued a PhD in Horticulture at the University of the Philippines Los Baños, completing it in 1980.

When the DA was reorganized in 1987, Dr. Dar was appointed as the first director of the DA-Bureau of Agricultural Research. He also served as executive director of PCARRD, from 1994 to 1998. The agency is now called the Philippine Council for Agriculture, Aquatic and Natural Resources Research and Development (PCAARRD), based in Los Baños, Laguna.

He received eight honorary doctorate degrees in various fields from several state universities and colleges in the Philippines.

In December 2016, President Rodrigo Roa Duterte honored Dr. Dar with The 2016 Outstanding Filipino Award for his exemplary achievements and selfless dedication to his profession that made significant contributions to the betterment of his countrymen and to his country as a whole.

Plenary Speakers

Dr. Francis de los Reyes is a Professor of Civil, Construction, and Environmental Engineering, an Associate Faculty of Microbiology, and a Training Faculty of Biotechnology at North Carolina State University. In 2013, he was named a University Faculty Scholar. He is a TED Fellow, a Water Environment Federation (WEF) Fellow, and Board Certified Environmental Engineer by Eminence by the American Academy of Environmental Engineers and Scientists.

He received his BS in Agricultural Engineering (magna cum laude) from UPLB in 1990, MS in Civil Engineering from Iowa State University in 1994, and PhD in Environmental Eng. from the University of Illinois at Urbana-Champaign in 2000.

Dr. de los Reyes has been a consultant for the industry on activated sludge operation, solids separation problems, sanitation technologies, and molecular microbiology techniques. He has conducted workshops for wastewater treatment plant operators and professionals in US and the Philippines. He has also worked in water and sanitation issues in developing countries, and has collaborations in Philippines, India, China, South Africa, Pakistan, Ghana, and Malawi. His group's pit emptying technology (Flexcrevator and Excluder) has won the RELX Group Environmental Challenge Award, and in 2020 has received the US Patents for Humanity Award.

Dr. Manuel "Manny" Reyes is a research professor at Kansas State University. He completed his BS and MS degrees at University of the Philippines Los Baños, an MPhil degree at Silsoe College, Cranfield University in England, and a PhD at Louisiana State University in Agricultural Engineering or related field.

Dr. Manny is an agroecological engineer ─ designing food production systems that mimic nature. He has more than 30 years of experience working with water quality modeling, natural resources management, and conservation agriculture. He has extensive expertise across the globe in research, extension, teaching and project implementation.

He is now focused on Cambodia, working with the Royal University of Agriculture, and the National University of Battambang as coordinator of the United States Agency for International Development (USAID) funded Center of Excellence on Sustainable Agricultural Intensification and Nutrition. Dr. Manny is also engaged with 18 higher education institutions in the Philippines. For both countries, he is passionate on extension, research and education of scholars, field practitioners, and youth in Conservation Agriculture─ a topic that he will talk about in his presentation.

Dr. Sergio Capareda is a full professor, Professional Engineer, and Faculty Fellow at the Biological and Agricultural Engineering Department (BAEN) of the College of Agriculture and Life Sciences (COALS), and College of Engineering (COE) at Texas A&M University (TAMU).

He has established the BioEnergy Testing and Analysis Laboratory at TAMU, and expanded it to cover renewable energy and agricultural air quality research. He was responsible for the establishment of emission factor for almond harvesting operations in California, and concentrated animal facilities in Texas. More recently, he established the carbon footprint for Texas A&M University Athletics.

Dr. Capareda is currently a Balik Scientist Awardee. He has written two textbooks on Biomass and Renewable Energy Conversions published by CRC Press. He has co-authored more than 116 refereed journal articles, and has presented more than 130 conference papers.

He received full patent for the Mobile Fluidized Gasification and Pyrolysis Technology he developed, which was licensed by numerous commercial start-ups. He consults for Circon Energy (Magnolia, Texas) which plans to build a 250 MW power plant powered by fuel from used rubber tires, plastics, and MSW.

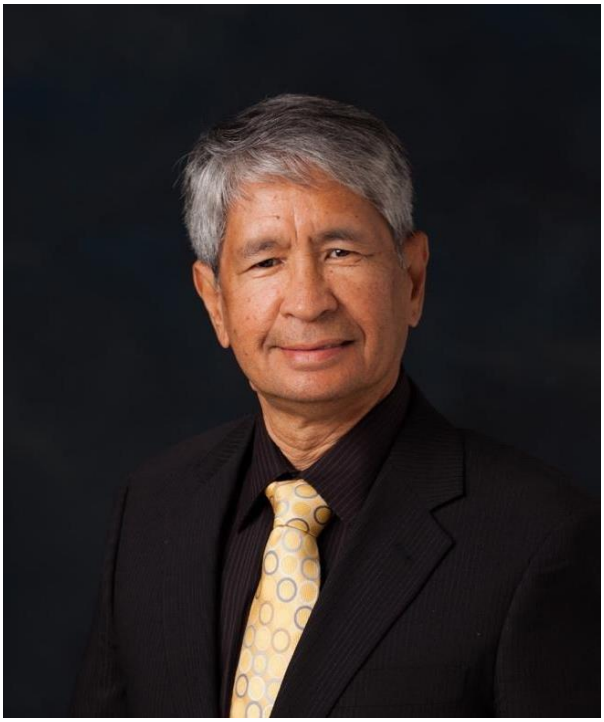

Dr. Isagani Sarmiento obtained his BS degree in Agricultural Engineering and MS degree in Agricultural Engineering and Operations Research at UPLB, and PhD in Biological and Agricultural Engineering at North Carolina State University.

Internationally, Dr. Sarmiento is an Instructor of Physics at Northern Carolina State University; owner of Crumbs Engineering, a biotechnology consultant to Fortune 500 companies in USA for quality assurance and engineering-related services, such as management, reliability engineering, validation, commissioning, calibration, and technical documentation; founder of not-for-profit companies ─ FISH for PEACE (Freeing Intelligence, Strength and Honor for Progress and Empowerment through Alliance, Collaboration, and Encouragement), and BSTC (Biotech Services Training Center); and a member of Board of Directors of several Northern California community organizations.

Locally, Dr. Sarmiento has extensive experience in teaching, research, and administration. He is a Balik Scientist awardee of DOST. He was an Associate Professor of Agricultural Engineering program in UPLB and Director of Agricultural Machinery Testing and Evaluation Center (AMTEC). He is a prolific author, project leader, and consultant to various institutions and local government units across the Philippines.

Dr. Isagani Sarmiento obtained his BS degree in Agricultural Engineering and MS degree in Agricultural Engineering and Operations Research at UPLB, and PhD in Biological and Agricultural Engineering at North Carolina State University.

Internationally, Dr. Sarmiento is an Instructor of Physics at Northern Carolina State University; owner of Crumbs Engineering, a biotechnology consultant to Fortune 500 companies in USA for quality assurance and engineering-related services, such as management, reliability engineering, validation, commissioning, calibration, and technical documentation; founder of not-for-profit companies ─ FISH for PEACE (Freeing Intelligence, Strength and Honor for Progress and Empowerment through Alliance, Collaboration, and Encouragement), and BSTC (Biotech Services Training Center); and a member of Board of Directors of several Northern California community organizations.

Locally, Dr. Sarmiento has extensive experience in teaching, research, and administration. He is a Balik Scientist awardee of DOST. He was an Associate Professor of Agricultural Engineering program in UPLB and Director of Agricultural Machinery Testing and Evaluation Center (AMTEC). He is a prolific author, project leader, and consultant to various institutions and local government units across the Philippines.

Dr. Siti Khairunniza Bejo is an Associate Professor at the Department of Biological and Agricultural Engineering, Head of Smart Farming Research Centre (SFTRC), and Research Associate at the Institute of Plantation Studies in Universiti Putra Malaysia (UPM). Dr. Bejo obtained her PhD degree in Image Processing from the University of Surrey, UK.

Dr. Bejo has served as an Academic Coordinator and Head of Department of Biological and Agricultural Engineering. Her contributions include curriculum development and accreditation by Washington Accord of USA, and Engineering Accreditation Council of Malaysia. She is also a committee member for the development of Bachelor Program of Smart Farming Technology at UPM. She has been appointed in the Editorial Board of 6 international journals, a reviewer for 18 journals, 14 conferences, 2 books, and an evaluator for research grant proposals and competitions.

She has authored more than 130 publications in the field of imaging technology, precision agriculture, remote sensing, and artificial intelligence, including 79 journals, 52 conference proceedings, 4 books, and 4 professional magazines. She has one patent granted, one patent pending, and nine copyrights. To date, her research works have received five international awards.

Dr. Lilik Soetiarso is a Professor of the Department of Agricultural and Bio-systems Engineering at the Universitas Gadjah Mada (UGM), Indonesia where he has been a faculty member since 1990. Starting 2021, he has been appointed as the Head of Department of Agricultural and Bio-systems Engineering. Dr. Soetiarso completed his PhD in Intelligent Control System on Agricultural Machinery at Tsukuba University, Japan; his MEng in Agricultural Information Support System at Asian Institute of Technology (AIT), Thailand; and his BEng in Agricultural Machinery Designat Universitas Gadjah Mada (UGM), Indonesia.

Dr. Soetiarso's specific areas of expertise include agricultural machinery and systems. In recent years, he is focused on model and simulation of agricultural systems, and in the application of soft computing for precision agriculture, and knowledge management system.

Dr. Soetiarso is likewise a member of the Institution of Engineers Indonesia (IEI). In 2017, he was certified by IEI as a Professional Engineer (PE). Currently, he is developing “Smart Agriculture - Research Center” in UGM.

Dr. Leslie Joy Diaz is a professor at the Department of Mining, Metallurgical, and Materials Engineering (DMMME) of the University of the Philippines Diliman, Quezon City (UPD), particularly teaching undergraduate subjects in Metallurgical and Materials Engineering; and graduate-level subjects in Materials Science and Engineering and Environmental Engineering.

Dr. Diaz obtained her DEng degree in Materials Science and Engineering from Tokyo Institute of Technology, while she finished her MS and BS degrees in Metallurgical Engineering at UPD. Her research efforts focus on the use of nanotechnology, green and indigenous materials in developing different kinds of composite materials for wastewater treatment, manufacturing, and biomedical applications.

Dr. Diaz is the first recognized professional materials engineer by the Materials Engineering Certification Board of the Philippines, where she currently leads as Chairman. She is also serving as a technical panel member for DOST-PCIEERD, Bureau of Products Standards of DTI, and the Food and Drug Administration of DOH. She has been instrumental in the establishment of the Materials R&D and Consulting Facility of the UP DMMME, which currently provides materials testing and characterization services employing state-of-the-art equipment needed by industry and researchers.

Technical Program

DAY 1: FEB 23, 2022 (1:20 – 5: 30 pm)

Parallel Session 1 (PS 1):

Food Systems, Bio Process Engineering, Agricultural and Fisheries Mechanization

Moderator: Asst. Prof. Rina A. Bawar

Co-moderator: Engr. Romulo E. Eusebio

Panel Chair: Dr. Roger C. Montepio

Members: Engr. Joseph M. Sandro

Engr. Wilfredo G. Tuso III

TIME (Philippine Time)	Title of Paper	Presenting Author
1:30 - 1:45	Integrating Innovation Equipment for Sustainable Food Engineering System	Alvarado, Urdujah G.
1:50 - 2:05	Rheological Properties of Avocado (Persea americana Mill.) Fruits at Different Ripening Stages	Valencia, Jovielyn L.
2:10 - 2:25	A Preliminary Study on LED Lighting and Growth Performance of Lettuce in an Indoor Vertical Hydroponic System	Saludes, Ronaldo B.
2:30 - 2:45	Sugar Recovery of a Standard Three-Pan Boiling System (CBCA) versus the Double Einwurf (CBA)	Matanguihan, Anna Elaine D.
2:50 - 3:05	Development of Banana Peduncle Juice Extractor for Ethanol and Fiber Production	Ang, Roejae Carlo A.
3:10 - 3:25	Development of a Mechanical Coffee Bean Demucilager	Crystal, Kelvin Michael A.
3:30 - 3:45	Development and Performance Evaluation of Modified Coconut Climbing Device	Tuyogon, Ruel F.
3:50 - 4:05	Performance Evaluation of Different Small Engines for Agricultural and Fishery Machinery Application	Ulgado, Ivan Eduardo A.
4:10 - 4:25	Local Tractor Manufacturing in the Philippines Using Open Systems Design Platform	Valencia, Ronnie C.
4:30 - 4:45	Development of a Manually Operated Checkrow Seeder for Rice Production Systems	Ranches, Mark Angelo F.
4:50 - 5:05	Vegetable Seeds and Seedlings Production: An Approach Towards Food Sustainability	Fernandez, Maribel L.

DAY 1: FEB 23, 2022 (1:20 – 5: 50 pm)

Parallel Session 2 (PS 2):

Land and Water Resources Engineering, Biomass and Biofuels - Renewable Energy

Moderator: Dr. Maurice A. Duka

Co-moderator: Asst. Prof. Kristelle Marie Dela Cruz

Panel Chair: Asst. Prof. Antonio Gabino P. Sobremisana

Members: Dr. Omar F. Zubia

Engr. Corazon D. Ditarro

TIME (Philippine Time)	Title of Paper	Presenting Author
1:30 - 1:45	Mobile Drip Irrigation: A New Tool in Water Management	Aguilar, Jonathan P.
1:50 - 2:05	Optimization of Bio-oil Production from Pyrolysis of Pigeon Pea Wood using Response Surface Methodology	Tanquilut, Mari Rowena C.
2:10 - 2:25	Carbon Footprint of a Direct Combustion Waste-to-Energy System for Municipal Solid Waste	Landoy, Rona Joyce B.
2:30 - 2:45	Integration of Life Cycle Analysis and System Dynamics for Carbon Footprint Assessment: The Case of Electricity Production from Rice Straw	Reaño, Resmond L.
2:50 - 3:05	Micro-hydropower generator feasibility study with inflow variations consideration	Jaurigue, Melvin A.
3:10 - 3:25	Air and Air-Steam Gasification of Coconut Shell in a Fluidized Bed	Magtoto, Keynty Boy V.
3:30 - 3:45	A P-graph Approach for Planning Sustainable Rice Straw Management Networks	Migo-Sumagang, Maria Victoria
3:50 - 4:05	Assessment of Factors Influencing Surface Irrigation Advance and Recession Phase using SIRMOD	Buela, Leunell Chris M.
4:10 - 4:25	Spatio-Temporal Projection of Water Balance Components Under Climate Change: Jalaur River Basin	Jaspe-Santander, Christsam Joy S.
4:30 - 4:45	Development of a Soil Erosion Control System Using Coconut Coir Net Integrated with Tropical Kudzu (Pueraria phaseoloides) Seeds	Reyes, Sherwin R.
4:50 - 5:05	Performance of Aerobic Rice Under Different Levels of N-fertilizer Using Surface Irrigation and Drip Fertigation	Barredo, Abigail R.
5:10 - 5:25	River Improvement Plan for Ungauged Micro Watershed	Tejada, Allan Jr. T.
5:30 - 5:45	Water resources development and management in estuaries during infrequent astronomical events	Haddout S

DAY 2: FEB 24, 2022 (12:50 – 4:40 pm)

Parallel Session 3 (PS 3):

Environmental Engineering and Waste Management,
ICT for SAFE Systems, and Industrial Engineering

Moderator: Dr. Ramon Christian P. Eusebio

Co-moderator: Asst. Prof. Clarissa M. Pesigan

Panel Chair: Prof. Jaderick Pabico

Members: Dr. Aurelio A. Delos Reyes

Dr. Marc Immanuel G. Isip

TIME (Philippine Time)	Title of Paper	Presenting Author
1:00 - 1:15	Computational Fluid Dynamics Simulation of Aerosol Particle Transport in Stored Product Facilities	Asuncion, Fei Xyza B.
1:20 - 1:35	GIS-Based Mapping of Appropriate Soil Texture-Based Four-Wheel Tractor Power Ratings in the Philippines	Pantano, Adrian Daniel L.
1:40 - 1:55	Level of Mechanization of the Rice and Corn Production and Post-Production Systems in Region IV	Amongo, Rossana Marie C.
2:00 - 2:15	Process Simulation of a Multi-Pressure Ethanol System Using Aspen Plus ® Software	Estante, Eros Paul V.
2:20 - 2:35	Rice Monitoring and Yield Estimation in Dumangas, Iloilo, Philippines Using Satellite Imagery	Brusola, Kezia Shem G.
2:40 - 2:55	Adsorption Study of Phosphates in a Fixed bed Utilizing Concrete Cement Wastes	Bautista-Patacsil, Liza
3:00 - 3:15	Prediction of Energy Expenditure (EE) in Construction Sites Using Artificial Neural Network (ANN)	Bautista, Catherine Mae E.
3:20 - 3:35	Determinants of Household Evacuation Mode Choice Behavior in a Rural Community	Gonzales, Maria Elaine A.
3:40 - 3:55	Effects of Various Grip Exertion Levels and Forearm Postures on Hand-Arm Transmitted Vibration	Revilla, Josefa Angelie D.
4:00 - 4:15	Efficiency Evaluation of the JXYS and ZQVR Ergonomic Keyboard Layouts	Cuevas, Eliza B.

DAY 2: FEB 24, 2022 (12:50 – 5:00 pm)

Parallel Session 4 (PS4):

Materials Engineering, Electrical Engineering, Infrastructure and Civil Engineering

Moderator: Asst. Prof. Jedidiah Joel C. Aguirre

Co-moderator: Dr. Ma. Bernadeth B. Lim

Panel Chair: Dr. Marloe B. Sundo

Members: Engr. Donny Rey Camus

Dr. Ronaldo B. Saludes

TIME (Philippine Time)	Title of Paper	Presenting Author
1:00 - 1:15	Classification of Grains using Near-Infrared Hyperspectral Imaging and Multivariate Analysis	Mendoza, Princess Tiffany D.
1:20 - 1:35	Rapid identification of the geographical origin and quality of paddy rice using near-infrared spectroscopy	Foliente, Joanne P.
1:40 - 1:55	COVID-19 Pandemic Activity Travel Patterns of the Commuters in Quezon City, Philippines	Rempillo, Joseph Amiel R.
2:00 - 2:15	Hydrophobic Anti-Corrosion Coatings for Steel Plates using Nanosilica Modified with Hexamethyldisilazane	Madlangbayan, Marish S.
2:20 - 2:35	Cradle-to-Grave Life Cycle Assessment of a Pedestrian Bridge in University of the Philippines-Los Baños, Laguna, Philippines	Fajardo, Adrian Carlo A.
2:40 - 2:55	Natural Fiber Reinforced Concrete: A Review on Mix Designs and Mechanical Properties	Beltran, Gil S.
3:00 - 3:15	A Cradle-to-Grave Life Cycle Assessment of a University Building	Alviar, Miguel Carlo S.
3:20 - 3:35	Use of Pineapple Core Sugar Extract as Set Retarder in Cement Paste	dela Cruz, Rondel A.
3:40 - 3:55	Characterization of harmonic distortion on office-academic buildings	Labalan, Robert Christian
4:00 - 4:15	Probabilistic Modelling of Vehicular Accidents by Collision Type in Metro Manila, Philippines	Tapang, Gracelou Marie B.
4:20 - 4:35	AC Conductivity of Gel Phantom with Varying Degree of Defect	Jusi, Arvin Lester C.
4:40 – 4:55	Gas Transmission Rates of Mango Peel with Chitosan-Nanosilica Composite Coating	Acabal, Ma. Camille G.

Awards

Best Paper Awardees

Session Topic	Title of Presentation	Authors	Ranking
Food Systems, Bio Process Engineering, Agricultural and Fisheries Mechanization	Development of Banana Peduncle Juice Extractor for Ethanol and Fiber Production	Roejae Carlo A. Ang, Rossana Marie C. Amongo, Fernando O. Paras, Jr., Delfin C. Suministrado, and Engelbert K. Peralta	1
	A Preliminary Study on LED Lighting and Growth Performance of Lettuce in an Indoor Vertical Hydroponic System	Ronaldo B. Saludes, Cyra Gail P. Fernandez, Jessica D. Rey, and Toni-An Mae C. Salcedo	2
	Development of a Mechanical Coffee Bean Demucilage	Kelvin Michael A. Crystal, Rossana Marie C. Amongo, Arthur L. Fajardo, and Glenn N. Baticados	3
Land and Water Resources Engineering, Biomass and Biofuels - Renewable Energy	Air and Air-Steam Gasification of Coconut Shell in a Fluidized Bed	Keynty Boy V. Magtoto, Rossana Marie C. Amongo, Sergio C. Capareda, Ronaldo B. Saludes	1
	A P-graph Approach for Planning Sustainable Rice Straw Management Networks	Maria Victoria Migo-Sumagang and Michael Angelo B. Promentilla	2
	Spatio-Temporal Projection of Water Balance Components Under Climate Change: Jalaur River Basin	Christsam Joy S. Jaspe-Santander and Mukand S. Babel	3
Environmental Engineering and Waste Management	Adsorption Study of Phosphates in a Fixed Bed Utilizing Concrete Cement Wastes	Liza Bautista-Patacsil, Marc Angelo V. Diongco & Czarina Jean N. Masicat	1

	Level of Mechanization of the Rice and Corn Production and Post-Production Systems in Region IV	Rossana Marie C. Amongo, Maria Victoria L. Larona, Ralph Kristoffer B. Gallegos, Mark Keylord S. Onal, Ronnie C. Valencia , Kit Ignatius S. Marticio, Andrea Elaine A. Antenor, Paul John S. Dizon, David L. Bondoc, Renz Kevin R. Ilagan, Gherlee Nelle L. Borja, Ria Salustia D. Duminding	2
	Effects of Various Grip Exertion Levels and Forearm Postures on Hand-Arm Transmitted Vibration	Josefa Angelie D. Revilla, Satoshi Muraki & Ping Yeap Loh	3
Materials Engineering, Electrical Engineering, Infrastructure and Civil Engineering	Hydrophobic Anti-Corrosion Coatings for Steel Plates using Nanosilica Modified with Hexamethyldisilazane	Marish S. Madlangbayan, Engelbert K. Peralta, Milagros M. Peralta, Carl Jerome N. Centeno, Paolo Miguel W. Abuan, Alvin Karlo G. Tapia, Rossana Marie C. Amongo, Francis M. Mulimbayan, Aidrean P. Opaco, and Maris Asuncion L. Bayhon	1
	Classification of Grains using Near-infrared Hyperspectral Imaging and Multivariate Analysis	Princess Tiffany Dantes-Mendoza	2
	Rapid Identification of the Geographical Origin and Quality of Paddy Rice using Near-infrared Spectroscopy	Joanne P. Foliente, Fidelina T. Flores, Mary Jane L. Quindoy & Kevin F. Yaptenco	3

Best Poster Awardees

Session Topic	Title of Presentation	Authors	Ranking
Food Systems, Bio Process Engineering, Agricultural and Fisheries Mechanization	Development of a Manually Operated Checkrow Seeder for Rice Production Systems	Mark Angelo F. Ranches, Rossana Marie C. Amongo, Ralph Kristoffer B. Gallegos, Erwin P. Quilloy and Patricia Ann J. Sanchez	1
Land and Water Resources Engineering, Biomass and Biofuels - Renewable Energy	A P-graph Approach for Planning Sustainable Rice Straw Management Networks	Maria Victoria Migo-Sumagang, Michael Angelo B. Promentilla	1
	Bi-Variate and CM Plotting of the Sediment Dynamic Process in the Sebou Estuary (Moroccan Atlantic Coast)	S. Haddout, K.L. Priya, Joan Cecilia C. Casila, and A.M. Hoguane	2
Environmental Engineering and Waste Management	GIS-based Mapping of Appropriate Soil Texture-Based Four-Wheel Tractor Power Ratings in the Philippines	Rossana Marie C. Amongo, Ronaldo B. Saludes, Ralph Kristoffer B. Gallegos, Patrick Lemuel P. Relativo, Adrian Daniel L. Pantano, Ria Salustia D.G. Duminding, Gherlee Nelle L. Lalap-Borja, Julius John Paul A. Cunan	1
Materials Engineering, Electrical Engineering, Infrastructure and Civil Engineering	Characterization of harmonic distortion on office-academic buildings	Robert Christian D. Labalan and Kim Jay R. Rosano	1
	A Cradle-to-Grave Life Cycle Assessment of a University Building	Miguel Carlo S. Alviar, Maricel A. Eneria, Resmond L. Reaño, Ma. Hazel T. Castillo, Richard Dean F. Morales	2

Oral Presentations

Integrating HITS Equipment for Sustainable Food Engineering System

Urdujah G. Alvarado [1, a *], Florentina S. Dumlao [1,b], Arthur G. Ibanez[1,c], Denis V. Policar[1,d] and Rosemarie B. Cabaña[1,e]

[1]Cagayan State University-Carig Campus, Cagayan, Philippines

[a]uat203@csu.edu.ph, [b]fsdumlao@gmail.com, [c]arthur_ibanez20@yahoo.com, [d]dv_policar@yahoo.com, [e]roseesor025@gmail.com

ABSTRACT

The Department of Science and Technology and Cagayan State University established in 2013 the Food Innovation Center (FIC) as the hub of research and innovation which focuses on transforming abundant raw materials in the region into food products using the High Impact Technology Solutions (HITS) equipment. Equipment integrated in sustaining food engineering system are vacuum fryer, spray dryer, water retort, and freeze dryer. The FIC is integrating the Sustainable Food Value Chain Framework from agricultural production, processing, manufacturing, and distribution up to consumption. It employs a systematic approach in the course of food innovation from raw material selection, transforming products using HITS equipment, laboratory analysis, sensory evaluation, packaging, and final product evaluation with Good Manufacturing Practices and Food Safety Standard. There are 302 products developed through the use of the equipment, wherein 12 are granted utility model protection, 11 products are adopted through technology licensing agreement and 630 clients served from the different FIC programs and services. In order to sustain agro-industrialization, there is a need to integrate food innovation equipment to enhance productivity, competitiveness and produce significant results that will help attain food security for the country.

KEYWORDS

Engineering equipment, Food engineering, innovation equipment

Rheological Properties of Avocado (Persea americana Mill.) Fruits at Different Ripening Stages

J. L. Valencia[1], E. K. Peralta[2], K. F. Yaptenco[3], and E. B. Esguerra[4]
[1]Minante I Cauayan City, Isabela 3305. Philippines
. [2]College, Los Baños, Laguna 4031. Philippines
[3] College, Los Baños, Laguna 4031. Philippines
[4] College, Los Baños, Laguna 4031. Philippines
[1] jlvalencia1@up.edu.ph [2] ekperalta@up.edu.ph [3] kfyaptenco@up.edu.ph [4] ebesguerra@up.edu.ph

ABSTRACT

Physical characterization and compression tests were conducted on avocados to develop an understanding of the rheological properties of avocados at different ripening stages, sizes, and compression loads. The appropriate equation in predicting volume from its weight and its shape signature that specifically represents the shape of the purple fruited avocado variety in a one-dimensional function was established. The mean values of sphericity and aspect ratio of the avocado fruits indicate that the shape tends toward being spherical and expected to roll not slide. The compressive strength of avocado varied with ripeness where small size can withstand up to 5 kg of load by weight after harvest without significant internal damage and 6 kg of load for medium size.

Avocado fruits had a time-dependent stress relaxation behavior like other viscoelastic materials. The three-term Maxwell model with six parameters described the stress relaxation behavior of avocado fruit at different compressive loads, ripeness, and sizes based on the maximum relative difference (MRD), R^2, and residual MSE. The advancing degree of ripeness has a corresponding decrease in the decay stress value (σ_1) and time of relaxation (τ_1) component of the model. To minimize mechanical damage, avocado should be packed in a vertical orientation with cushion (bubble wrap, foam, or paper) and can be stacked up to 10 layers for small size and 12 layers for medium size at harvest using 10 kg capacity cartons.

Keywords: avocado, compression, rheology, postharvest handling, physical properties

A Preliminary Study on LED Lighting and Growth Performance of Lettuce in an Indoor Vertical Hydroponic System

Ronaldo B. Saludes[1, a *], Cyra Gail P. Fernandez[1,b], Jessica D. Rey[2,c], and Toni-An Mae C. Salcedo[1,c]
[1]Agrometeorology, Biostructures & Environment Engineering Division,
IABE, CEAT, UPLB, Philippines
[2]Institute of Biology, College of Science, UP Diliman, Philippines
[a]rbsaludes@up.edu.ph, [b]cpfernandez2@up.edu.ph, [c]jdrey@up.edu.ph, [d]tcsalcedo@up.edu.ph

Controlled Environment Agriculture (CEA) is a technology established to address the limitations in open-field farming. In CEAs, different crop and environmental conditions can be optimized and maintained to achieve higher and more efficient production. Plant factories with artificial lighting are examples of such systems[1].

In this study, the experiment was carried out at the Plant Factory with Artificial Lighting (PFAL) research laboratory of ABSEED, IABE from 14 June – 22 December 2021. Three cropping trials were done to evaluate the performance of three different artificial lightings, i.e., T5 cool daylight (T1), T5 daylight (T2), and fixed spectrum LED grow lights (R/W) (T3). Each treatment was applied to a single rack of a 4-layer recirculating deep water culture (DWC) hydroponic system (Fig. 1). Green span lettuce is grown indoors for 21 DAT using artificial grow lights, air conditioning unit, dehumidifier, CO_2 supply tank, and recirculating nutrient solution (SNAP A&B) at a photoperiod of 16/8 hrs of light/dark. The crop and environmental conditions for indoor crop production recommended by Kozai[1] were followed.

Shown in Table 1, are the photosynthetic photon flux density (PPFD) readings and Red/Blue (R/B) ratio of the grow lights, measured using LI-COR LI-250A light meter and Lighting Passport Pro Essence spectrometer with the accompanying Spectrum Genius Agricultural Lighting (SGAL) mobile application, respectively. The spectral distribution of the three light treatments used in the study is shown in Figure 3. This visually shows the relative ratio of red and blue wavelength for the three grow lights, supporting the R/B ratio.

T1 T2 T3

Fig. 1. Experimental setup.

Table 1. PPFD and R/B ratio of artificial lights.

Treatment	PPFD (µmol/m²/s)	R/B
T1	115	2.25
T2	126	0.99
T3	236	5.22

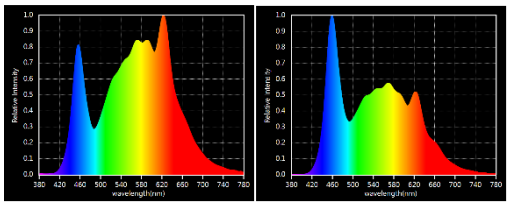

a. (b)

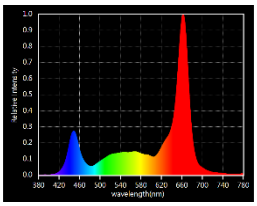

(c)

Fig 2. Spectral distribution of the growing lights used for (a) T1, (b) T2, and (c) T3.

The morphological differences among the treatments were evident as shown in Figure 3, wherein, lettuce grown under lower PPFD (T1 & T2) appeared to be bright green in color, slender, and loose while T3, with higher PPFD, appeared dark green and denser. However, under increased PPFD, tip burn injury appeared on the younger leaves.

Figure 3. Morphological comparison of lettuce under different light treatments at 21 DAT.

The fresh weight (fresh shoot weight) and the final weight (marketable yield or fresh shoot weight less

rejected leaves) were measured. The fresh and final weight were highest when grown under T3 as shown in Figure 4. Whereas, both T1 and T2 showed relatively similar results. Lettuce subjected to a higher PPFD and R/B ratio resulted to a higher yield. The final weight under fixed spectrum significantly increased by 55% and 53% compared to T1 and T2, respectively.

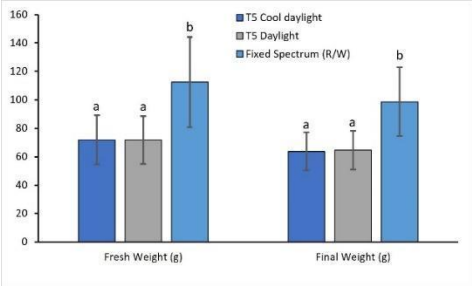

Fig. 4. Average weight of lettuce for three cropping under different light treatments. Bars represent means ± SE. Different letters for the same parameter indicate significant differences at 5% level based on Tukey's test.

Data was analyzed using one-way ANOVA (α=0.05), with assumptions satisfied in all cases. Tukey's test was used for post-hoc comparison of the significant mean difference. Using R software, analysis showed that there is significant effect between light treatments and the fresh and final weight of lettuce for all cropping trials. Post-hoc comparison showed significant mean difference between T3-T1 and T3-T2.

As observed from the results, the difference in the light intensity and quality used in the growing lights can affect the performance of the crop grown [2]. The measured PPFD of the artificial lights indicated that T3 provides more wavelength that the plants can convert to biomass. The significant mean difference in fresh and final weight of T3 to T1 and T2 suggests a more effective energy conversion from the fixed spectrum (R/W) artificial light. Moreover, findings of this study were consistent with those previously observed where, lettuce subjected to a higher PPFD resulted to an increase in biomass [3],[4].

The waveband, blue and red light within the 400-700 nm spectrum, is important for plant growth and development since this is the region most absorbed by the plants for photosynthesis and photomorphogenesis [5],[6],[7]. As absorbed wavelengths increases, photosynthesis becomes more effective, thus contributing to better plant growth [8]. Leaf anatomy, morphology, and physiology is also affected by changes in the light spectrum it was exposed to [9]. Previous studies on lettuce showed that higher portion of red light resulted to higher biomass, leaf count, and increase in plant height as red wavelengths get absorbed more [10],[11]. In addition, a study conducted on lettuce showed that an increase of R/B from 0.5 to 3.0, at 200 μmol/m^2/s intensity, increased the yield 1.6x [12]. Similar findings were observed in this study, wherein T3, having the highest R/B ratio, with PPFD of 236 μmol/m^2/s, had the highest initial and final weight among the treatments.

This study analyzes the effects of light intensity and quality on lettuce grown in an indoor vertical hydroponic system. It was observed that light treatments significantly affect plant biomass and leaf development, showing positive relationship between yield and light intensity and R/B ratio. Although there are also other factors that may affect plant growth, these should be maintained within an acceptable range. Thus, to achieve higher and better-quality lettuce yield, the R/B ratio and PPFD of the grow lights used can be optimized according to the requirements of the crop grown.

KEYWORDS

PFAL, hydroponics, artificial lights, light intensity, R/B ratio

ACKNOWLEDGEMENT

The authors would like to acknowledge the funding support from the Center for Agri-Fisheries and Biosystems Mechanization (BIOMECH), DOST-PCIEERD, and the DOST-SEI's Career Incentive Program (CIP).

REFERENCES

[1] Kozai T. 2018. Smart plant factory: the next generation indoor vertical farms. Singapore: Springer. ISBN 978-981-13-1065-2

[2] Macedo AF, Leal-Costa MV, Tavares ES, Lage CLS, Esquibel MA. 2011. The effect of light quality on leaf production and development of *in vitro*-cultured plants of *Alternanthera brasiliana* Kuntze. *Environmental and Experimental Botany*, 70(2011): 43-50. DOI: https://10.1016/j.envexpbot.2010.05.012

[3] Loconsole D, Cocetta G, Santoro P, Ferrante A. 2019. Optimization of LED lighting and quality evaluation of romaine lettuce grown in an innovative cultivation system. *Sustainability* 11: 841. DOI: 10.3390/su11030841.

[4] Fu Y, Li HY, Yu J, Liu H, Cao Z, Manukovsky NS, Liu H. 2017. Interaction effects of light intensity and nitrogen concentration on growth, photosynthetic characteristics, and quality of lettuce (*Lactuca sativa L.*

Va. Youmaicai). *Scientia Horticulturae.* 214: 51-57. DOI. https://www.sciencedirect.com/science/article/abs/pii/S0304423816305799

[5] Ouzounis, T, Rosenqvist E, Ottosen C. 2015. Spectral effects of artificial light on plant physiology and secondary metabolism: a review. *HortScience,* 50(8): 1128-1135. DOI: https://doi.org/10.21273/HORTSCI.50.8.1128

[6] Li Y, Xin G, Liu C, Shi Q, Yang F, Wei M. 2020. Effects of red and blue light on leaf anatomy, CO_2 assimilation and the photosynthetic electron transport capacity of sweet pepper (*Capsicum annuum* L.) seedlings. *BMC Plant Biology,* 20: 318. DOI: https://doi.org/10.1186/s12870-020-02523-z.

[7] Lumigrow. 2019. The definitive guide to grow light spectrum. Retrieved on January 21, 2022 at https://www.lumigrow.com/learning-center/blogs/the-definitive-guide-to-grow-light-spectrum/

[8] Runkle, E. 2016. Red light and plant growth. Michigan State University: Extension Floriculture Team. Retrieved on January 17, 2022 at https://gpnmag.com/article/red-light-and-plant-growth/

[9] Fan X, Xu Z, Liu X, Tang C, Wang L, Han X. 2013. Effects of light intensity on the growth and leaf development of young tomato plants grown under a combination of red and blue light. *Scientia Horticulturae,* 153 (2013): 50-55. DOI:http://dx.doi.org/10.1016/j.scienta.2013.01.017

[10] Massa GD, Kim H, Wheeler RM, Mitchell CA. December 2008. Plant productivity in response to LED lighting. *HortScience,* 43 (7): 1951-1956.

[11] Lin K, Huang Z, Xu Y. 2018. Influence of light quality and intensity on biomass and biochemical contents of hydroponically grown lettuce. *HortScience* 53 (8): 1157-1163.

[12] Mohamed SJ, Rihan HZ, Aljafer N, Fuller MP. 2021. The impact of light spectrum and intensity on the growth, physiology, and antioxidant activity of lettuce (*Lactuca sativa* L.). *Plants* 10: 2162. DOI: https://doi.org/10.3390/plants10102162

Sugar Recovery of a Standard Three-Pan Boiling System Versus the Double Einwurf

Anna Elaine D. Matanguihan[1, a *], Rex B. Demafelis[1,b], Manolito E. Bambase, Jr[1,c], U-Primo E. Rodriguez[2,d], and Canesio D. Predo[3,e]

[1]Department of Chemical Engineering, College of Engineering and Agro-Industrial Technology, University of the Philippines Los Baños, Laguna, Philippines

[2]Department of Economics, College of Economics and Management, University of the Philippines Los Baños, Laguna, Philippines

[3]Institute of Renewable Natural Resources, College of Forestry and Natural Resources, University of the Philippines Los Baños, Laguna, Philippines

[a]admatanguihan@up.edu.ph, [b]rbdemafelis@up.edu.ph, [c]mebambase@up.edu.ph, [d]uerodriguez1@up.edu.ph, [e]cdpredo@up.edu.ph

Abstract

In the Philippines, the two most employed pan boiling configurations of sugar factories in the recovery of sugar are the 1) Standard three-pan (CBCA), and the 2) Double Einwurf (CBA or double magma). These two configurations were compared through simulation modeling using Sugars™ for Windows using typical operating values from the milling station up to the production of raw sugar in the pan boiling station, using the same feedstock quality (18°Bx) and quantity (10,000 TCD), and configurations of the other pre-boiling stations. The study aims to address the low sugar recovery of sugar mills in the Philippines by focusing on the boiling house section of the mills, where sugar losses in this area majority falls beyond the 10%, while it is typical in the US to lose only 6-10%. It was concluded that the Double Einwurf pan boiling configuration is more efficient in extracting sugar than the CBCA, with 91.39% and 86.60% pol extraction efficiency, respectively. It recovers 5.53% more raw sugar than the CBCA, yielding 2.28 L-kg/TC versus 2.16, but produces 16.71% less molasses, and uses 1.35% more bagasse. This result can be used for decision making on the overall production goal and financials of the sugar factory. Also, it is expensive to conduct process modifications in a commercial scale, more so waste away feedstock for experiments given the current sugar industry condition of almost only 50% utilization for most mills, hence conducting this simulation study should be practicable to the industry. The application of the result (i.e., that mills adopt the Double Einwurf configuration), which should primarily increase the sugar recovered in their mills, may give them a leeway to lower the price of molasses (the by-product of sugar manufacturing) and eventually effect to lower the price of fuel ethanol.

KEYWORDS

sugarmill, simulation, Sugars™ for Windows, L-kg/TC, Philippines

Development of Banana Peduncle Juice Extractor for Ethanol and Fiber Production

Roejae Carlo A. Ang[1, a *], Rossana Marie C. Amongo[2,b], Fernando O. Paras, Jr.[3,c], Delfin C. Suministrado[4,d], and Engelbert K. Peralta[5,e]
[1]Central Mindanao University, Philippines
[2,3,4,5]University of the Philippines – Los Banos, Philippines
[a]raang2@up.edu.ph, [b]rcamongo@up.edu.ph, [c]foparas1@up.edu.ph,
[d]dcsuministrado@up.edu.ph, [e]ekperalta@up.edu.ph

A juice extractor was developed to extract juice from banana peduncle without rupturing its fiber structure for the purpose of processing the juice into ethanol and recover the fiber as co-product. Banana peduncle is a byproduct in commercial banana plantations in the Philippines, which is generated at roughly 2.3 MT every year[1]. While naturally biodegradable, this organic residue, when left to decay in open landfills, emits gaseous pollutants that are harmful to the environment. It was reasoned that this agricultural waste is a cheap and easily accessible sugar-containing biomass that can be efficiently converted by microbes into ethanol and at the same time, recover high quality fiber for various products and uses[2],[3].

Fig. 1. Crushing rolls system

A system of crushing rolls was employed as extraction mechanism to extract as much juice possible without the unnecessary rupture of the cellulosic fiber. The machine was studied under the effect of the rolls' rotational speed and the crushing load. Roll rotational speed was varied in three levels based on recommended rotational speed for similar agricultural products – 50, 70, and 90 RPM[4],[5]. Crushing load was varied in three levels based on the crushing load or rupture force required to break the peduncle – 0.8, 1.2, and 1.6 kN. This was done by employing a spring load mechanism attached to the main crushing roll.

Performance of the machine was evaluated in terms of input capacity,

$$Ci=WiTi \quad (1)$$

where, Ci is the input capacity in kg/h, Wi is the weight in kg of banana peduncle sample fed into the machine, and Ti is the time it took from feeding the sample into the machine until it leaves the exit chute in hours.

Juice or fiber extraction rate,

$$Er=WfTi \quad (2)$$

where, Er is the extraction rate in kg/h for juice or fiber and Wf is the weight in kg of juice or fiber extracted per sample.

Juice or fiber recovery,

$$Ro=WfWi\times100 \quad (3)$$

where, Ro is the juice or fiber recovery in percent.

Extraction losses,

$$El=WLWTJ\times100 \quad (4)$$

where, El is the extraction losses in percent, WL is the weight of juice collected other than from the juice outlet, WTJ is the total weight of extracted juice (Wf+WL).

Extraction efficiency,

$$Eff=WTJPJC\times100 \quad (5)$$

where, Eff is the extraction efficiency in percent, PJC is the potential juice content or the initial moisture content in percent.

Fuel consumption,

$$FC=FiTi \quad (6)$$

where, FC is the rate of fuel consumption in L/h, Fi is the volume of fuel consumed in L.

Optimization analysis for multiple responses using 2-factor interaction model and surface response methodology (RSM) reveals that the optimal setting is found at 71.4 rpm and 0.8 kN combination. The optimum values are presented in Table 1.

Table 1. Optimum values of responses

Response	Significance at α=0.05		Optimum Value**
	Roll Speed	Crushing Load	
Ci	*	*	307.24 kg/h
Juice Er	*	*	82.92 kg/h
Juice Ro	*	*	26.08 %
El	*	ns	4.21 %
Eff	*	*	18.46 %
Fiber Er	*	*	54.83 kg/h
Fiber Ro	*	*	42.29 %
FC	ns	*	0.391 L/h

*means are significant, ~means are not significant, **desirability of 92.3%

ANOVA reveals that higher roll rotational speed and lower crushing load increases input capacity, juice and fiber extraction rates, and fiber recovery. Lower roll rotational speed and higher crushing load increases juice recovery and extraction efficiency. Higher roll rotational speed increases extraction losses while higher crushing load increases fuel consumption rate.

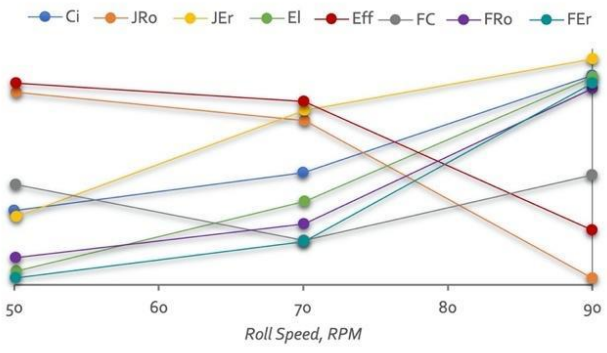

Fig. 2. Machine performance at different roll rotational speed and 0.8 kN crushing load

The extracted juice was concentrated by removing 65%-75% of its moisture to increase sugar concentration to 15-18 °Brix, sustainable for metabolic activity of microorganisms. After 14-day fermentation using *Saccharomyces cerevisiae,* ethanol analysis showed that the fermented broth contains 10-11% ethanol v/v.

The fiber extracted from the pressed peduncles was soak-washed with water daily for 14 days. It was sundried to 9-10% $MC_{w.b.}$. Results showed an average fiber tensile strength of ~300 MPa.

In conclusion, the banana peduncle juice extractor extracts juice while preserving the cellulosic fibers. Performance of the machine is affected by roll rotational speed and crushing load, but no significant effect was observed in terms of ºBrix of extracted juice and tensile strength of fibers. As the case, it is recommended to study other factors that may improve extraction efficiency and recovery and minimize extraction losses and fuel consumption.

KEYWORDS

Peduncle, extractor, ethanol, fiber

REFERENCES

[1] Bureau of Agricultural Research. 2013. Banana Peduncle: To Waste or Not To Waste? BAR Research and Development Digest, January-March Issue (Vol. 15, No. 1). Accessed 20 March 2018

[2] Pazmiño-Hernandez M, Moreira CM, Pullammanappallil P. 2017. Feasibility assessment of waste banana peduncle as feedstock for biofuel production. Biofuels, ISSN: 1759-7269/1759-7277

[3] Vigneswaran C, Pavithra V, Gayathri V, Mythili K. 2015. Banana fiber: scope and value-added product development. Journal of Textile and Apparel, Technology and Management, Volume 9, Issue 2

[4] Gbabo A. 2002. Development and testing of sugarcane juice extractor. Sugar Technology, Volume 4, (3&4):103-107

[5] Oriola KO, Jekayinfa SO, Ola FA, Adedoyin AS, Akande FB. 2017. Some mechanical properties of sugarcane at different sizes and loadings relevant to design and construction of sugarcane juice extractor. International Journal of Engineering Research and Application, Volume 7, Issue 7, Pages 62-70, ISSN 2248-962

Development of a Mechanical Coffee Bean Demucilager

Kelvin Michael A. Crystal[1, a *], Rossana Marie C. Amongo[2, b], Arthur L. Fajardo[2, 3, c], and Glenn N. Baticados[4. d]
[1]Master of Science in Agricultural Engineering, Institute of Agricultural and Biosystems Engineering, College of Engineering and Agro-industrial Technology, University of the Philippines Los Baños, Los Baños, Philippines
[2]Institute of Agricultural and Biosystems Engineering, College of Engineering and Agro-industrial Technology, University of the Philippines Los Baños, Philippines
[3]Agricultural Machinery Testing and Evaluation Center, University of the Philippines Los Baños, Philippines
[4]Department of Agribusiness Management and Entrepreneurship, College of Economics and Management, University of the Philippines Los Baños, Philippines
[a]kacrystal@up.edu.ph, [b]rcamongo@up.edu.ph, [c]alfajardo@up.edu.ph, [d]gnbaticados@up.edu.ph

Coffee ranked as the second most traded global commodity with 1.9% increase on global consumption. The quality and volume of coffee products largely depend on the postharvest processing and handling. A Mechanical Coffee Bean Demucilager is developed to mechanize coffee wet postharvest processing. Design criteria and results from coffee farmers' survey were used in crafting the design. The machine was fabricated using locally available materials and was evaluated based on PNS/PAES 253:2011 and 252:2011 but was tailored for the demucilaging process. Arabica and Robusta were used as test materials. Three speeds and three angles were used to determine the optimum characteristic of the machine. The machine was evaluated in terms of demucilaging efficiency, demucilaging recovery and output capacity. Additional indicators such as mechanically damaged green beans, purity, scattering loss and undemucilaged loss were considered to further understand the effect of speed and angle on the overall machine performance. Results showed that the best setting for Arabica and Robusta were 650 rpm at 15 degrees worm shaft inclination, and 650 rpm at 30 degrees worm shaft inclination, respectively. Statistically, the effect of speed or angle or both are highly significant on the effect on demucilaging efficiency, demucilaging recovery and output capacity.

The Mechanical Coffee Bean Demucilager was fabricated based on the set specification and design suggested by the end-users during the focused group discussion (FGD). FGD was conducted to coffee producer-organization (PO) members across Region IV-A. There was no major change in the actual fabrication. The machine has overall length of 700 mm, overall width of 610 mm, and overall height of 630 mm. The main body (removing the hopper, counterweight, and prime mover) has a dimension of 350 mm x 350 mm x 600 mm (LxWxH). The main frame has a dimension of 700 mm x 350 mm x 600 mm (LxWxH). The demucilaging drum has a diameter of 306 mm and height of 500 mm. The worm worm shaft has a diameter of 298 mm. The machine costs Php 56,760 for the material cost and Php 32,000 for the fabrication cost. Preliminary runs were conducted to check for possible adjustments. A total of 3 preliminary runs were conducted wherein the third run lasted for one straight hour.

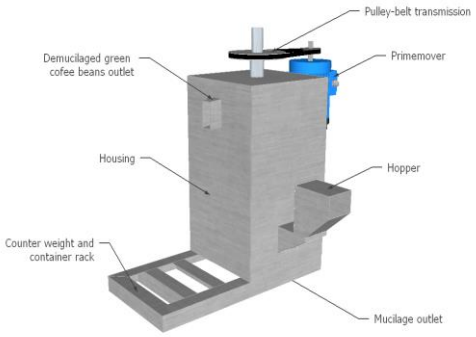

Fig. 1. External parts of the Mechanical Coffee Bean Demucilager.

Test results for Arabica beans showed that changes in the speed and the angle will cause a change on the effect to demucilaging efficiency, demucilaging recovery, and output capacity. An increasing angle decreases the demucilaging efficiency, and it was highest (89.41%) at 650 rpm and significantly higher when angle is set to 15 degrees. On the other hand, a decreasing speed increases the demucilaging recovery, and it was highest (99.41%) at 500 rpm and significantly higher when angle was set to 45 degrees. For the output capacity, an increasing speed increases the output capacity, and it was highest (221.45 kg/h) at 800 rpm and significantly higher when the angle was set to 45 degrees. Furthermore, the correlation between demucilaging efficiency and demucilaging recovery as highly significant and has a positive Pearson correlation value. This implied that as the

demucilaging efficiency increases, the demucilaging recovery also increases. On the other hand, the correlation between output capacity to demucilaging efficiency and to demucilaging recovery had highly significant effect but with negative Pearson correlation values. This suggested that as the output capacity increases, the demucilaging efficiency and the demucilaging recovery decreases.

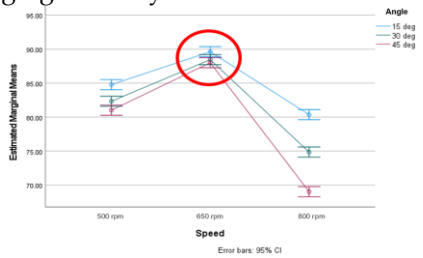

Fig. 2. Profile plot of estimated marginal means of demucilaging efficiency for Arabica.

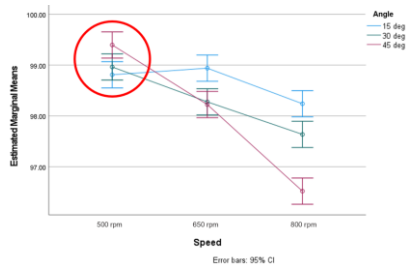

Fig. 3. Profile plot of estimated marginal means of demucilaging recovery for Arabica.

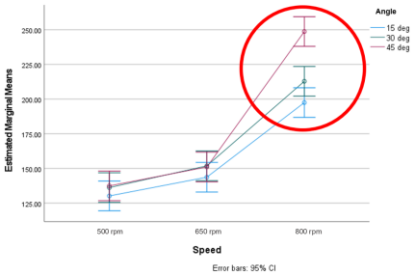

Fig. 4. Profile plot of estimated marginal means of output capacity for Arabica.

Test results for Robusta beans showed that a change in the speed and the angle caused no change on the effect to demucilaging efficiency. However, effect of changing only speed caused a change on the effect to demucilaging efficiency, and it was highest (93.61%) at 650 rpm and significantly higher when angle was set to 30 degrees. On the other hand, a change in the speed and the angle caused a change on the effect to demucilaging recovery. A decreasing speed and angle increase the demucilaging recovery, and it was highest (94.29%) at 500 rpm and significantly higher when angle was set to 15 degrees. For the output capacity, an increasing speed increases the output capacity, and it was highest (169.46 kg/h) at 800 rpm and significantly higher when the angle was set to 45 degrees. Similarly, a change in the speed and the angle caused a change on the effect to output capacity. Furthermore, the correlation between demucilaging efficiency and demucilaging recovery was highly significant and had a positive Pearson correlation value. This implied that the demucilaging efficiency increases, the demucilaging recovery also increases. On the other hand, the correlation between output capacity to demucilaging efficiency and to demucilaging recovery had highly significant effect but had negative Pearson correlation values. This implied that as the output capacity increases, the demucilaging efficiency and the demucilaging recovery decreases.

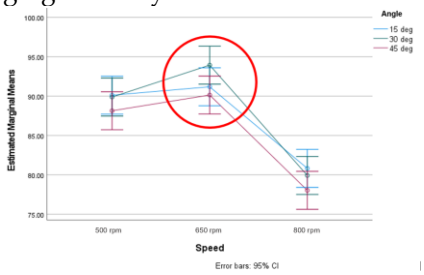

Fig. 5. Profile plot of estimated marginal means of demucilaging efficiency for Robusta.

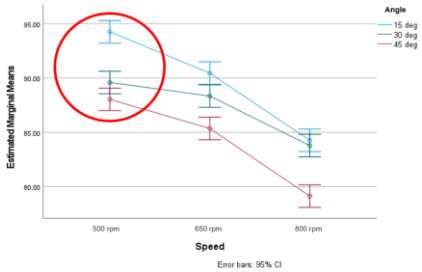

Fig. 6. Profile plot of estimated marginal means of demucilaging recovery for Robusta.

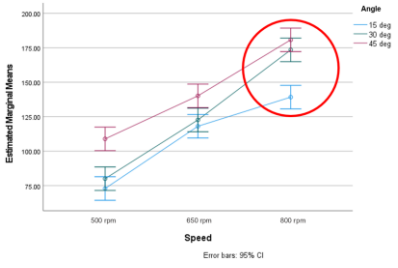

Figure 7. Profile plot of estimated marginal means of output capacity for Robusta.

Keywords *– mechanical coffee bean demucilager, green coffee bean (GCB), demucilaging efficiency, demucilaging recovery, machine design, coffee wet processin*

Development and Performance Evaluation of a Modified Coconut Climbing Device

Ruel F. Tuyogon[1, a *], Ryan M. Abenoja[2,b], , Lourenze Karl C. Lanticse[3,c], and Eldie S. Daffon[4,d]
[1]Brgy. Visayan, Tagum City, Davao del Norte, Philippines
[2]Mesaoy, New Corella, Davao del Norte, Philippines
[3]Haguimitan, Monkayo, Davao de Oro, Philippines
[4]Paloc, Maragusan, Davao de Oro, Philippines
[a]r.tuyogon@usep.edu.ph, , [b]ryan.abenoja@usep.edu.ph, [c]lkclanticse@usep.edu.ph, [d]esdaffon00474@usep.edu.ph

It will take years of experience to develop an expert skill in coconut climbing. Nowadays, the coconut industry of the Philippines is facing a shortage of laborers to do the conventional operations due to aging manual coconut climbers and an insufficient number of predecessors. Problems in coconut harvesting by manual climbing include a high risk of injury, occupational marks, and injuries like callosities, abrasions, amputation. Moreover, it can cause death to some climbers [3]. Thus, a mechanical coconut climbing device with a Philippine-setting-based design was developed to address the problems and lower the risks in coconut climbing.

Methodology

The design was based on the existing model from Mahamuni Agro Equipments in India, several parameters such as the characteristic of the tree (trunk orientation, trunk base, and crown diameter, and presence of obstacles like vines and V-shaped notches or hak-hak) were considered in the modification of the design to suit its performance for the Philippine coconut tree conditions. The field trial was conducted at USeP Tagum Campus and was laid out see Table 1 in a completely randomized 2-level complete factorial design with three factors resulting in six (6) experimental treatments replicated four times.

Table 1. Experiment factors

Factors	Levels	
	1	2
A – Climbing Direction	Up	Down
B – Type of User	Experienced	Inexperienced
C – Mode of Climbing	Manual	By Climbing Device

Two (2) male climbers (experienced and inexperienced in traditional coconut climbing) were selected to experiment with different climbing modes. Both climbers' climbing up/down speed and health parameters were compared.

Results and Discussion

The coconut climbing device

The developed coconut climbing device inf Figure 2 had a frame height of 1 meter, 6 kgs total weight, easy

locking mechanism using a steel carabiner. High tensile strength cable rope was used added with plastic rollers to avoid entanglement on coconut tree trunk deformities. The homing mechanism was installed that enables the user to leave the climbing device at the top of the trunk for safety. Handles and footrests were installed to lessen the users' muscles' fatigue during the operation. The device was cheaper than the device developed in Bangladesh [2].

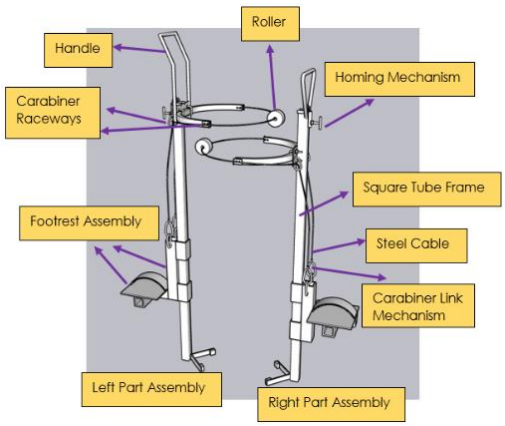

*Figure SEQ Figure * ARABIC 2.The Modified UseP Coconut Climbing Device*

Climbing direction speed

Results revealed in Table 2 that the climbing up speed was statistically equal to the climbing down the speed in both types of users. The mechanism for climbing up is the same as climbing down. However, there was a significant difference in the climbing speed between the different users. Table 3 shows that the user who had experience in manual climbing is faster (13.08m/min) than the user with no experience (10.62m/min). The climbing ability of the farmer is highly affected by the length of experience [4]. Constant training and practice may increase the speed and boost the user's confidence in using the device.

Table 2. Mean of Climbing Speed with respect to Climbing Direction

Factor A – Climbing Direction	Speed, m/min
1 – Climbing up	12.22[a]
2 – Climbing down	11.41[a]

Table 3. Mean of Climbing Speed with Respect to Trained Users Experience

Factor B – Type of Trained Users	Speed, m/min
1 – With experience in manual Climbing	13.08[a]
2 – Without experience in manual Climbing	10.62[b]

Manual climbing vs. device

It was also found that manual climbing (16.38m/min) was faster than the coconut climbing device (7.25m/min) in Table 4. Furthermore, there was a high variation in the users' performance in climbing manually than using the device (Table 4.). The inconsistency was caused by the pain experienced by the user in manual climbing caused by the deformities and notches around the coconut trunk.

Figure 3. The before and after effect of blood pressure,

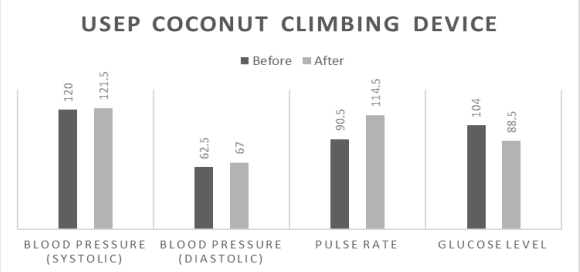

Although the device would not compete with the manual method, the safety during the operation of the farmers and the opportunity of all rural youths and women are the main factors that drive the farmer to use new devices [3].

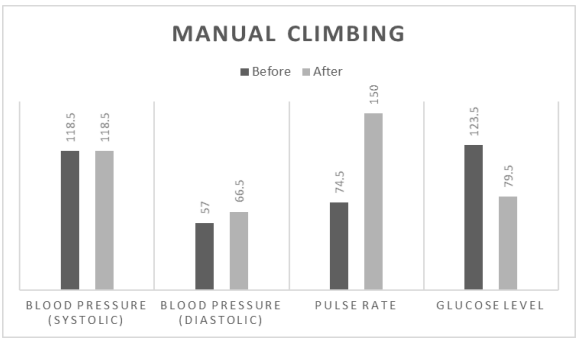

Table 4. Coefficient of Variance of Climbers' Performance for Different Climbing Modes

Mode of Climbing	Direction	Mean (m/min)	C.V. %
Manual	Climbing up	19.97	24.65
	Climbing down	18.67	22.57
With climbing device	Climbing up	7.496	7.56
	Climbing down	6.765	10.42

Figure 4. The before and after effect of blood pressure, pulse rate, and glucose level using the manual method

Health parameters

Figure 3 and 4 shows that the user's blood pressure and body temperature were not heavily affected during the climbing operations. However, there was a difference in the pulse rate and glucose level change. The pulse rate increase in manual climbing ranges 57-94 beats/min while the device ranges 16-32 beats/min. In terms of the users' glucose level changes before and after the operation, manual climbing shows a decrease in glucose level with a range of 33-55 dg/mL, while with the climbing device, the difference only ranges from 13-18 dg. The results show that manual climbing is much more tiring and requires more energy than climbing using the developed manual climbing device.

Although the device and manual method obtained changes in the pulse rate and glucose level, the manual method exhibited a significant difference compared to the device; hence the drudgery was lessened when the device was used during operation [4].

Conclusion

Therefore, the speed or rate of climbing is affected by the mode of climbing and the users' experience. Manual climbing exhibits a higher speed rate; however, pain on the sole and other parts of the subject's body was reported, and tiring. The performance of manual climbing is affected by the characteristics of the V-shaped notches in the tree trunk. On the other hand, climbing using the developed climbing device is much more user-friendly since minimum to no pain was reported by the subject persons. The users' performance was not affected by the characteristics of the V-shaped notches when assisted by the developed climbing device.

References

[1] Deepthi, V., Karunasree, E., Subbaiah, K.V., Reddy, R.V.S.K., Shali, G., Raju, A., Nirmala, T.V., and Prasad, J.V., Impact of FoCT training

[2] Dhafir, M., Idkham, M., Munawar, A.A. and Azrial, P., 2021, November. Operator workload analysis on coconut tree climbing using portable coconut climbing equipment. IOP Conference Series: Earth and Environmental Science (Vol. 922, No. 1, p. 012074). IOP Publishing.

[3] George, M Bincy R., Rao, S Muddanna, Kumar A., Suvarna, N., D'souza, JS.,(2012). "Health of coconut Tree climber of Rural Southern India-Medical Emergencies, Body Mass Index and occupational Marks: A Quantitative and survey study ."J.ClinDiagn. Res.Vol.6 (1)pp. 57-60.

[4] Nusrat Jahan. “Development of a Low-Cost Coconut Tree Climber for Small Farmers in Bangladesh.” International Journal of Engineering Research And, vol. V7, no. 03, 22 Mar. 2018, 10.17577/ijertv7is030034. Accessed 10 Dec. 2021.

Performance Evaluation of Different Small Engines for Agricultural and Fishery Machinery Application

Ivan Eduardo A. Ulgado[1, a *], Arthur L. Fajardo[1,b], Rossana Marie C. Amongo [1,b], Ralph Kristoffer B. Gallegos[3,d], and Romulo E. Eusebio[2,e]

[1]Agribiosystems Machinery and Power Engineering Division, IABE, CEAT, UPLB

[2]Agricultural Machinery Testing and Evaluation Center, CEAT, UPLB

[3]Department of Mechanical Engineering, CEAT, UPLB

[a*]iaulgado@up.edu.ph, [b]alfajardo@up.edu.ph, [c]rcamongo@up.edu.ph,

[d]rbgallegos@up.edu.ph, and [e]reeusebio@up.edu.ph

Over a thousand agricultural machineries such as engines, tractors, pumps, production, and postharvest machineries were being tested and evaluated by AMTEC[1]. However, the copy of test reports are only available to the one who requested the test. To make all these test data available to everybody, it should be published in other forms such as Test Data Bulletin and compilation.

In this study, the general data of small engines tested in AMTEC from 1995-2019[1] were compared with the standards set in PAES 116:2001 to observe and evaluate the data that will fall within the set standards. Trends and distribution on the small engines tested at AMTEC were also done to build a database of its performance. The database consisted of the actual test results on percent rated maximum power at varying load (MBP), percent rated continuous power at rated speed (CBP), noise level (NL), and specific fuel consumption (SFC).

This study showed how the performance features of the small engine have improved over the years. Moreover, the performance evaluation scheme or point system established in the study of Resurreccion, et.al. (2008)[2] was adopted and evaluated using the data generated in the study. The performance evaluation scheme was set by allocating different rating points on different parameters such as specific fuel consumption, power ratings, and noise level of small engines.

Table 1 shows the overall performance of the engines tested from 1995-2019 based on minimum, maximum, and average values. The average engine performance based on the maximum and continuous brake power and the noise level of both varying load test and continuous running test were within the standard set in PAES 116:2001 of at least 80% of the rated maximum output power and not more than 92 dB of the noise emitted by the engine at 50mm away from the operator's ear level.

In terms of maximum and continuous brake power, 73.52% and 53.60% of the small engines tested fall within the standards set in PAES 116:2001, respectively (Table 2) whereas 25.32% and 45.50% fall below the standards, respectively. For the noise level during the varying load tests, 52.06% fall within the standards set in PAES and about 59% (under continuous running test (Table 3). About 46.14% and 38.82% of the engines tested fall below the standards set in PAES for varying and continuous running test, respectively.

Table 1. Summary of the overall engine performance from 1995-2019.

Overall	Min	Max	Ave
MBP	44.00	139.70	87.80
SFC (varying)	185.70	2041.10	512.53
NL (varying)	76.50	107.50	91.99
CBP	9.12	124.65	77.89
SFC (continuous)	2.83	1811.70	362.64
NL (continuous)	3.40	109.20	90.83

Table 2. Summary of engine performance based on PAES 116:2001 for engines tested from 1995-2019.

PAES Standard	Maximum Brake Power	Continuous Brake Power
Within PAES	572	417
Below PAES	197	354
No Data	9	7
Total	778	778

Table 3. Summary of noise level performance of engines tested from 1995-2019.

PAES Standard	Varying Load Test	Continuous Running Test
Within PAES	405	459
Below PAES	359	302
No Data	7	15

Not Readable	7	2
Total	778	778

Table 4 showed the test report counts for each rating points based on power ratings, SFC, and NL. For varying load tests, 46.29% of all small engines earned the highest point in terms of MBP whereas majority of the engines has a rating point of 6 (27.05%) and 2 (27.7%) in terms of CBP. Under varying load test, majority of the engines' SFC has a rating of 2 (52.8%) as well as its noise level performance (33.2%). As for the continuous running test, majority of the engines has a rating of 6 (41.68%) and a rating of 10 (27%) for the noise level performance. Overall, majority of the engines performed within the rating score of 6 and above except for SFC at varying load test where 72.75% of all the engines tested earned a rating score of below 6.

Table 4. Number of engines per rating points based on its performance.

Rating Points	**Varying Load Test**			**Continuous Running Test**		
	MBP	SFC	NL	CBP	SFC	NL
10	356	1	149	69	13	206
8	98	45	111	140	115	124
6	118	168	145	208	318	129
4	83	148	110	139	182	117
2	114	405	256	213	135	187
No Data	9	5	7	9	14	15
Not readable	---	6	---	---	1	---

After assigning the rating points of the small engine based on its performance, the average weights of the six parameters was computed to determine the number of test reports that fall within the minimum and above minimum rating points regardless of whether the engine performance falls within the standard set in PAES 116. Majority of the engines fall below the minimum requirement (57.51% or 429 out of 746). Whereas only 34.85% (260 out of 746) and 7.64% (57 out of 746) fall above and within the minimum requirements, respectively. Out of the 317 small engines with minimum and above minimum ratings, the type of engine based on cooling system were determined and is summarized in Table 5. Diesel water-cooled engines has the highest total number of engines (61.83%) that fall within the minimum and above minimum rating points. The 317 small engines that fall within the minimum and above minimum ratings were further analyzed to determine the number of engines that fall within the standards set in PAES 116. Results showed that only 58.68% (186 out of 317) of the engines with a weighted average of 6 and above fall within the standards in PAES 116. Diesel water-cooled engines has the highest count (69.35% or 129 out of 186) followed by gasoline air-cooled (17.74% or 33 out of 186), and diesel air-cooled (12.90% or 24 out of 186).

Based on the evaluated performance rating scheme, further analysis of the engine performance can be done in terms of assigning weights on specific parameters. The use of different statistical analysis such as the Analytic Hierarchy Process (AHP) or Multi Criteria Decision Analysis (MCDA) can be useful tools in expanding the limitations of the study. Further calibrations can be made in terms of weight percentages of specific parameters used in the study. Moreover, development of evaluation scheme/system may consider other different parameters in the standards set in PAES.

Table 5. Summary of average weight based on the engine performance per type of engine and cooling system.

Rating	**Gasoline air-cooled**	**Diesel air-cooled**	**Diesel water-cooled**
Above Min	60	30	170
Minimum	20	11	26
Total	80	41	196

Table 6. Summary of engines with six and above weighted average that fall within the standard set in PAES 116.

Rating	**Gasoline air-cooled**	**Diesel air-cooled**	**Diesel water-cooled**
Above Min	29	22	125
Minimum	4	2	4
Total	33	24	129

Local Tractor Manufacturing in the Philippines Using Open Systems Design Platform

Victor A. Rodulfo, Jr.[1, a], Alexis C. del Rosario[1, b], Maria Victoria L. Larona[1, c], Ronel S. Pangan[1, d], Jose D. de Ramos[1, e], and Ronnie C. Valencia[1, f*]

[1]Center for Agri-Fisheries and Biosystems Mechanization, College of Engineering and Agro-Industrial Technology, University of the Philippines Los Baños, Los Baños, Laguna, Philippines

[a]varodulfo@up.edu.ph, [b]acdelrosario2@up.edu.ph, [c]mllarona@up.edu.ph, [d]rspagan1@up.edu.ph, [e]jdderamos@up.edu.ph, [f]rcvalencia1@up.edu.ph

The utilization and number of four-wheel tractors in the Philippines, especially for rice and corn farming areas, has been increasing over the years. This can be attributed to the implementation of national policies like the Republic Act No. 8435[1], known as the "Agricultural and Fisheries Modernization Act (AFMA) of 1997", and the Republic Act No. 10601[2], otherwise known as the "Agricultural and Fisheries Mechanization (AFMech) Law of 2013". AFMA law aims to modernize the agriculture and fisheries sectors to enhance profitability while AFMech law promotes agricultural and fisheries mechanization development in the country. Another recent initiative of the government was the "Rice Tariffication Law" or the Republic Act No. 11203[3], which is envisioned to improve rice farmers' competitiveness and income with the lifting of quantitative restrictions on rice imports and replacing them with tariffs, among others. With the government's policy shift to adopt mechanization as a necessary input for farming, Filipino farmers are shifting to the use of machines to allow more efficient, more cost-effective, and more productive farming systems. Such farming systems have the potential to provide more benefits for the country and improve the competitiveness of the agricultural sector. Despite this, local tractor manufacturing capability in the country is still lacking and the current supply is highly dependent on imports. Thus, there is a need to stimulate the local machinery manufacturing industry to manufacture and assemble more advanced machines like tractors. One way to fast-track the manufacturing capability of local manufacturers is the use of open systems design as the manufacturing platform. The mechanisms of an open systems design manufacturing platform are like free and open-source computer applications in which developers provide all the design details of the technology and allow the modifications and improvement of the technology based on the needs and local conditions of the community. This paper focuses on the strategies and methodologies for the development of local tractor assembly and manufacturing in the country using the open systems design platform.

METHODOLOGY

The Center for Agri-Fisheries and Biosystems Mechanization (BIOMECH) of the College of Engineering and Agro-Industrial Technology (CEAT) in the University of the Philippines Los Baños (UPLB) conducted a two-day national workshop at the Obdulia F. Sison Hall Conference Room and the CEAT shop to introduce the concept of open systems design for the local assembly and manufacture of the Ronnie Baugh tractor (formerly Oggun tractor) designed by Clebber Limited Liability Company (CleBer LLC) on January 13-14, 2020. This activity was in collaboration with the CleBer LLC, Kansas State University (KSU), Southeast Asian Regional Center for Graduate Study and Research in Agriculture (SEARCA), Department of Agriculture - Philippine Council for Agriculture and Fisheries (DA-PCAF), and Department of Agriculture - Bureau of Agricultural and Fisheries Engineering (DA-BAFE). After the workshop, the Open Systems Agricultural Machinery Manufacturing (OSAMM) network was organized through the efforts of BIOMECH, together with KSU, SEARCA, identified manufacturers, and other cooperators like the Danfoss, supplier of hydraulic system components. Regular meetings were conducted to monitor the progress in manufacture, assure the quality of components, and map out plans for the eventual commercialization of the RB tractor in the Philippines.

RESULTS AND DISCUSSION

The 2020 workshop was a multi-organizational activity wherein the status of the local machinery manufacturing industry, the open systems design and architecture, conservation agriculture practices, SMART agriculture initiatives in the country, machines developed by USDA for CA and the Oggun tractor, and SEARCA initiatives on innovations and

collaboration in agriculture were discussed. But the key activity of the workshop was the actual assembly and test drive of the tractor. The assembly of the RB tractor components was completed in about five and a half hours with about ten (10) CEAT and BIOMECH technicians doing the work. Figure 1 shows the photos taken during the workshop.

Fig. 1. National workshop on local tractor manufacture and conservation agriculture, 2020.

Among the participants from the manufacturing sector, five (5) manufacturers, namely RU Foundry and Machine Shop Corporation (RUFMC), Global Manufacturing, AGRICOM, Machines Systems Corporation, and Diestro Engineering expressed their interest to manufacture the tractor locally. This suggests a good potential that the open system design platform for the tractor is acceptable to stakeholders, and they are willing to adopt the technology. Through the workshop, the OSAMM network was created and further strengthened the collaboration among the technology generators, suppliers, manufacturers, research institutions, and the government. With the regular meetings and discussions, the issues and concerns of all the stakeholders were being promptly addressed. In February 2022, RUFMC has successfully fabricated and assembled the first locally made agricultural tractor in the country and named it "UR Tractor"

Other initiatives undertaken by BIOMECH were the initial efforts for the research and development of agricultural implements to be attached to the tractor and policy studies on Philippine agricultural machinery manufacturing. The study of Larona, et. al[4], included the commercialization of the open system tractor in the short-term period of the roadmap implementation given the positive reception of the manufacturing sector stakeholders of the project. Furthermore, recent activities on the performance testing and evaluation of the tractor and its implements in local conditions are currently being carried out together with the Agricultural Machinery Testing and Evaluation Center (AMTEC), CEAT, UPLB. It is envisioned that through open systems design, local manufacturing of agricultural technologies will accelerate, become cheaper, and be more available to farmers over the years

CONCLUSION AND RECOMMENDATION

With the open systems design platform, the manufacture of locally made tractors can be realistically pursued. With design improvements, additional innovations, and sourcing of local parts, the utility of the machine under local conditions can be further enhanced. The open systems design in agricultural machinery assembly and manufacturing will allow various stakeholders such as State Universities and Colleges, distribution companies, manufacturers, farmers, and interested adopters to collaborate and further improve the design through the coordination of BIOMECH. The collaboration will allow the manufacturing of parts to be more efficient, sourcing materials localized, manufacturing and maintenance costs reduced, and the majority of the revenue is retained in the community.

ACKNOWLEDGEMENT

The authors would like to acknowledge Dr. Manny R. Reyes of KSU, Mr. Horace Clemmons of Cleber, LLC, Mr. Ramon Uy and Mr. Ronald Margen of R.U. Foundry and Machine Shop Corporation, Mr. Nam Siew Han of Danfoss, the Southeast Asian Regional Center for Graduate Study and Research in Agriculture (SEARCA), and the other members of the Open System Agricultural Machinery Manufacturing (OSSAM) network for their continued support in this undertaking.

KEYWORDS

open systems design, local manufacturing, agricultural mechanization, Ronnie Baugh tractor, four-wheel tractor

REFERENCES

[1] Republic Act No. 8435. 1997. Agriculture and Fisheries Modernization Act of 1997. Accessed on 17 February 2022 at https://www.officialgazette.gov.ph/1997/12/22/republic-act-no-8435-s-1997/.

[2] Republic Act No. 10601. 2013. Agricultural and Fisheries Mechanization (AFMech) Law. Accessed on 17 February 2022 at https://www.officialgazette.gov.ph/2013/06/05/republic-act-no-10601/.

[3] Republic Act No. 11203. 2018. Rice Tariffication Law. Accessed on 17 February 2022 at https://www.officialgazette.gov.ph/downloads/2019/02feb/20190214-RA-11203-RRD.pdf

[4] Larona M, Rodulfo, Jr V, Del Rosario A, Querijero N, Eusebio M, Gumasing R, Bautista M, Salandanan A,

& Talaro N. 2022. Roadmap to Transform the Philippine Agricultural Machinery Manufacturing into a Competitive, Productive, Innovative and Sustainable Industry: Progress Report. Project funded by Department of Agriculture – Bureau of Agricultural and Fisheries Engineering (DA-BAFE) and implemented by the Center for Agri-Fisheries and Biosystems Mechanization (BIOMECH), College of Engineering and Agro-Industrial Technology, University of the Philippines Los Baňos, 4031 College, Laguna, Philippines.

Development of a Manually Operated Checkrow Seeder for Rice Production Systems

Mark Angelo F. Ranches [1, a *], Rossana Marie C. Amongo[2,b], Ralph Kristoffer B. Gallegos[3,c], Erwin P. Quilloy[4,d] and Patricia Ann J. Sanchez[5,e]

[1,2,3,4] Agribiosystems Machinery and Power Engineering Division, Institute of Agricultural and Biosystems Engineering, College of Engineering and Agro-industrial Technology, University of the Philippines Los Baños, Laguna, Philippines

[5] School of Environmental Science and Management, University of the Philippines Los Baños, Laguna, Philippines

[a]mfranches1@up.edu.ph, [b]rcamongo@up.edu.ph, [c]rbgallegos@up.edu.ph, [d]epquilloy@up.edu.ph, [e]pjsanchez@up.edu.ph

The study focused on the development of a manually operated checkrow seeder for rice production systems. According to Amongo (2020), the level of agricultural mechanization in the Philippines only ranged from 3.351 hp/ha to 5.103 hp/ha which is still low[1]. The addition of the checkrow seeder is seen to improve the mechanization level of the country. It was designed and fabricated in Alaminos City, Pangasinan where majority of farmers still utilize traditional methods of rice establishment. The three-dimensional drawing is shown in Figure 1.

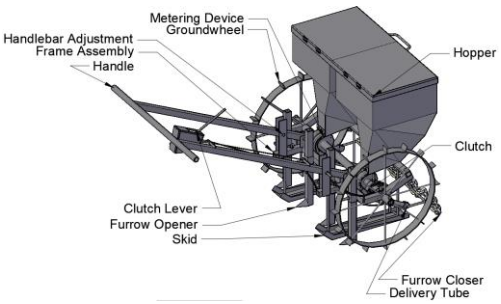

Fig. 1. Isometric view of the checkrow seeder.

The fabricated checkrow seeder is shown in Figure 2. The seeder is mostly made of steel components welded or connected using nuts and bolts.

Fig. 2. Fabricated checkrow seeder.

The general specification of the seeder is shown in Table 1.

Table 1. General specifications of the checkrow seeder.

ITEMS	DIMENSIONS/ SPECIFICATIONS
Overall length, mm	1360
Overall width, mm	880
Overall height, mm	855
Weight (hoppers empty), kg	32
Number of rows and row spacing, mm	4 x 200 mm
Nominal working width, mm	800
Hill distance, mm (if applicable)	200
Capacity, kg	20
Recommended traveling speed, kph	2
Working capacity, ha/h	0.149

Laboratory testing was done where the optimized and calibrated settings were determined. A two-factor, three-level full factorial was done as presented in Table 2. Each setting is repeated thrice resulting to a total of 27 trials. The dependent variables gathered during the tests include seeds per drop, % damaged seeds, and % missed hills.

Table 2. Settings for laboratory testing of the checkrow seeder.

A: METERING DEVICE HOLE DIAMETER, mm	B: HOPPER CAPACITY, %
5	20
5	60
5	100
7	20
7	60
7	100
9	20
9	60
9	100

Using Design expert ® 11 for optimization, it was discovered that at a metering device hole diameter of 6 mm and 60% hopper capacity, the checkrow seeder can drop 3.45 seeds per hill with only 3.14% damaged seeds, and 13.33 % missed hills. The generated solution has a desirability of 0.59 which shows that the response variable values are met 59% of the time. The results were verified through confirmation runs indicating that the generated predictive equations (shown below) are reliable for the machine tests.

$$Seeds\ per\ drop = -10.3832 + 3.29504 * A + 0.0423 * B - 0.002307 * AB - 0.1899 * A^2 - 0.000052 * B^2 \quad (1)$$

$$\%\ Damaged\ Seeds = +2.2503 \quad (2)$$

$$\%\ Missed\ Hills = +180.4167 - 38.6111 * A - 0.2917 * B - 0.01389 * AB + 2.3611 * A^2 + 0.002083B^2 \quad (3)$$

where A is the metering device hole diameter and B is the hopper capacity.

Using the optimum solution, the row and hill spacin of the seeder were measured at 1/8, ½, and full capacity. Test results showed a range of 20.67 to 21.33 cm for hill spacing and 20 cm for row spacing. The seeder was then tested by male and female operators under field conditions. Each trial was done on a 512 square-meter prepared area. The field test results are shown in Table 3.

Table 3. Field test results of the checkrow seeder.

	OPERATOR	
ITEM	**MAL**	**FEMAI**
Seeds/Drop	3.23	3.28
Seeding Depth, mm	14.06	10
Missed hills, %	20	16.67
Field Efficiency, %	93.13	56.25
Hill Spacing, cm	19.8	19.76
Row Spacing, cm	20	20

The apparent impacts of the checkrow seeder were also determined.

KEYWORDS

Manual rice seeder, checkrow seeder, hopper capacity, seed drop per hill, damaged seeds

REFERENCES

[1] Amongo. R. (2020). Philippines Level of Rice Agricultural Mechanization

Vegetable Seeds and Seedlings Production: An Approach Towards Food Sustainability

Maribel L. Fernandez[1, a*] and Florante Victor M. Balatico[2,b]
[1]Cagayan State University, Sta Maria, Lal-lo Cagayan, Philippines
[2]Cagayan State University, Sta Maria, Lal-lo Cagayan, Philippines
[a] maribelfernandezcsu@gmail.com, [b]fvmb42830@gmail.com

The study was conducted in San Mariano, Lal-lo, Cagayan, Philippines, from January 2021 to September 2021 to support the Bayanihan Act 2 program of Department of Agriculture to assess the immediate outcomes of massive seeds and seedlings production of bitter gourd, ladies finger, eggplant, tomato, bush sitao, pole sitao, pepper and bottle gourd vegetables among vegetable growers affected with Covid-19 pandemic and determine their socio demographic and socioeconomic statuses.

The profiling was conducted with the assistance of Municipal Agriculture Office of the Local Government Unit of Lal-lo, Cagayan and barangay officials of San Mariano, Lal-lo, Cagayan. The gathering of data was done by the campus project team of Cagayan State University Lal-lo, Cagayan, particularly faculty researchers and extensionists. During the gathering phase, fifty (50) vegetable growers were selected and identified as beneficiaries and interviewed utilizing the structured questionnaires largely comprising of close ended questions. These vegetable beneficiaries are the original vegetable growers in the said barangay. The questionnaire were consisted of three parts. Part I elicited the socio demographic profile of the respondents, including age, sex, civil status, ethnicity, religion, and highest educational attainment, For part II elicited the socioeconomic profile of the respondents such as occupation, family type, tenurial status, area cultivated, estimated net sales, highest income commodity, number of cropping season and reasons why growing vegetables. Part III contains the problems encountered by the beneficiaries during production, harvesting and post-harvest operation, and marketing, other problems met and alternative sources of income.

Data collected were processed through Statistical Package for Social Sciences Software. Table 1 shows the distribution of respondents in terms of personal information. Results revealed that vegetable farmers are predominantly male (54%), aged 41-50, married, Ilokano, with elementary and tertiary educational attainment belonging to nuclear type family with 3-4 members.

Table 1. Distribution of the respondents in terms of personal information

Variable	Frequency (n=50)	Percentage	Rank
Age			
30 and Below	4	8	4
31 to 40	12	24	2
41 to 50	15	30	1
51 to 60	12	24	2
Above 60	7	14	3
Mean=47.25	**SD=10.78**		
Gender			
Male	27	54	1
Female	23	46	2
Religion			
Roman Catholic	37	74	1
Born Again	6	12	2
Union Espiritista	3	6	3
Church of Christ	2	4	4
Free Believers of Christ	1	2	5
I.N.C.	1	2	5
Ethnicity			
Ilokano	38	76	1
Kalinga	10	20	2
Agta	2	4	3
Type of Family			
Nuclear	44	88	1
Extended	6	12	2
Family Size (DF)			
1 to 2	6	12	3
3 to 4	27	54	1
5 to 6	13	26	2
7 to 8	3	6	4
9 to 10	1	2	5
Mean=4.29	**SD=1.55**		
Civil Status			
Married	44	88	1
Single	3	6	2
Widow	3	6	3
Highest Educational Attainment			
College graduate	10	20	1
College level	9	18	2
Vocational	1	2	5
High school graduate	6	12	4
High school level	7	14	3
Elementary graduate	7	14	3
Elementary level	10	20	1

As shown in table 2, the majority of respondents (66%) are full-time members of the San Mariano Vegetable

Growers Association, earning an average income of Php33,480.39 from a 0.25 to 1.0-hectare vegetable-corn land. All of the beneficiaries (100%) are affected with a high cost of inputs, high labor cost and absence of hauling vehicles during harvesting and post-harvest operations and a very low price of products also exists during marketing.

Table 2. Distribution of the respondents in terms of socio-economic profile

Variable	Frequency (n=50)	Percentage	Rank
Occupation			
Vegetable and Corn Farmer	27	54	1
Vegetable and rice farmer	9	18	2
Vegetable, Rice Farmer and Corn Farmer	8	16	3
Vegetable farmer	2	4	4
Corn, Carabao and vegetable Farmer	1	2	5
Rubber tree and vegetable farmer	1	2	5
Vegetable, Corn, and fruit bearing trees Farmer	1	2	5
Vegetable, and other plantation crops Farmer	1	2	5
Community Organization			
San Mariano Vegetable Growers Association	33	66	1
Tribal Alliance of Indigenous People (TAIP)	10	20	2
Agrarian Reform Beneficiaries Cooperative	4	8	3
Rural Improvement Club	3	6	4
Area Cultivated			
0.25 -1 ha	33	66	1
1.25-2 ha	15	30	2
2.25 to 3 ha	2	4	3
Net Sales/Income			
10,000 and Below	6	11.8	4
10,001 to 20,000	9	17.6	2
20,001 to 30,000	11	23.5	1
30,001 to 40,000	6	11.8	4
40,001 to 50,000	8	15.7	3
50,001 to 60,000	5	9.8	5
More than 60,000	5	9.8	5
Mean=33,480.39	**SD=20,684.53**		
Number of Cropping per Year			
1	6	12	2
2	43	84	1
3	1	2	3
Mean=1.94	**SD=0.47**		
Tenurial Status			
Tenant	26	52	1
Owner	22	44	2
Owner/ Tenant	2	4	3
Harvesting/post-harvest			
High labor cost	25	50	1
Scarcity of labor	17	34	2
Absence of hauling vehicle	8	16	3

Furthermore, vegetable yields average to 3,520 kilograms with a net income of Php45, 306.40, and an ROI ranging from 20% to 247% per cropping season. The results implied that the *Bayanihan* II program significantly increased the income of vegetable farmers from Php33,480.39 to Php45,306.40. Hence, the massive vegetable seeds and seedlings production program was recommended to provide additional funds, closed supervision, and proper management. The program sustainability is vital for the sustainable supply of safe and quality vegetables in the local market, to help farmers generate income in a short period of time and provide them immediate and alternative sources of healthy food during this time of the pandemic.

KEYWORDS

Vegetables, Seeds, Seedlings, Bayanihan, Covid19 pandemic

REFERENCES

[1] Castillo J, Martin A, Rocha L, Sabio V. 2017. Assessment of farmers' knowledge, attitude and perceptions towards organic farming in Cagayan Valley. Philippine Journal of CropScience 42: 131- 132.

[2] Conrado VD, Antonio A, Pattaguan JM. 2013. Profitability of Vegetables Production in Region 02. CSU Research Journal 7:1.

[3] Masuku MB, Xaba B. 2013. Factors Affecting the Productivity & Profitability of Vegetables Production in Swaziland. Journal of Agricultural Studies 1 2:37-52.

[4] Mavengahama S, McLachlan M, De Clercq W. 2013. The role of wild vegetable species in household hood security in maize subsistence cropping systems. Journal of Food Science 5 2: 227-233.

Mobile Drip Irrigation: A New Tool in Water Management

Jonathan Aguilar[1, a *], Bill Golden[2, b], and Dan Devlin[3,c]
[1]Kansas State University, Southwest Research - Extension Center, 4500 E. Mary St., Garden City, Kansas, USA 67846
[2]3627 FM 1473, Meridian, Texas, USA 76665
[3] Kansas State University, 44 Waters Hall, 1712 Claflin Road, Manhattan, Kansas, USA 66506
[a]jaguilar@ksu.edu, [b]ddevlin@ksu.edu, [c]bgolden@ksu.edu

ABSTRACT

Water management in the changing climate conditions and burgeoning world population plays a critical role in the agricultural food production. Irrigated agriculture in particular will be crucial in maximizing crop production under limited land resource. Different irrigation systems deliver valuable water resource to the crops depending on various climatic, topographic, and economic conditions. One of the most versatile and automated system which can have relatively high application efficiency yet still cost effective is the center pivot (and linear) irrigation system. Center pivot irrigation works by irrigating crops using sprinklers mounted on a machine primarily made of radial pipes supported by towers rotating around a pivot or a center point. Center pivot system is the dominant irrigation systems used in the High Plains region of the United States of America and in many other arid regions of the world. While it is more efficient than gravity or surface irrigation, the use of sprinklers and spray nozzles introduces water losses such as spray droplet evaporation, wind drift, and canopy evaporation. Mobile drip irrigation, which integrates drip line onto a mechanical irrigation system such as a center pivot, has attracted attention lately due to its potential of reducing water losses associated with spray nozzles. After five years of conducting research, including data and observations from water technology farms, there is now enough information to share with the public regarding this technology.

KEYWORDS

Mobile Drip Irrigation, Irrigation System, Water Management, Center Pivot, Irrigation

Optimization of Bio-oil Production from Pyrolysis of Pigeon Pea Wood using Response Surface Methodology

Mari Rowena C. Tanquilut[1], Jessie C. Elauria[2], Rossana Marie C. Amongo[2],
Delfin C. Suministrado[2], Kevin F. Yaptenco[2], and Marilyn M. Elauria

[1] *College of Engineering and Computer Studies, Pampanga State Agricultural University, PAC Magalang, 2011 Pampanga, Phil.*

[2] *Institute of Agricultural Engineering, College of Engineering and Agro-Industrial Technology, University of the Philippines Los Baños, College, Laguna, Philippines*

[3] *Department of Agricultural and Applied Economics, College of Economics and Management, University of the Philippines Los Baños, College, Laguna, Philippines*

ABSTRACT

Pyrolysis is an important technology to convert lignocellulosic biomass to a renewable liquid energy carrier known as pyrolysis oil or bio-oil. Bio-oil yield from pigeon pea (*Cajanus cajan*) wood was conducted using a small, semi-continuous reactor at gram- scale level. Response surface methodology using the Box-Behnken three-level, three-factor fractional factorial design was carried out to establish process-product yield relations. The factor variables are temperature (400 to 600°C), particle size of biomass feed (0.5 to 1.3 mm), and N flow rate (7 to 15 mL min^{-1}), with yield of bio-oil and other products as the response variables. The effects of these process conditions on the product yields were also determined. Of particular interest is the liquid product (bio-oil), of which the yield was shown to depend on all independent variables in a complex manner. The optimal conditions for highest bio-oil yield (54 wt.% on dry feed intake) were a temperature of 465.96 ◦C, particle size of biomass feed 1.30 mm, and N flow rate of 14.2 mL min^{-1}. The optimum region has an area of 0.7 cm^2 with its centroid at 1.33 cm from left and 0.45 cm from top of the shaded area. Validation of the optimum condition proved that experimental bio-oil yield (53.33 wt.%) is in good agreement with the predicted value from the model. The bio-oils were shown to have low ash content (0.2%), and high heating value (29 MJ kg^{-1}) and contain high value-added phenolics compounds (41%, GC peak area) as well as low molecular weight aldehydes and carboxylic acids, based on GC–MS analysis. Gel-permeation chromatography analysis indicated the presence of a considerable amount of higher molecular weight compounds. Nuclear magnetic resonance spectroscopy measurements showed that a large proportion of bio-oil contains aliphatic carbons (~60%), likely formed from the decomposition of (hemi)cellulose components, which are abundantly present in the starting pigeon pea wood.

Based on these results, pigeon pea wood is proven as a new potential lignocellulosic bio-resource to replace petroleum-based fuels due to its several attractive agro-energy features. The bio-oil production at optimized condition proved to be a profitable investment and highly viable. Use of catalyst or hydro-treatment or hydro-cracking, further fractionation and/or processing are recommended to upgrade these bio-oils to biofuels and biobased chemicals. Upscaling of pyrolysis system for industrial purposes is also recommended.

KEYWORDS

Optimization, pyrolysis, bio-oil, pigeon pea, characterization, techno-economic analysis

Carbon Footprint of a Direct Combustion Waste-to-Energy System for Municipal Solid Waste

Rona Joyce B. Landoy[1, a*], Rex B. Demafelis[1, b], Manolito E. Bambase, Jr.[1, c], Veronica P. Migo[1, d], and Bernadette T. Magadia[1, e]

[1]Department of Chemical Engineering, College of Engineering and Agro-Industrial Technology, University of the Philippines Los Baños, College, Laguna, Philippines 4031

[a]rblandoy@up.edu.ph, [b]rbdemafelis@up.edu.ph, [c]mebambase@up.edu.ph, [d]vpmigo@up.edu.ph, [e]btmagadia@up.edu.ph

Energy and waste sectors are two of the major areas contributing about 52% and 7%, respectively, of the country's GHG emissions along with the agriculture (33%) and industry (8%). Within the energy sector, production of electricity and heat results to the highest GHG emissions caused mainly by heavy reliance on depleting fossil fuel resources and imported energy. On the waste sector, on the other hand, various waste management activities such as landfilling and wastewater treatment are the identified leading contributors to GHG emissions. [1] Likewise, considering the status of existing dumpsites and sanitary landfills in the Philippines which mostly are already filled up to its capacity, the continuously increasing volume of garbage is becoming a significant concern over time. In response to these concerns, the Philippines recognizes the need to provide mitigation strategies and intensive efforts in view of sustainable development leading to the adoption of cleaner and sustainable technologies.

Across the world, waste-to-energy (WTE) has become the promising alternative in response to the looming garbage and energy crisis. According to the World Energy Council, thermal WTE was the leading technology that accounts for 88.2% of total market revenue in 2013. Globally, around 1700 thermal WTE facilities process over 216 million tons of municipal solid waste (MSW) each year.[2] Several WTE technologies such as direct combustion, gasification, pyrolysis, and anaerobic digestion are mostly applied in converting MSW into heat and electricity.[3] In the Philippines, extensive research and development on the viability of these technologies has been initiated with the release of guidelines and regulations governing the establishment and operation of WTE technologies in the country. However, with the intensive materials and energy required for the construction and operation of a WTE facility, this technology requires further evaluation in terms of carbon footprint and energetics to gain its potential as a sustainable and environmentally benign option in the country.

In this study, life cycle assessment in terms of carbon footprint of a 25-kW direct combustion WTE system for MSW was performed to assess its potential as an environmentally sound option for solid waste management in the country. The carbon footprint analysis was based on the functional unit of analysis – disposal of one (1) kilogram of MSW, wherein the WTE technology was compared to the business-as-usual scenario of landfilling. Based on design parameters, the WTE process was simulated using Aspen Plus ® software while SimaPro ® was the software used for life cycle assessment. The system boundary established in this study includes the transport and sorting of MSW as well as the processing of these wastes for power generation (Figure 1).

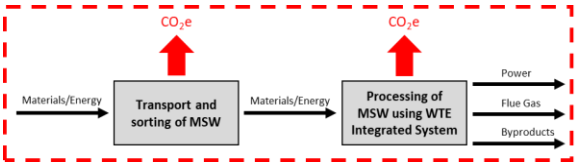

Fig. 1. Overall System Boundary

As compared to other WTE technologies, direct combustion is a thermal conversion technology that operates by direct burning of waste primarily to convert chemical energy into heat and electricity. The end products of a direct combustion process are high temperature flue gas and waste ash.[3] In this study, the direct combustion WTE facility is comprised of a direct combustion system, flue gas cleaning system, and Organic Rankine Cycle (ORC) system for power generation.

Results of the process simulation revealed that a gross power of 27 kW is generated by the system for a 50 kg/hr input of combustible MSW. This translates to a WTE plant capacity factor of about 84%. Considering all the inflows and outflows of the system during operation, it was found out that the total GHG emissions of the direct

combustion WTE system is 1.55 kg CO2e/kg MSW. Figure 2 shows the percent contribution of all the process inputs in terms of GHG emissions. As observed, lime used in the absorption process during flue gas cleaning contributes the largest GHG emissions. To possibly reduce the environmental impact of this process input, further utilization of the potential byproduct in the absorption process may be explored. Since calcium hydroxide, upon reaction with carbon dioxide results to precipitated calcium carbonate, this byproduct being widely used as fillers, additives, and reinforcements in paper, plastic, and cement industry can be considered as an avoided product of the system thereby contributing to GHG emissions reduction. [4]

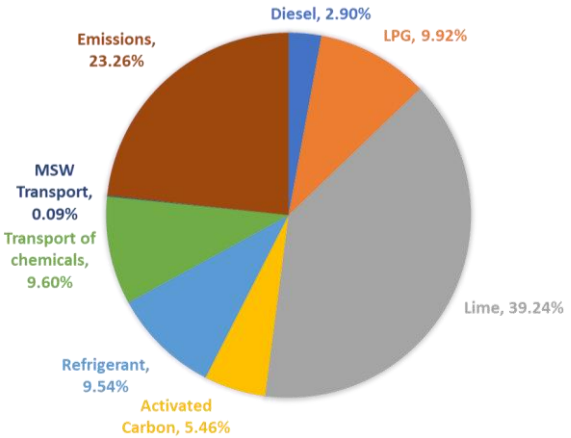

Fig. 2. Percent contribution of process inputs in terms of GHG emissions

As compared to the direct combustion WTE system, the business-as-usual scenario of landfilling results to a relatively higher GHG emissions equal to 3.11 kg CO2e/kg MSW. This was based on the available database in SimaPro ® while methane emissions from solid waste disposal was calculated based on IPCC default method.[5] Landfilling was found to have much higher environmental impact in terms of GHG emissions primarily due to high emissions of methane which is an extremely potent greenhouse gas. Consequently, the carbon debt that comprised the GHG emissions from the production of materials during equipment fabrication up to plant installation was also calculated to be 1.40 x 10^5 kg CO2e. Steel production and metal working accounts the largest percentage of about 88% since most of the equipment is made using this material of construction. Accordingly, the result of this study can serve as a basis of action plans and policy recommendations for the adoption and implementation of WTE via direct combustion in the Philippines.

Integration of Life Cycle Analysis and System Dynamics for Carbon Footprint Assessment of Bioelectricity Production from Rice Straw

Resmond L. Reaño[1a], Victor Antonio N. de Padua[1b]
[1]Department of Engineering Science, College of Engineering and Agro-Industrial Technology, University of the Philippines, Los Baños, College, Los Baños, Laguna, 4031, Philippines
[a]rlreano@up.edu.ph, [b]vndepadua@up.edu.ph

Electricity production from biomass has become an attractive avenue in alternative energy and climate change mitigation research. This study assessed the carbon footprint of bioelectricity produced from rice straw using combined gasification and internal combustion engine. Life cycle assessment was performed, following the ISO 14040 and 14044 guidelines[1], accounting for the material and energy flows within a cradle-to-gate system boundary.

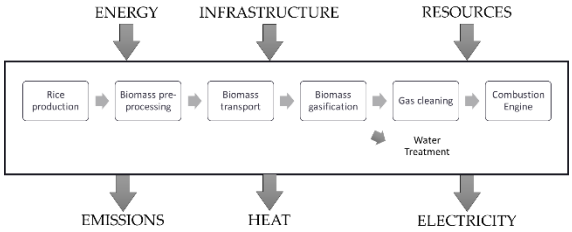

Fig. 1. LCI System boundary

Life cycle inventory (LCI) was performed based on Fig. 1, wherein data from Ecoinvent v.3.7.1 database and literature values were used to calculate the associated emissions for each process. The greenhouse gas (GHG) emission from rice production is allocated based on the mass percentage of milled rice and rice straw as a co-product. Due to lack of literature and actual data for the gasification process, a stoichiometric and thermodynamic equilibrium model was used to calculate the gasification products, using Newton-Raphson method [2]. Table 1 shows the gasification parameters, the rice straw ultimate analysis, and the gasification products.

Table 1. Input and output parameters for the gasification process

Biomass ultimate analysis, wt%	
Components	Weight %
Carbon	33.50
Hydrogen	4.62
Oxygen	58.83
Nitrogen	0.99
Sulfur	0.06
Ash	19.86

Gasification parameters	
Biomass feed rate, kg/hr	1,500.00
Gasification temperature, K	1,273.00
Equivalence ratio	0.20
Steam to biomass ratio	0.25
Biomass moisture content, wt%	0.05
Air supplied, kg/hr	831.23
Carbon conversion (alpha)	0.81
Steam flowrate, kg/hr (1 bar; 300degC	375.00

Product gas components	kmoles
Hydrogen, H_2	8.07
Carbon monoxide, CO	16.06
Carbon dioxide, CO_2	13.30
Methane, CH_4	1.09
Steam, H_2O	46.72
Nitrogen, N_2	22.87

Elemental C, kg/hr	88.67
Tar, kg/hr	22.58
Ash, kg/hr	297.90
H_2S, kg/hr	0.93

Gas yield, Nm^3/kg biomass	0.92
LHV gas (MJ/Nm^3)	5.26
Gasification efficiency	0.33

The gasification efficiency is low due to the high ash and oxygen content of rice straw. Life cycle impact assessment (LCIA) was performed using OpenLCA v.1.10.3 with ReCiPe 2016 methodology to compute the climate change – global warming potential (GWP_{100}). GWP_{100} accounts the total GHG emissions in terms of equivalent amount of carbon dioxide (CO_2)[3]. The result of the impact assessment for climate change is presented using a Sankey diagram (Fig. 2), showing the contributions of each process and the carbon sink

caused by carbon sequestration to support plant growth. Fig. 2 shows that the over-all system results into a surplus of GHG emissions, due to high biogenic methane emission from anaerobic decomposition of plant residues in the flooded rice field.

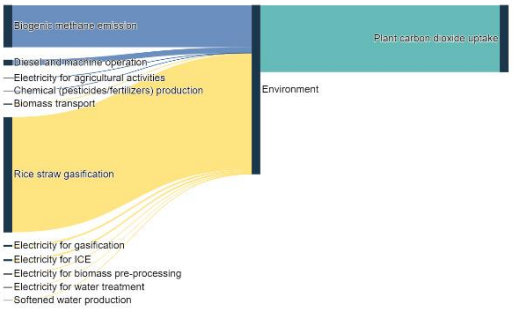

Fig. 2. Sankey Diagram showing the contributions of each process within the product system boundary to climate change

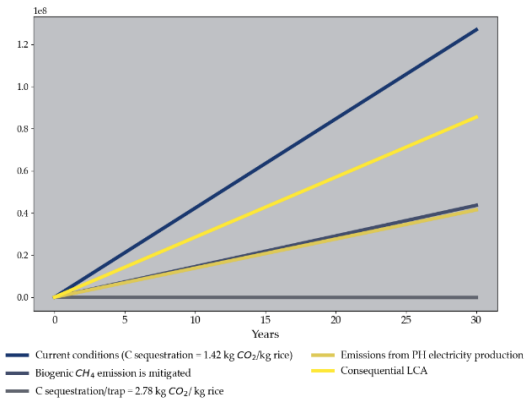

Fig. 3. System dynamics showing GHG accumulation over 30-yr period and the result of various scenario

The result of the LCIA is used in a system dynamic model to show the accumulation of GHG over a 30-yr period (Fig. 3). A net-zero greenhouse gas emissions can be achieved by mitigating biogenic methane emissions and improving carbon sequestration. Consequential LCA accounts the avoided emissions and subtract it from the total emission of the system, thus resulting into a lower carbon footprint.

KEYWORDS

system dynamics, gasification, rice straw, internal combustion engine, bioelectricity

REFERENCES

[1] International Organization for Standardization. 2006. Environmental management: life cycle assessment; requirements and guidelines (Vol. 14044). Geneva, Switzerland.

[2] Rupesh S, Muraleedharan C, Arun P. 2015. A comparative study on gaseous fuel generation capability of biomass materials by thermo-chemical gasification using stoichiometric quasi-steady-state model. Int J Energy Environ Eng 6:375–384.

[3] Levasseur A, Cavalett O, Fuglestvedt J S, Gasser T, Johansson D J, Jørgensen S V, ... & Cherubini F. 2016. Enhancing life cycle impact assessment from climate science: Review of recent findings and recommendations for application to LCA. Ecological Indicators, 71, 163-174.Marine Drugs. 9: 1761-180

Micro-hydropower generator feasibility study with inflow variations consideration

Melvin A. Jaurigue[1,a*] , Kim Jay R. Rosano[1,b*], Gabriela Monica M. Gonzales[1,c], Kyrstynne D. Ureta[1,d]
[1]Department of Electrical Engineering, College of Engineering and Agro-Industrial Technology, University of Philippines in Los Baños (UPLB), 4031, College, Laguna, Philippines
[a]majaurigue1@up.edu.ph, [b]krrosano@up.edu.ph, [c]gmgonzales1@up.edu.ph , [d]kdureta@up.edu.ph

Variability of water inflow makes the conventional methods for calculation of expected power generation of small hydropower plants impractical. Unlike large dams that has controlled flow rate through water gates, inflow variations are a natural occurrence in small hydropower generation systems as they are highly affected by seasons and weather [1]. Without consideration of the disparities in water velocity experienced frequently by water streams, calculated generation capacity may easily be overestimated [2]. Some methods utilize the flow duration curve, assuming the 5th and 95th percentile to be the dry and wet seasons, but still fails to account for the variability in between [3]. This study takes into consideration inflow variations in conducting a feasibility study for micro-hydropower generator by considering these variations as different generation states.

The study evaluated a location along an irrigation network in Maragundon Cavite, which is a part of the Cavite Friar Lands Irrigation System [4], where three months of water flow data was gathered. The irrigation provides a continuous flow of water at 2.22 m^3/s average from a total head of 8.6m. Both human and environmental factors affect the water flow, causing variations that ranges from 0.72 m^3/s to 5.43 m^3/s.

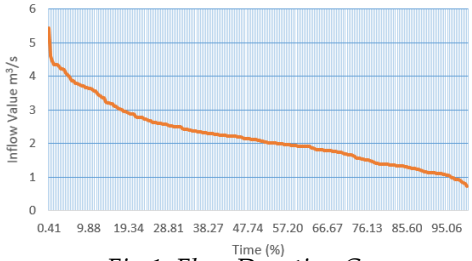

Fig 1. Flow Duration Curve

The flow duration curve is illustrated in Figure 1, where at least 1.07 m^3/s occurs 95% of the time. Water inflow data was clustered through K-means clustering. Using the elbow method [5] shown in Figure 2, the elbow point of the average point-to-centroid distances was identified to be at four clusters, leading to the final generation having five states (with the failure state included).

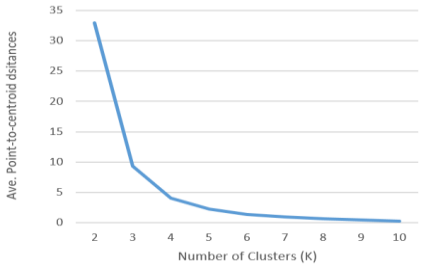

Fig 2. Average Point-to-Centroid distances of the different clusters

A generator failure of 7.6% [6] and turbine efficiency of 85% [7] was used in this study and was maintained to all the transitions with the other states. With the transition between states considered [8], the resulting generation availability from the study is five generation states with their respective capacities [9] and probabilities shown in Table 1.

Table 1. Generation States

State	Capacity, kW	Individual Probability	Cumulative Probability
1	0	7.60%	7.6%
2	89.57	23.52%	31.12%
3	146.75	36.24%	67.70%
4	199.97	19.87%	87.23%
5	283.37	12.76%	100%

The method used in this study identified the different generation states available in the location under study. Using the mean value, Q_{ave}, and neglecting inflow variations, the projected power capacity available at the location is 159 kW, which tends to undermine the potential of the area for power generation that could reach up to 283.37 kW. In comparison to the power generated if the average water flow was used, Q_{ave} tends to undermine the potential of the area for power generation. On the other hand, using the flow rate at the 95th percentile, Q_{95} as used in most studies, will result to at least 76.69 kW capacity available 95% of the time. However, the use of generation

state probability reduces that to only 68.88%, accounting for uncertainties brought by generator failure and inflow variation.

This approach in small-hydropower generation projection gives a more practical solution in determining the power availability in a location. Longer observation and monitoring could improve the results of this study to include the effects of seasons on the water flow rate, but overall, the inclusion of inflow variation in analyzing the small hydro power plant capacity provided better insights in energy planning and future developments of the area.

KEYWORDS

Small hydro power plant, Intermittency, Transition rate, Generation state

REFERENCES

[1] M. S. Rahman, I. M. Nabil and M. M. Alam, "Global analysis of a renewable micro hydro power generation plant," in 1st International Conference on Mechanical Engineering and Applied Science (ICMEAS 2017), Dhaka, Bangladesh, 2017.

[2] C. L. Borges and R. J. Pinto, "Small Hydro Power Plants Energy Availability Modeling for Generation Reliability Evaluation," IEEE Transaction on Power Systems, vol. 23, no. 3, pp. 1125-1135, 2008.

[3] L. Liucci, D. Valigi and S. Casadei, "A new application of Flow Duration Curve (FDC) in designing run-of-river power plants," Water Resources Management, vol. 28, no. 3, pp. 881-895, 2014.

[4] A. Of, Cavite Integrated Water Resource Management Master Plan, 2011.

[5] C. Yuan and H. Yang, "Research on K-Value Selection Method of K-Means Clustering Algorithm," Multidisciplinary Scientific Journal, vol. 2, no. 2, pp. 226-235, 2019.

[6] J. Carroll, . A. McDonald and D. McMillan, Reliability Comparison of Wind Turbines With DFIG and PMG Drive Trains, IEEE Transactions on Energy Conversion, 2015.

[7] A. Kumar, T. Schei, A. Ahenkorah, R. C. Rodriguez, J. Devernay, M. Freitas, D. Hall, Å. Killingtveit and Z. Liu, "Hydropower. In IPCC Special Report on Renewable Energy Sources and Climate Change Mitigation," Cambridge University Press, Cambridge, UK, 2011.

[8] T. Konstantopoulos, "Markov Chains and Random Walks," 2009. [Online]. Available: https://mcube.lab.nycu.edu.tw/~cfung/docs/books/konstantopoulous2009_mcrw.pdf. [Accessed 25 January 2022].

[9] A. Hatata, M. El-Saadawi and S. Saad, "A feasibility study of small hydro power for selected locations in Egypt," Energy Strategy Reviews, vol. 24, pp. 300-313, 2019.

Air and Air-Steam Gasification of Coconut Shell in a Fluidized Bed

Keynty Boy V. Magtoto[1, a*], Rossana Marie C. Amongo[1,b], Sergio C. Capareda[2,c], Ronaldo B. Saludes[1,d]
[1]Institute of Agricultural and Biosystems Engineering, CEAT, UPLB, Philippines
[2]Texas A&M University, Texas, USA
[a]kvmagtoto@up.edu.ph, [b]rcamongo@up.edu.ph, [c]scapareda@tamu.edu, [d]rbsaludes@up.edu.ph

The Philippines, being situated in the tropics, is blessed with vegetation. With almost 33% of its area allotted for agricultural production, biomass wastes also come in considerably large volumes. In the Philippine coconut industry, biomass waste generation contributes to almost 10.4 million tons [1]. These wastes are considered as a potential biomass resource because they can be sourced out almost anywhere in the country and do not compete with food consumption [2]. One method to convert biomass into energy is by thermochemical processes like gasification where biomass is subjected to an oxygen-starved environment while under heat and pressure.

In gasification, different gasifying agents such as air, steam, and oxygen or combinations can be used to react with the solid carbon and heavier hydrocarbons of the biomass. The conversion produces low-molecular-weight gases such as carbon monoxide and hydrogen gas [3]. The type of gasifying agent affects the reaction hence, the study explored the potential of mixing steam in the gasifying agent of the conventional air gasification commonly used in the Philippines. The study aimed to evaluate the effect of using air and air-steam mixture as gasifying agents for fluidized bed gasification of coconut shells on the composition of syngas, higher heating value (HHV), cold gas efficiency (CGE), and carbon conversion efficiency (CCE).

The coconut shell used as a feedstock came from a plantation in Nagcarlan, Laguna, Philippines. After pre-processing the coconut shells for sun-drying and meat-removal, they were then subjected to size reduction using a hammer mill with a 2mm sieve size. Proximate and ultimate analyses, HHV, and moisture content of coconut shells were determined following the ASTM standards. The steam-to-carbon ratio (SCR) was varied to 0 (no steam), 0.3, 0.6, 0.9 and 1.2, computed on a molar basis, to evaluate its effect on the resulting syngas composition, yield, and heating value. During the experiment, the fluidized bed temperature was maintained at 690°C to 700°C only due to equipment limitations. The equivalence ratio (ER) was held at 0.25 as the determined optimum for air gasification of coconut shell [4]. For each SCR setting, the gas samples were analyzed using gas chromatography to determine the relative concentrations of syngas. One-way ANOVA was used for the statistical analysis. The parameters such as H_2, H_2/CO, CCE, CGE, and HHV were also analyzed.

Based on the proximate analysis, the coconut shell has 83.51%$_{wt}$ volatile combustible matter, 15.55%$_{wt}$ fixed carbon, and 0.95%$_{wt}$ ash content, as-received moisture content of 6.94%$_{wt}$, and an HHV of 18.68 MJ/kg. These characteristics are ideal for gasification due to high VCM, high HHV and low ash content. On the other hand, the complete combustion equations for air and air-steam gasification were derived based on the results of the ultimate analysis. Fig. 1 shows the average composition of resulting syngas from the SCR settings.

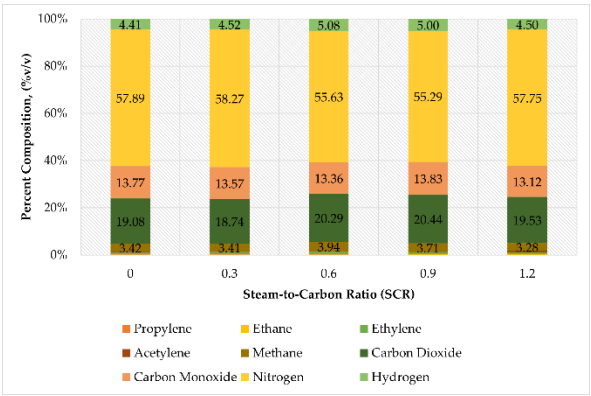

Fig. 1. Average composition of syngas produced at different SCR.

In general, it was observed that 70-75% of the syngas composition is made up of nitrogen and carbon dioxide which are zero-energy gases. The high concentration of nitrogen in the syngas was due to the usage of air as a part of the gasifying agent. Conversely, the hydrocarbons like acetylene, ethylene, ethane, and propylene account for an average of 1.5%$_{v/v}$. Although these hydrocarbons shared only a small portion of the syngas, they were accounted for 18.21% (0.79–1.06 MJ Nm-3) of the total energy content because of their relatively higher HHV equivalents.

As shown in fig. 2a, hydrogen content displayed an increasing trend where it peaked at SCR 0.6 with a value of 5.08 %$_{v/v}$. The increasing trend of hydrogen content was due to water-gas (WG) and water-gas shift

(WGS) reactions promoted by mixing steam in the gasifying agent. However, since both the WG and hydrogasification are highly endothermic, excessive steam decreased the operating temperature which is not favorable to hydrogen production according to the Le Chatelier's principle [5]. ANOVA revealed that in terms of hydrogen content, SCRs have statistically similar results (p-value = 0.1332). The SCRs having no significant effect on hydrogen content suggests that steam had undergone minimal reforming which can be attributed to a low operating temperature [6].

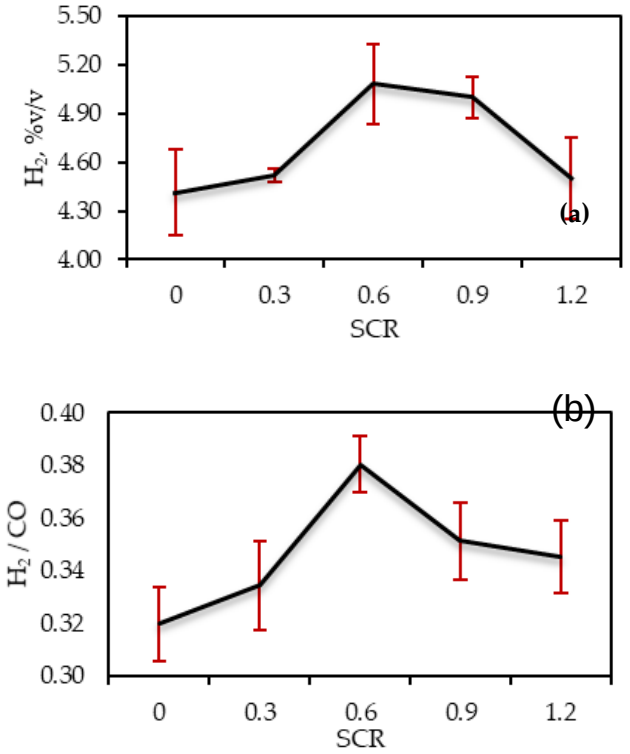

Fig. 2. The H_2 (a) and H_2/CO (b) concentrations of syngas produced at varying SCR.

The H_2/CO ratio represents the degree of WGS reactions that happened during gasification wherein steam reacts with CO to produce H_2 and CO_2. The use of steam as a gasifying agent increased the hydrogen content at the expense of carbon monoxide. As shown in fig. 2b, H_2/CO increased at SCR up to 0.6 then decreased at further SCRs. A higher H_2/CO value means better syngas quality as it has a potential for further synthesis of methanol, ethanol, and dimethyl ester [7].

Carbon conversion efficiency (CCE) and cold gasification efficiency (CGE) are parameters used to evaluate the gasification process. CCE reflects the percentage of carbon atoms of biomass that have been converted to syngas. However, CO_2 is one of the carbon-containing components of syngas that has no heating value. Thus, the performance of the gasification process can be better explained using CGE which represents the total energy of biomass that has been transferred to the syngas. As shown in Table 1, CCE had peaked at SCR 0.9 with a value of 75.49% while CGE had a peak value of 47.50% at SCR 0.6. This implies that among the SCR values considered, the gasification process was most efficient at 0.6 setting. Further increase in steam flow rate results to a decreasing pattern which are like other studies [8, 9]. Many studies concluded that using steam as a gasifying agent should be limited to an optimum flow rate to prevent a decrease in operating temperature. The lowering of temperature due to excessive steam decreases the syngas quality [10, 11, 12]. This conclusion was also reflected in the pattern of HHV that peaked at SCR 0.6 (5.28 MJ/Nm^3).

Table 1. The HHV and gasification efficiencies at different SCR.

Parameters	Steam-to-carbon ratio, SCR				
	0	0.3	0.6	0.9	1.2
Steam flow rate, kg/h	0	0.65	1.30	1.95	2.60
HHV, MJ/Nm^3	5.13	5.16	5.28	5.02	5.04
CGE, %	43.5	45.3	47.5	44.9	44.8
CCE, %	72.9	74.8	74.9	75.5	71.4

ACKNOWLEDGEMENT

This research was funded by the Engineering Research and Development for Technology (ERDT) scholarship program of the Department of Science and Technology (DOST) and the experiment was carried out at the Bio-Energy Testing and Analysis (BETA) Laboratory, Texas A&M University, USA.

KEYWORDS

Coconut shell, fluidized bed gasification, gasifying agents, steam-to-carbon ratio

REFERENCES

[1] Zafar S. 2014. Agricultural wastes in the Philippines<http://www.bioenergyconsult.com/agricultural-resources-in-philippines/>. 9 March 2015.

[2] Canabarro N, Soares JF, Achieta CG, Kelling CS, MazuttI MA. 2013. Thermochemical processes for biofuels production from biomass. Sustainable Chemical Processes, 1:22

[3] Basi P. 2013. Biomass gasification, pyrolysis and torrefaction: Practical design and theory (2nd ed.). Saint Louis, MO, USA. Academic Press.

[4] Wan AK, Ghani WA, Moghadam RA, Mohd Salleh MA, Alias AB. 2009. Air gasification of agricultural wastes in a fluidized bed gasifier: hydrogen production performance. Energies. 2:258-268.

[5] Maglinao AL Jr, Capareda SC, Hyungseok N. 2015. Fluidized bed gasification of high tonnage sorghum, cotton gin trash and beef cattle manure: Evaluation of synthesis gas production. Energy conversion and management. 105:578-587.

[6] Kumar A, Eskridge K, Jones D, Hanna M. 2009. Steam-air fluidized bed gasification of distiller grains: Effects of steam to biomass ratio, equivalence ratio and gasification temperature. Bioresource Technology. 100:2062-2068.

[7] Zheng J-L, Zhu Y-H, Zhu M-Q, Wu H-T, Sun R-C. 2018. Bio-oil gasification using air – steam as gasifying agents in an entrained flow gasifier. Energy. 142:426-435.

[8] Lv PM, Xiong ZH, Chang J, Wu CZ, Chen Y, Zhu JX. 2004. An experimental study on biomass air–steam gasification in a fluidized bed. Bioresource Technology. 95:95–101.

[9] Salami N, Skala Z. 2015. Use of the steam as gasifying agent in fluidized bed gasifier. Chem. Biochem. 29(1):13-18.

[10] Wang Y, Yoshikawa K, Namioka T, Hashimoto Y. 2007. Performance optimization of two-staged gasification system for woody biomass. Fuel Processing Technology. 88(3):243–250.

[11] Alauddin ZABZ, Lahijani P, Mohammadi M, Mohamed AR. 2010. Gasification of lignocellulosic biomass in fluidized beds for renewable energy development: a review. Renew Sust Energy Rev. 14:2852-2862.

[12] Alauddin ZABZ, Lahijani P, Mohammadi M, Mohamed AR. 2010. Gasification of lignocellulosic biomass in fluidized beds for renewable energy development: a review. Renew Sust Energy Rev. 14:2852-2862.

A P-graph Approach for Planning Sustainable Rice Straw Management Networks

Maria Victoria Migo-Sumagang[1,2,a], Michael Angelo B. Promentilla[2,b]
[1] Department of Engineering Science, College of Engineering and Agro-Industrial Technology, University of the Philippines, Los Baños, College, Los Baños, Laguna, 4031, Philippines [2] Chemical Engineering Department, Gokongwei College of Engineering, De La Salle University, 2401 Taft Avenue, 0922 Manila, Philippines
[a]mpmigo@up.edu.ph, [b]michael.promentilla@dlsu.edu.ph

Best rice straw management can lead to sustainable by-product development and reduce pollution from open-field burning. Rice straw agricultural waste can be used sustainably to produce valuable products such as mushrooms, fodder, pellets, or bioenergy, in a rice straw waste management system. Such systems can be optimized using Process Integration tools so that the raw materials are used efficiently at the maximum profit and with a minimal carbon footprint. The P-graph framework is an efficient Process Integration tool that solves Process Network Synthesis problems. P-graph finds the optimal and near-optimal solutions for further analysis, which is useful in decision making. The P-graph framework has been applied to optimize bioenergy systems using agricultural wastes [1, 2]; however, no studies have been found optimizing rice straw networks considering non-bioenergy products. In addition, literature studies do not consider the collection and storage steps of rice straw which are energy and cost-intensive. To address this research gap, the current work developed a P graph model of rice straw management networks, considering collecting, storing, and producing non-bioenergy such as fodder and mushroom in addition to bioenergy products. Disruption scenarios considering reduced raw materials were investigated.

The formal problem statement is stated as follows,

- Given the raw materials (rice straw, diesel, and labor), and various final products (pellets, mushroom, fodder, biogas, biochar, and heat.), with their corresponding process streams data (unit cost/price, availability, etc.).
- Given the various operating units (balers, tractor, storage, pelletizer, fodder pretreatment, anaerobic digester, pyrolizer, and furnace) and their corresponding techno
- economic data and input/output rates.
- The problem is to find the optimal (and sub optimal) allocation of rice straw in terms of maximum profit.

The maximal structure of the p-graph model was constructed using the software P-graph Studio as shown in Fig. 1. The model's performance was illustrated by a case study. The process streams data, techno-economic data, input/output rates were obtained from published literature [3–7]. Rice straw, diesel, and labor as raw materials were considered as they are the main source of energy consumption and cost of production.

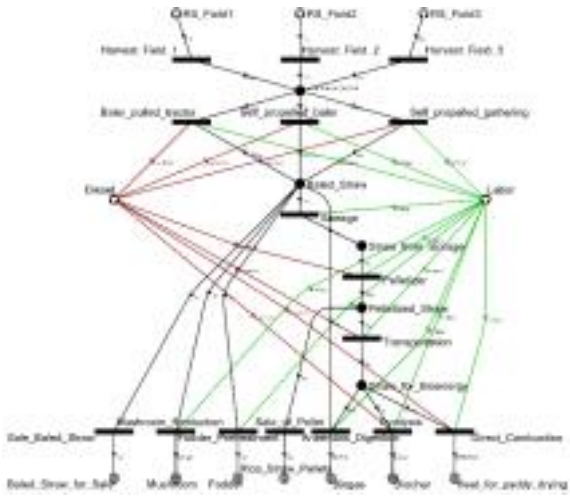

Fig. 1. Maximal P-graph structure of the problem

Four scenarios were investigated. The baseline scenario assumes three different rice fields with a total rice straw yield of 96.84 t/y, and unlimited diesel and manual labor. Scenarios 2 to 4 are disruption scenarios wherein the availabilities of the diesel, manual labor, and rice straw are reduced to 100 L/y, 500 MJ/y, and 75.32/y, respectively.

The results of the baseline scenario show that mushroom production is the optimum solution with an annual profit of USD 14,658.60/yr, followed by rice straw pellet production with an annual profit of USD 12,626.90/yr. The top ten solutions only consist of networks with mushroom or pellet production as final products. Configurations with multiple products are not present in the top ten solutions. Biogas was not selected in the solutions. Other unique solutions are found in Table 1. Fodder production, biochar and heat, and baled straw and heat production come in ranks 19, 29, and 52, respectively. The other unique

solutions have much lower profits compared to the optimal solution (Table 1). The solutions have varying diesel and labor consumption, but all solutions maximized the available rice straw (96.84 t/y).

Table 1. Unique solutions from the baseline scenario.

Solution Rank	Diesel (L/y)	Labor (MJ/y)	Product(s)	Profit (USD/y)
1	404.79	549.08	Mushroom	14,658.60
2	5,547.00	643.02	Pellets	12,626.90
19	404.79	549.08	Fodder	6,993.67
29	6,309.61	1,137.19	Biochar and Heat	5,269.13
52	2,369.54	441.07	Baled Straw and Heat	3,473.04

Scenario 2, which is a disruption in diesel consumption, simulates future decarbonization. Based on the results, mushroom production is still the optimum but at a much-reduced profit of USD 4,437.14/yr as shown in Table 2. Fodder production is another unique solution that comes in rank 14 and a lower profit. Scenario 3, which is a disruption in manual labor, simulates the possible disinterest of the future generation in agriculture. Based on the results, mushroom production is still the optimum with the same profit as the baseline scenario as shown in Table 2. Reduction in the available rice straw (Scenario 4) simulates a future change in land use. Mushroom production is still the optimum solution but at a reduced capacity (Table 2).

Mushroom production using rice straw is an attractive product due to its low production cost and many benefits [7].

Table 2. Disruption scenarios.

Scenario	Rank	Product(s)	Profit (USD/y)
2	1	Mushroom	4,437.14
	14	Fodder	2,053.54
3	1	Mushroom	14,658.60
	5	Baled Straw and Pellets	9,984.86
4	1	Mushroom	11,401.10
	2	Pellets	9,820.91

A P-graph model for rice straw management network was developed considering collection and storage of the rice straw, and production of non-bioenergy products. The model can generate optimal and near-optimal solutions (based on profit) and can simulate raw material disruption scenarios. Based on the illustrative case study, mushroom production is the optimal solution in terms of profit, followed by pellet production. Disruption scenarios at reduced diesel, manual labor, and rice straw show that mushroom production is still the optimum solution, showing the robustness of the solution. This basic model demonstrates that P-graph can be applied to rice straw management networks, to aid with decision making for sustainability. Future work includes carbon footprint accounting, integration with multi-criteria decision analysis (MCDA) techniques to evaluate the near-optimal solutions and considering demand constraints and uncertainty in the data.

KEYWORDS

sustainability, P-graph, process integration, rice straw, decision support systems

REFERENCES

[1] Sangalang KPH, Belmonte BA, Ventura JRS, Andiappan V, Benjamin MFD. 2021. P-graph method for optimal synthesis of philippine agricultural waste-based integrated biorefinery. Chem Eng Trans 83:103–108.

[2] Vance L, Heckl I, Bertok B, Cabezas H, Friedler F. 2015. Designing sustainable energy supply chains by the P-graph method for minimal cost, environmental burden, energy resources input. J Clean Prod 94:144–154.

[3] Migo-Sumagang MVP, Van Hung N, Detras MCM, Alfafara CG, Borines MG, Capunitan JA, Gummert M. 2020. Optimization of a downdraft furnace for rice straw-based heat generation. Renew Energy. doi: 10.1016/j.renene.2019.11.001.

[4] Ishii K, Furuichi T, Fujiyama A, Watanabe S. 2016. Logistics cost analysis of rice straw pellets for feasible production capacity and spatial scale in heat utilization systems: A case study in Nanporo town, Hokkaido, Japan. Biomass and Bioenergy 94:155–166.

[5] Nguyen H Van, Nguyen CD, Tran T Van, Hau HD, Nguyen NT, Gummert M. 2016. Energy efficiency, greenhouse gas emissions, and cost of rice straw collection in the mekong river delta of vietnam. F Crop Res 198:16–22.

[6] Nguyen VH, Topno S, Balingbing C, Nguyen V, Röder M, Quilty J, Jamieson C, Thornley P, Gummert M. 2016. Generating a positive energy balance from using rice straw for anaerobic digestion. Energy Reports 2:117–122.

[7] Vinh Thuc L, Corales RG, Sajor JT, Thi Thanh Truc N, Hieu Hien P, Ramos RE, Bautista E, Joventino Tado CM, Ompad V, Thanh Son D, Van Hung N, Thuc L V, T Truc NT, Corales RG, Sajor JT, Ramos RE, Bautista E, M Tado CJ, Ompad V, Hien PH, Son DT, Hung N V. 2020. Rice Straw Mushroom Production. In: Sustain. Rice Straw Manag. Springer, Cham, pp 93–109.

Assessment of Factors Influencing Surface Irrigation Advance and Recession Phase using SIRMOD

Leunell Chris M. Buela[1, a *], Rubenito M. Lampayan[1,b], Sudhir Yadav[2,c], and Olivyn R. Angeles[2,d]
[1]University of the Philippines Los Baños, College, Laguna, Philippines
[2]International Rice Research Institute, Los Baños, Laguna, Philippines
[a]lmbuela@up.edu.ph, [b]rmlampayan@up.edu.ph, [c]s.yadav@irri.org, [d]o.angeles@irri.org

Surface irrigation is the most common method used in the Philippines, accounting for 1.8 out of 3.1 million ha of irrigable land[1,2]. However, this strategy is known to exhibit low efficiency, resulting to more water waste and energy use[3]. Therefore, it is critical to assess the dynamics of surface irrigation through coupled field experiment and simulation study to potentially increase water use efficiency in surface irrigated lowland rice field.

Various surface irrigation simulation models have been developed over time to evaluate the efficiency and performance of surface irrigation systems. The Surface Irrigation Simulation, Evaluation, and Design (SIRMOD) Model[4] developed by Utah State University is one of these. At the field level, this numerical model simulates the hydraulics of surface irrigation (border, basin, and furrow)[5]. SIRMOD's simulation routine is based on the numerical solution of Walker and Skogerboe's Saint-Venant equations for mass (Eq. 1) and momentum (Eq. 2) conservation[6]. The water efficiency determination for border, basin, and furrow systems was determined to be 70.3, 63.6, and 54.5%, respectively, using this approach[7].

$$\frac{\partial A}{\partial t}+\frac{\partial Q}{\partial x}+\frac{\partial Z}{\partial \tau}=0 \qquad (1)$$

$$\frac{1}{Ag}\frac{\partial Q}{\partial t}+\frac{2Q}{A^2 g}\frac{\partial Q}{\partial x}+\left(1-\frac{Q^2 T}{A^3 g}\right)\frac{\partial y}{\partial x}-S_o+S_f=0 \qquad (2)$$

Only a few research studies have recently been dedicated to determining the relationship between the water advance rate and recession time to the rice establishment method using field experimental and numerical modeling approach. Thus, emphasizing the significance of addressing the primary objective of this research study. Direct seeding of rice is becoming more popular than traditional transplanting[8]. This abrupt change in rice planting methods is owing to the new method's ability to save irrigation water. In earlier years, the impact of rice development stage on surface irrigation hydraulics was investigated. Because there is less impediment on the soil surface during the vegetative stage than during the reproductive stage, water advances faster during the vegetative stage than during the reproductive stage[9].

The field experiment was carried out for two consecutive cropping seasons at the DSR Field Laboratory of IRRI in Los Baños, Laguna, Philippines, where the major soil type belongs to the Maahas clay series. Rice was planted in the wet season (WS) employing a wet tillage strategy that included manual broadcasting, line seeding, and mechanical transplanting. Alternatively, crops were planted using wet tillage technique (manual transplanting, wet direct seeding) and dry tillage system (dry direct seeding) during the dry season (DS). The key water management practice during WS was alternate wetting and drying (AWD). Saturated soil culture was employed in the puddled transplanted rice treatment (T1), while AWD was used for the rest of the setup during DS: wet direct-seeded rice (T2); dry direct-seeded rice (T3), and dry direct-seeded corn (T4).

For the numerical modeling part of the study, SIRMOD III software was used to simulate the surface irrigation system at the field level. The data gathered on the ground served as input parameters for the software. The soil's infiltration characteristic was determined using the Mezencev model (Eq. 3). Meanwhile, infiltration characteristics and Manning's roughness coefficient were used to calibrate and fine-tune the result of the simulation model.

$$i(t) = i_o + (i_1 - i_f)t^{-b} \qquad (3)$$

During the DS experiment, the grain yield data was compared using the Games-Howell Post-hoc Test[10] at a 95% confidence level, implemented through the IBM SPSS Statistics Software. STAR[11] was used to do analysis of variance (ANOVA) throughout the WS. The least significant difference (LSD) test was used to compare the mean of the treatments at a 5% level of significance. Finally, Microsoft Excel was used to do further descriptive statistical analyses such as mean, RMSE, standard error, standard deviation, and linear regression analysis.

Due to the increased surface roughness caused by the development in crop biomass, advance time increased towards its maturity. For the two cropping seasons considered in the study, the advance time of manually broadcasted plots and puddled transplanted rice (PTR) were the lowest. Furthermore, the PTR system's recession time was highest in both experiments due to the formation of hardpan layer. In Fig. 1, the water recession time in the four treatments investigated during DS was compared. Experimental result showed that T1 has the greatest average recession time (1640 to 2144 minutes), whereas T4 has the smallest average recession time (372 to 819 minutes). Additionally, wet tillage systems were also found to have a much longer recession time than dry tillage systems.

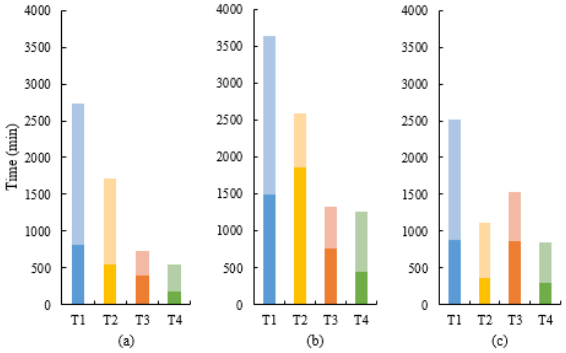

Fig. 1. Recession time of rice: (a) early vegetative stage, (b) tillering stage, and (c) panicle initiation stage; and corn: (a) third leaf collar stage, (b) seventh leaf collar stage, and (c) silking stage.

Irrigation water advance and recession times were measured at three different development stages to evaluate the performance of SIRMOD in simulating surface irrigation using hydrodynamic model. The relationship between observed and simulated advance time was established using linear regression analysis and RMSE to validate SIRMOD model under experimental settings (Fig. 2). The three establishment methods during WS had a very significant association, with R2 values of 0.99 and RMSE ranging from 1.05 to 10.08 minutes, respectively. Through the conjunctive use of field experiment and numerical modelling approach, the study revealed that advance and recession phase are affected by crop establishment method and growth stage owing to the variations in soil physical properties and surface roughness. Additionally, results showed that SIRMOD is thus a useful tool for simulating surface irrigation.

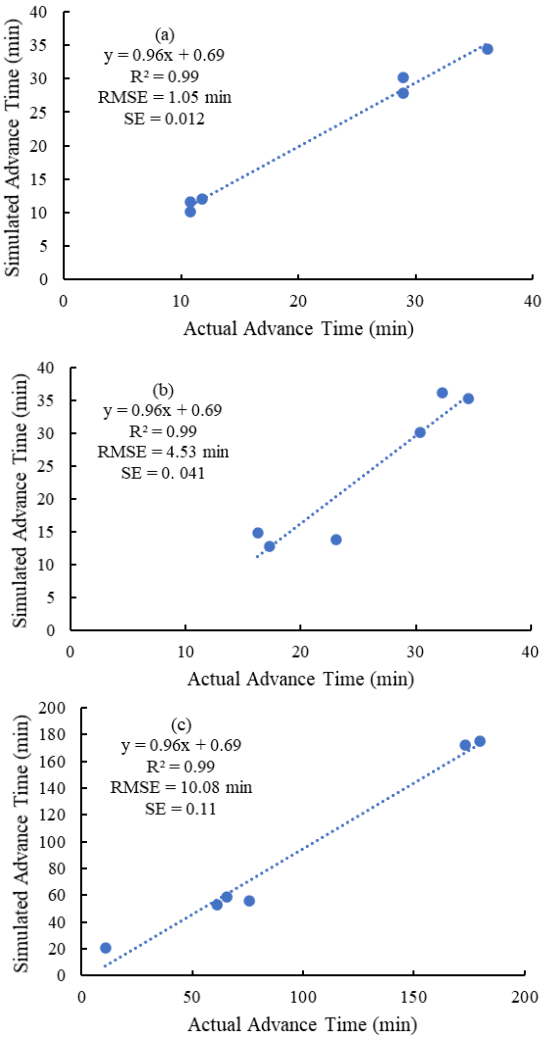

Fig. 2. Scatter plots of simulated and actual advance time for (a) manual broadcasting, (b) line seeding, and (c) transplanting.

Spatio-Temporal Projection of Water Balance Components Under Climate Change: Jalaur River Basin

Christsam Joy S. Jaspe-Santander[1, a *], Mukand S. Babel[2,b]
[1]Central Philippine University, Iloilo City, Philippines
[2]Asian Institute of Technology, Pathum Thani, Thailand
[a]cjjaspe@cpu.edu.ph, [b]msbabel@ait.ac.th

The 2017 World Risk Index[1] and the Germanwatch Climate Risk Index[2] ranked the country third and fifth, respectively, as to be highly impacted by the occurrence of climate change in terms of fatalities and economic losses. The Philippine Atmospheric Geophysical and Astronomical Services Administration (PAGASA) reported that the country's temperature increases by an average of 0.1 °C every decade, with expected continuous warming by as much as 0.9°C to 1.9°C. Seasonal mean rainfall is projected to vary by as much as ±40%. Water resource is considered as among the highly vulnerable resource to be affected by these events[3]. Among the 18 major watersheds in the country, Jalaur River Basin (JRB) is classified as critical in terms of water availability and accessibility.

This study investigates the impacts of climate change to water balance components under climate change scenario by assessing the spatio-temporal variation of precipitation, evapotranspiration, surface run-off, groundwater flow and water yield in the Jalaur River Basin.

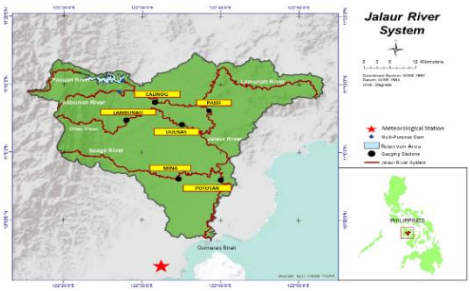

Fig. 1 Jalaur River Basin

Methodology

Baseline climate data of maximum and minimum temperature, and rainfall for the period 1981-2005 were obtained from global sources due to lack of meteorological station. Downscaling was done at the Iloilo station, located outside of the basin. Statistical correlation, using R^2, RMSE, Mean and Standard Deviation methods was used to compare observed climate data to global resources.

Three RCMs (Table 1) at two emission scenarios, RCP4.5 and RCP8.5, at three time periods, 2030s (2025-2049), 2055s (2050-2074) and 2080s (2075-2099) were used to represent future scenario. Linear scaling[4,5,6] was applied as bias correction method. Correction factor for precipitation was developed as a multiplier, while temperature as an additive.

GCM	Institution	Resolution
CCSM4	Community Climate System Model (CCSM)	0.5° x 0.5°
CNRM-CM5	Centre National de Recherches Météorologiques	0.5° x 0.5°
NorESM1-M	Norwegian Climate Center's Earth System Model	0.5° x 0.5°

Table 1. Regional Climate Models

SWAT was used to determine water balance components of rainfall, evapotranspiration, surface runoff, groundwater flow and water yield[7]. SUFI-2 implemented in SWAT-CUP[8] and manual standardization was utilized for model calibration. Goodness-of-fit was determined by graphical comparison, along with Coefficient of Determination (R^2)[9], Nash-Sutcliffe Efficiency (NSE)[10], percent bias (PBIAS) and the RMSE-observation standard deviation ratio (RSR)[11].

Results and Discussion

The use of meteorological data from global sources showed that mean monthly values for both climate parameters have been captured reasonably well for APHRODITE and CPC-UNEP (Table 2).

Table 2. Observed and Global Meteorological Data

Rainfall / Mean Temperature				
Global Climate	Mean	R^2	SD	RMSE
Observed	182.3 / 28.01		174.5 / 0.74	
APHRODITE	143.9 / 27.61	0.82 / 0.98	99.21 / 0.69	130.02 / 0.41
CPC-UNEP	158.6 / 24.94	0.81 / 0.99	130.97 / 0.71	102.36 / 0.11

CFSR	208.5 / 25.96	0.50 / 0.71	154.3 / 1.70	83.91 / 2.36

Analyzing future climate showed that the maximum and minimum temperature in the JRB will increase by 0.39°C to 2.82°C and 0.84°C to 2.69°C respectivley (Fig. 2a, 2b). Absolute change in mean annual precipitation varies from -723 mm to +1150 mm with a declining trend observed throughout the century (Fig. 2c).

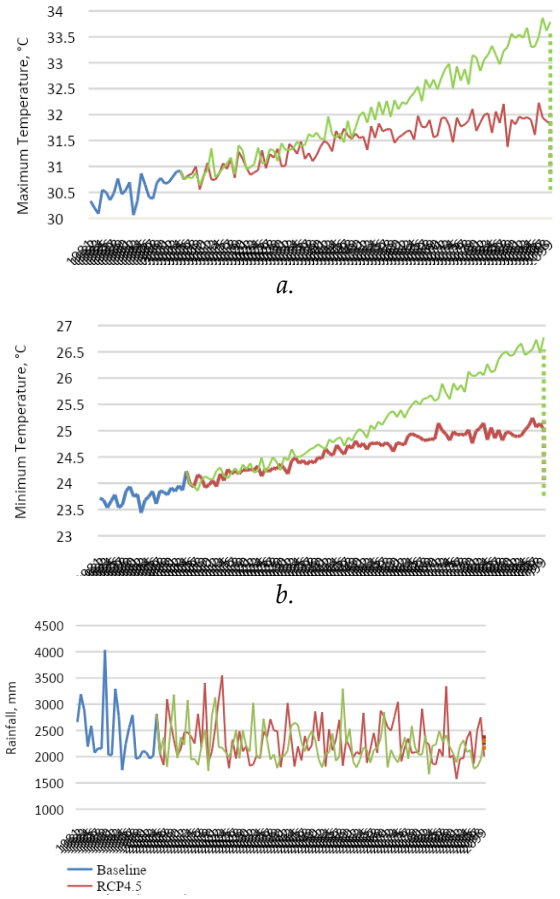

Fig. 2 Average of annual a. maximum, b. minimum temperature and c. rainfall for baseline period (1981-2005) to future period (2025-2099)

The projected decrease in rainfall generally decreases the water supply in the JRB. Over-all water yield will have an average monthly decrease of 5-50 mm (Table 2). The increase in surface temperature results to drier lands with 1 to 7 mm increase in evapotranspiration.

Table 2. Projected average variation in monthly water supply

Component	Supply
Surface Run-off	30-45 mm
Groundwater Flow	5-18 mm
Water Yield	5-50 mm

Considering spatial parameters, the increase in temperature and evapotranspiration (Fig. 3a) and decrease in rainfall and overall water yield (Fig. 3b), will occur all throughout the JRB with the worst occurring in high-elevated areas during the 2055s and 2080s.

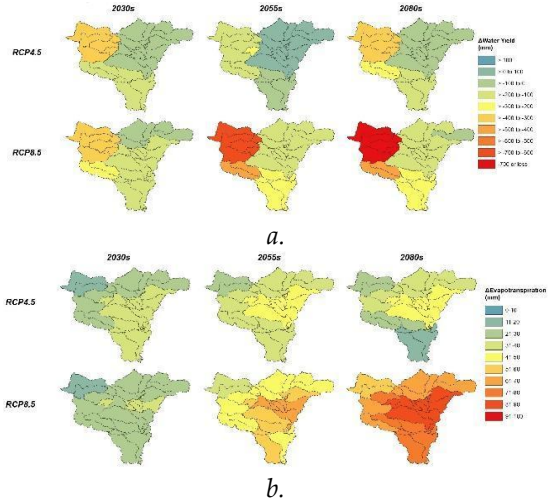

Fig. 3 Multi-annual average of variation a. evapotranspiration and b. rainfall

IV. Conclusion

The future water balance of the JRB is significantly affected by the projected changes in climate. The increase in temperature and decrease in rainfall directly results to the decrease in future water supply of the JRB. The limitation in water resource will disrupt agricultural productivity, food security, employment and price stability causing imbalance to the communities highly dependent on the JRB for its water supply. Management and mitigation strategies should be immediately put in place to alleviate these outcomes.

Development of a Soil Erosion Control System Using Coconut Coir Net Integrated With Tropical Kudzu (*Pueraria phaseoloides*) Seeds

Sherwin R. Reyes[1,a*], Arthur L. Fajardo[2,b], Fernando O. Paras, Jr.[3,c], Roger A. Luyun, Jr.[4,d]
[1]Brgy. Pangpang, Labo, Camarines Norte
[2]University of the Philippines Los Baños, Los Baños, Laguna
[3]University of the Philippines Los Baños, Los Baños, Laguna
[4]University of the Philippines Los Baños, Los Baños, Laguna
[a]srreyes@up.edu.ph, [b]alfajardo@up.edu.ph, [c]foparas1@up.edu.ph, [d]raluyun1@up.edu.ph

Abstract

This study describes the development of a soil erosion control system comprised of tropical kudzu seeds incorporated in the coconet twines. The performance of the system was determined by installing the net (2x3m) in a sloping plot using a 2 by 3 complete factorial design experiment. The three factors are fertilizer (with and without), seed spacing (6"x6", 247 seeds and 12"x12", 123 seeds), and seeding (direct seed to soil and seed integrated into the net) with three replications. Response variables were germination rate and vegetation index and the volume of soil collected. Results showed (figure 1) that the average germination rate ranged from 51% to 84%, with the highest rate yielded from the treatment with no fertilizer.

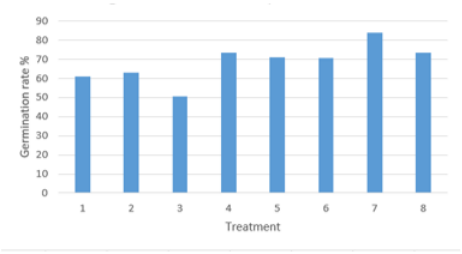

Figure 1. Average germination rate of Tropical Kudzu seeds in Coconut Wire Coir Net Plus

The germination rate of treatments with seeds incorporated into the net was relatively higher and was within the 70% rate of the preliminary trials. The average vegetation index for all treatments was more than 92% for the 12-week duration. No soil particles were collected at the bottom of the plots due to the low frequency and intensity of rainfall during the conduct of the study. In the long run, the Coconut Coir Net Plus is found to be a more economical soil erosion solution as it will not require re-installation as compared to a regular coconet (table 1 and table 2).

Table 1. Coconut coir net cost per hectare

Description	unit	Unit Cost (Peso)	Total cost (Peso)
Dried cocofiber (500 rolls x 50kg)	kgs	14.00	350,000.00
Labor cost			
a. Twining with seeds integration (500 roll x 24 twine)	Per twine	2.50	30,000.00
b. Weaving (500 roll)	Per roll	100.00	50,000.00
Installation fee (per roll, included clearing of area)	Per roll	700.00	350,000.00
		Total	**750,000.00**

Table 2. Coconut Coir Net Plus Cost per hectare

Description	unit	unit Cost (Peso)	Total Cost (Peso)
Dried cocofiber (500 rolls x 50kg)	kgs	14.00	350,000.00
Tropical Kudzu seeds (3 kgs)	kgs	300.00	900.00
SMYERG Bio compound Fertilizer (Coating fertilizer) (1500/kg)	Pack @ 1kg (per 3 kg seed)	1,500.00	1,500.00
Labor cost			
c. Twining with seeds integration (500 roll x 24 twine)	Per twine	2.50	30,000.00
d. Weaving (500 roll)	Per roll	100.00	50,000.00
e. Mixing fertilizer and seeds (1 day)			500.00
Installation fee (per roll, included clearing of area) (500 rolls)	Per roll	700.00	350,000.00
		Total	**782,900.00**

The design of a mechanical system in the incorporation of seeds during the twining process is recommended to increase the production capacity. Furthermore, it is recommended to further study the establishment of tropical kudzu considering a longer period of time.

Keywords - coconut coir net, soil erosion control system, germination rate, vegetation index

REFERENCES

[1] Benik, S.R., Wilson, B.N., Hansen, B.J. "The Efficacy of Erosion Control Blankets and Soil Stabilizers", 2000. https://www.lrrb.org/pdf/200015.pdf. Accessed (September 15, 2019).

[2] Bubb, Philip, Arnout Van Soesbergen, Neha Bisht, Gajendra Singh, Srijana Joshi, Kamal Aryal, Fiona S. Danks, Gopal Singh Rawat, Sanjeev Bhuchar, Wu Ning, Rajan Kotru, Yi Shaoliang. "Planning Management for Ecosystem Services An Operations Manual",2017. http://lib.icimod.org/record/21492/files/Sloping%20Agricultural%20Land%20Technology%20(SALT).pdf. Accessed (September 15, 2019).

[3] Clavecillas, Ryan C., Martin, Ramon M., Andal, Efren A., Morla, Simplicio N., And Velasco, Jenny C. "Development of Paper Twining Machine. Philippine Metals", Vol. 2, 2015. Metals Industry Research and Development Center, Department of Science and Technology, Bicutan, Taguig City 1631

[4] Contreras, S.M.. "The Philippine Agriculture and the threats of Land Degradation, BSWM, DA", 2018. https://lcluc.umd.edu/sites/default/files/Phil_Ag_0.pdf. Accessed (September 15, 2019).

[5] Decano, Cristina S., Malamug, Vitaliana U., Agulto, Melissa E. And Gavino, Helen F., "Corn (Zea mays L.) Stalk Geotextile Net for Soil Erosion Mitigation". http://www.joaat.com/uploadfile/2016/1230/20161230111218350.pdf Accessed (September 30, 2019)

[6] Echo Inc. "Echo Plant Information Sheet: Tropical Kudzu" ,2019. ECHO 17391 Durrance Rd, N. Fort Myers FL 33917 USA. https://www.echocommunity.org/en/resources/66dc56cc-d33a-417e-b29e-6ebb15caf3b9.pdf. Accessed (September 30, 2019)

Performance of Aerobic Rice Under Different Levels of N-fertilizer Using Surface Irrigation and Drip Fertigation

Abigail R. Barredo[1,2,a], Rubenito M. Lampayan[2,b], Aurelio A. Delos Reyes Jr[2,c], Ronaldo B. Saludes[2,d], Kristine S. Pascual[3,e]

[1]Bureau of Agriculture and Fisheries Engineering, Department of Agriculture, Diliman, Quezon City

[2]College of Engineering and Agro-industrial Technology, University of the Philippines Los Baños, College, Laguna, Philippines

[3]Philippine Rice Research Institute, Munoz, Nueva Ecija, Philippines

[a]arbarredo@up.edu.ph, [b]rmlampayan@up.edu.ph, [c]aadelosreyes2@up.edu.ph, [d]rbsaludes@up.edu.ph, [e]kspascual@exchange.philrice.gov.ph

With the increasing demand for food and a looming water crisis, shifting away from the conventional practice of growing rice in continuously flooded condition, to being partly or even completely aerobic field condition under water-scarce environment, or during period of short drought is very necessary. A system called 'aerobic rice' was developed in which rice is grown in non-puddled and non-saturated soil, just like an upland crop. The target environments for aerobic rice are irrigated lowlands with water shortage and favorable uplands with access to supplementary irrigation[1]. The conventional application of irrigation water on aerobic rice is done by surface "flash" irrigation, and standing water in the field is not desired in each irrigation event. However, the potential use and application of modern irrigation systems like drip fertigation system, for example has not been fully explored for aerobic rice, at least in the Philippines.

The field experiment was conducted at the Block 9 Experiment Station of the University of the Philippines Los Baños during 2021 dry season to evaluate the performance of aerobic rice NSIC Rc222 under different levels of N-fertilizer using surface irrigation (SI) and drip fertigation (DF). It was laid out in a split plot design with irrigation methods (surface irrigation and drip fertigation) as the main plot and four levels of N fertilizer (0%, 50%, 75%, and 100% of Recommended Nitrogen Dose of Fertilization or RNDF) as the subplot. Total RNDF was 120 kg/ha. N was applied in 4 splits at the following stages: 1) at seed sowing, 2) mid-tillering, 3) panicle initiation, and 4) flowering. For balanced fertilization, 40 kg/ha of phosphorus (P) and 40 kg/ha of potassium (K) were applied during seeding (except in N0%). In drip fertigation, Urea fertilizer was dissolved in the separate mixing tank to facilitate drip fertigation at drip lines spaced at 60 cm apart. For surface irrigation treatment, N fertilizer (Urea and Complete) were applied manually along the plant rows based on the fertilizer application schedule. During seeding, seeds were manually dibbled continuously along the furrows at about 7-10 cm depth spaced at 30 cm between rows and were covered with 1-2 cm layer of soil. Irrigation was scheduled every other day from early emergence up to panicle initiation stage in all treatments. The water application frequency was then adjusted to daily application during the panicle initiation up to end of flowering stage; and thereafter, was adjusted back again to every two days until 15 days before harvesting. Surface irrigation was done with flexible hose attached to a water tap.

Results showed that the irrigation method did not significantly affect plant growth parameters such as the plant height, tillering ability and the total above ground biomass of the aerobic rice in the experiment. Similarly, grain yield and yield components (except 1000-grain weight) (Table 1) and water productivity (Table 2) were not also influenced by the irrigation method. Plant height was mainly influenced by the amount of nitrogen fertilizer with highest plant height -observed under N100% RDNF with an average value of 74.7 cm. The average plant height measured under drip fertigated and surface irrigated plots were 70 cm and 69 cm, respectively. Nitrogen treatments significantly affected total above ground biomass, with unfertilized plot (N0%) attaining the lowest biomass (6952.9 kg/ha), while N50% (8264.1 kg/ha), N75% (8483.6 kg/ha), and N100% (8562.6 kg/ha) treatments were similar. This indicated that application of N fertilizer results in higher biomass accumulation, however, 50% application of recommended dose of N fertilizer (in this case 60 kg/ha) was enough to achieve the optimum plant biomass. Harvest Index was greatly influenced by the amount of fertilizer but not by irrigation method. Treatments under N100% and N75% had the highest harvest index of 0.6 kg/kg. Other harvest indices of the remaining treatments ranged from 0.4 kg/kg to 0.5 kg/kg.

Table 1. Yield and yield components.

Treat-ments	No. panicles per m^2	No. spikelets per panicle	% Filled spike-lets	1000-grain weigh t (g)	Yield at 14% MC (kg/ha)
N-level					
N0%	351.7b	45.3b	76.7b	24.0a	3020.4c
N50%	503.3a	50.6b	82.6a	25.0a	4291.9b
N75%	513.3a	51.0ab	79.3ab	25.5a	4771.3ab
N100%	460.0a	61.3a	76.3b	25.1a	4872.0a
Irrigation					
DF	433.3Y	57.8Y	76.4Y	24.1Z	4095.3Y
SI	480.8Y	46.3Z	81.0Y	25.7Y	4382.6Y

In a column , values with the same letter are not significantly at 5% level of probability.

In general, grain yield was significantly affected by the amount of nitrogen fertilizer applied, but not by the irrigation method. Highest grain yield was obtained under the N100% treatments with 4, 872.03 kg/ha (Table 2). The study showed that applying N100% RDNF does not vary significantly from N75% RDNF, just as there were no significant difference between N100% RDNF and N75% RDNF nitrogen treatments.

The total amount of water input under drip fertigation was about 40% lower compared to surface irrigation with values of 783.50 mm and 1181.83 mm, respectively. This implies that 34% of water can be saved using drip fertigation without significantly affecting the crop yield. In terms of the irrigation methods used (drip fertigation and surface irrigation), highest water productivity was attained under drip fertigation system, ranging from 0.36 to 0.59 kg per m^3.

In terms of nitrogen efficiency, partial factor productivity (PFP) was highest at N50% treatments on drip fertigation and surface irrigation with 42.5 kg grain per kg of N applied and 45.2 kg grain per kg of N applied, respectively. Lower levels of PFP indicate less responsive soil or over application of nutrients. On the other hand, high level of PFP suggest that nutrient supply is likely limiting the productivity. Furthermore, agronomic efficiency (AE) was observed highest at N75% treatment under drip fertigation with 14.3 kg grain increase per kg of N fertilizer applied. In surface irrigation AE was observed highest at N50% with 11.8 kg grain increase per kg of N fertilizer applied.

Table 2. Input water productivity.

N Levels	Water Productivity (kg/m^3)		
	Drip Fertigation	Surface Irrigation	Mean
N0%	0.36c	0.28c	0.32
N50%	0.53b	0.b37	0.45
N75%	0.62a	0.40ab	0.51
N100%	0.59ab	0.44a	0.52
Mean	0.53A	0.37B	0.45

In a column, values with the same letter are not significantly at 5% level of probability.

In conclusion, surface irrigation and drip fertigation had no effect on the agronomic and yield performance of aerobic rice, except for the number of spikelets per number of panicles and the 1000 grain-weight, but the different levels of N-fertilizer did. With drip fertigation, water input was reduced by 34% without reducing the yield levels, thus resulted to higher water productivity. Growing aerobic rice either under drip irrigation or surface irrigation only requires about 90 kg/ha of N to get yields above 4000 kg/ha.

KEYWORDS

Aerobic rice, nitrogen use efficiency, water productivity, drip fertigation, surface irrigation

REFERENCES

[1] Bouman BAM, Lampayan RM, Tuong TP. (2007). Water management in irrigated rice: coping with water scarcity. Los Baños (Philippines): International Rice Research Institute. 54 p.

River Improvement Plan for Ungauged Micro Watershed

Allan T. Tejada, Jr. [1,a *], Joseph Daniel Sandoval [2,b]
[1]MS Graduate Fellow, Interdisciplinary Studies Center for Water, School of Environmental Science and Management, University of the Philippines Los Baños, Philippines
[2]PhD Candidate, Water Resources Management Group, Department of Environmental Sciences, Wageningen University and Research, The Netherlands
[a]attejada@up.edu.ph , [b]joseph.sandoval@wur.nl

Hydrologic model have been extensively developed for its application in the study of water resources management scenarios [1–3], assessment on the impacts of future changes in climate and land use [4,5], and design and valuation of river engineering works [6,7]. However, for developing countries, rivers in micro watersheds (<10 km2) are mostly not equipped with stream gauging stations which could limit the proper calibration process of hydrologic model. Recently, interdisciplinary approach by incorporating the experiences and knowledge of flood-affected communities collected through social media posts, field interviews, and surveys were increasingly recognized to address the issue of hydrologic model development for data-scarce watersheds [8–10].

There are different river engineering works that can be implemented to reduce flood damages along the river reaches[11]. These measures are categorized according to its purpose which includes (1) increasing the river flow capacity (2) reducing the peak discharge of the flood, (3) preventing the bank collapse and riverbed degradation, and (4) maintaining the good condition of the river. For this study, we developed hydrologic model for ungauged micro-watershed which we utilized for valuation of river engineering works to increase river flow capacity through one or combination of widening, excavating, and culvert resizing.

MATERIALS AND METHODS

This study considered the ungauged micro watershed in Brgy. Tuntungin-Putho, Laguna with designated outlet at the culvert along IPB road, which covers a total area of 2.81 km2. The methodology framework for the development of hydrologic model, and evaluation of proposed river improvement plan is shown in Figure 1.

RESULTS AND DISCUSSION

The simulated flood levels from the developed hydrologic model show a good resemblance on data on the experiences of the locals during Typhoon Milenyo (2006) and Ondoy (2009), collected from the conducted key-informant interview (KII). The result entails that the used parameters for loss, transform, and routing methods in HEC-HMS are adequate in modeling the watershed's hydrological response to storm events. Furthermore, the discharge (Q, m3/sec) computed at the outlet simulated from HEC-HMS and the classical Rational formula differs 7% at most across return periods (Table 1). Rationale formula is a widely used method by DPWH for hydrologic modeling of watershed smaller than 100 km2 [11].

Table 1. Computed Q (m3/s) in the outlet using HEC-HMS and Rationale Equation

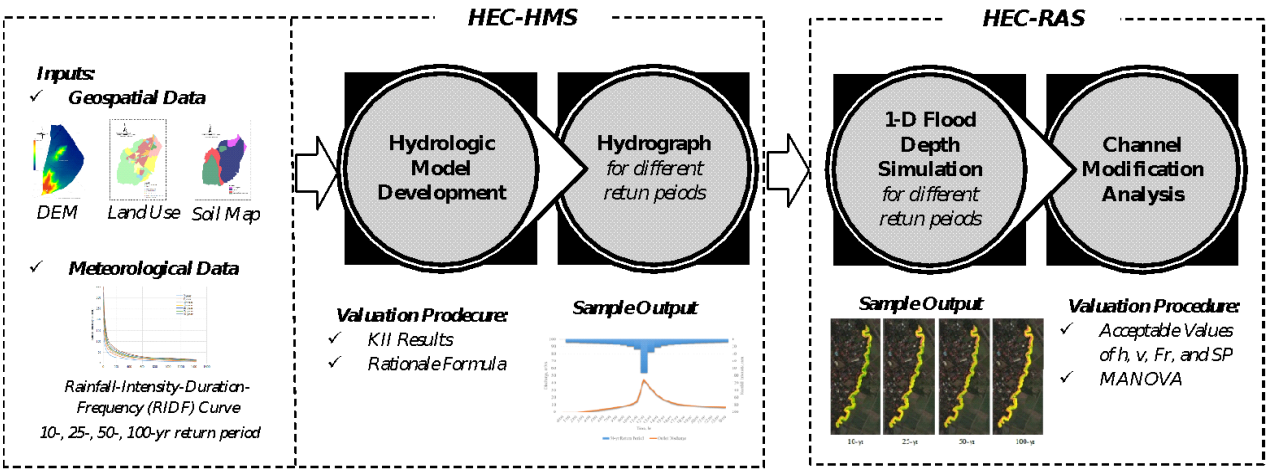

Figure . Methodological Framework of the study

Return Period	HEC-HMS	Rationale
10-yr	30.9	31.6
25-yr	38.6	37.5
50-yr	44.2	42.0
100-yr	49.8	46.3

The developed hydrologic model was then used to simulate a 1-D flood depth map for different storm return periods, which showed that the existing channel cannot convey flood from at least a 10-yr storm (Figure 2).

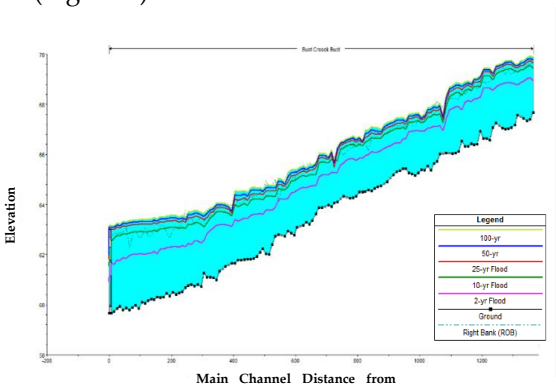

Four river improvement plans through widening and excavating were developed and modeled in HEC-RAS by varying the right-side channel inverse slope and channel roughness. The plans are classified into: Plan A: non-vegetated channel with inverse slope of 1:1.5, Plan B: non-vegetated channel with inverse slope of 1:2, Plan C: riprap with inverse slope of 1:2; and Plan D: non-vegetated channel with inverse slope of 1:2.5. The improvement was based on a 50-yr storm since this design return period is recommended for this kind of engineering work[11]. The results of MANOVA (α=5%) shows that only Plan D has significant difference to the existing cross section in terms of discharge (Q, m3/sec), flood depth (h, m), flow velocity (v, m/s), Froude number (Fr, dimensionless), and shear power (SP, N/m2). Also, among the alternative plans, only Plan D could sufficiently convey the flood of a 50-yr storm without overflowing. Plan D was also able to sustain the permissible value of Fr (0.58) and SP (34.8 N/m2). The simulation also shows that the culvert span located in the outlet should be resized at least 3m compared to its present size of 2.3m to avoid the overflowing in the area during a 50-yr storm.

CONCLUSION AND RECOMMENDATIONS

This study demonstrates the potential of social interview data in the valuation of hydrologic model of ungauged watershed, necessary for proper simulation and assessment of river engineering works. Alteration on specific stages in the development of hydrologic model, consideration of other river improvement strategies, and inclusion of economic analysis may be explored to further improve the study.

KEYWORDS

River Improvement, Ungauged Watershed, Hydrologic Model

ABBREVIATIONS

DPWH – Philippine's Department of Public Works and Highways
HEC-HMS – Hydrologic Engineering Center's Hydrologic Modeling System
HEC-RAS – Hydrologic Engineering Center's River Analysis System
MANOVA – Multivariate Analysis of Variance

REFERENCES

[1] Ella VB . 2016. Simple hydrologic model for predicting streamflow in small watersheds for irrigation system planning. Int Agric Eng J 4: 1-13.

[2] Jaranilla-Sanchez PA, Wang L, Koike T . 2011. Modeling the hydrologic responses of the Pampanga River basin, Philippines: A quantitative approach for identifying droughts. Water Resour Res 3: 1-21.

[3] Singh VP . 2018. Hydrologic modeling: progress and future directions. Geosci Lett 1.

[4] Arceo MGAS, Cruz RVO, Tiburan CL, Balatibat JB, Alibuyog NR . 2018. Modeling the hydrologic responses to land cover and climate changes of selected watersheds in the Philippines using soil and water assessment tool (SWAT) model. DLSU Bus Econ Rev Special issue: 84-101.

[5] Briones RU, Ella VB, Bantayan NC . 2016. Hydrologic impact evaluation of land use and land cover change in Palico Watershed, Batangas, Philippines Using the SWAT model. J Environ Sci Manag 1: 96-107.

[6] Bharath A, Shivapur A V., Hiremath CG, Maddamsetty R . 2021. Dam break analysis using

HEC-RAS and HEC-GeoRAS: A case study of Hidkal dam, Karnataka state, India. Environ Challenges November: 100401.

[7] Abdelal Q, Al-Rawabdeh A, Al Qudah K, Hamarneh C, Abu-Jaber N . 2021. Hydrological assessment and management implications for the ancient Nabataean flood control system in Petra, Jordan. J Hydrol January: 126583.

[8] Malgwi MB, Ramirez JA, Zischg A, Zimmermann M, Schürmann S, et al. . 2021. A method to reconstruct flood scenarios using field interviews and hydrodynamic modelling: application to the 2017 Suleja and Tafa, Nigeria flood. Nat Hazards 2: 1781-1805.

[9] Assumpção TH, Popescu I, Jonoski A, Solomatine DP . 2018. Citizen observations contributing to flood modelling: Opportunities and challenges. Hydrol Earth Syst Sci 2: 1473-1489.

[10] Sy B, Frischknecht C, Dao H, Consuegra D, Giuliani G . 2020. Reconstituting past flood events: The contribution of citizen science. Hydrol Earth Syst Sci 1: 61-74.

[11] DPWH . 2015. DPWH Design Guidelines, Criteria & Standards - Volume 3 – Water Engineering Projects. Dpwh: 1-278.

Water resources development and management in estuaries during infrequent astronomical events

S. Haddout[1a*], K.L. Priya[2b], and Joan Cecilia C. Casila[3c]
[1a]Department of Physics, Faculty of Science, Ibn Tofail University, B.P. 133 Kenitra, Morocco.
[2b]Department of Civil Engineering, TKM College of Engineering, Kollam 691005, India.
[3c]Land and Water Resources Engineering Division, IABE, CEAT, University of the Philippines Los Baños, College, Laguna 4031, Philippine.
[a]soufian.haddout@gmail.com , [b]klpriyaram@gmail.com, and [c]jmcatubigcasila@up.edu.ph

Estuaries, where rivers with fresh water meet the salty open sea, play an essential role in the human-earth system. The estuary serves as a superb habitat for a vast array of plants and animals. Humans rely on estuaries for water, food, leisure, transport, and coastal protection. In addition, estuarine ecosystems are affected by changes in global systems and cycles such as climate and weather cycles. Infrequent events, such as periodical total moon or sun eclipses can affect the water resources in the estuaries.

Salt intrusion in the estuaries reduces the quality of the water used for industrial and agricultural purposes and may result in other environmental problems such as stratification and anoxia of bottom waters due to the trapping of saline water [1] and even sedimentation (e.g., [2]). Hence, salt intrusion length has been used as an environmental standard [3]. The effects of human activities on salt intrusion are of major interest for engineers as well as scientists. Therefore, several analytical, field and numerical studies have been conducted to address this issue worldwide (e.g. [4] and [5]).

The application of a numerical model is not an easy task because the model must be calibrated and verified for each case [6]. For, semi-empirical models, such as those of [7] and [8], are a trade-off between correlation models and numerical models. These models are based on both scaling arguments and field measurements, and therefore have a wider applicability. These equations are even more complicated at predicting intrusion length if data of one parameter is not available or not well estimated. In recent years, several researchers have attempted to use semi-empirical approaches to predict the salinity intrusion in estuaries. Brockway et al. (2006) [9] solved the dispersion equation analytically in simplified conditions to derive a formula for the limit of salt intrusion in the Incomati estuary. As the geometrical characteristics of the Incomati estuary can be explained by exponential functions, they modified the previously presented theories of [10] and [11] to develop their formula. The satisfactory results they obtained indicated that their simplified formula was justified in that case. Gay and O'Donnell (2007) [12] developed a simple model for the longitudinal structure of the salinity in a linearly tapered tidal estuary. They found that the convergence or divergence of the channel had an important effect on the salinity distribution along the estuary.

A number of systematic attempts have been made with varying levels of success to correlate the salt intrusion length to the freshwater discharge/or tidal range based on measurements of the salinity structure (e.g. [13] and [14]).

A nonlinear multiple regression analysis, which incorporated both driving variables tide range and river flow were used in this work; and this formula is more effective at predicting intrusion length in site-specific during astronomical event.

Study area

The Bouregreg estuary is located in northwestern part of Morocco, stretching about 240 km from its source in the Middle Atlas Mountains to the Atlantic Ocean. The Bouregreg estuary is located on the Atlantic between the two cities Rabat and Sale 34N and 650'W (Figure 1). It has a length of 23 km, limited by the dam of Sidi Mohammed Ben Abdellah and an average width of 150 m. Its average freshwater flow varied from 3–84 m^3s^1. Additionally, the tide near the estuary mouth is mainly semi-diurnal with a 44,100 s tidal cycle and is a meso-/micro-tidal estuary an average tidal range of only 2.3 m [15, 16]. The stratification parameter was less than 0.55 indicating that this estuary is well-mixed generally and partially stratified in some cases [15, 16].

Figure 1. Map showing Bouregreg estuary (Morocco). Image is taken from Google Earth.

Data collection

The Super Blue Blood Moon on (31 January 2018) and Total Solar eclipse on (21 August 2017) were investigated at 7-stations (S1->S7, see Fig.1). Results showed that during these phenomena, the gravitational pull on the ocean was strong, so the high water was at its highest point and the low water at its lowest point. Water level rise affects the hydrodynamic balance and can increase salt water intrusion into the river estuaries, causing many ecological problems.

Although there may be some stratification in the estuaries during normal condition, the hydrodynamic and salinity distribution responses of the estuaries under the effects of the extreme events were evaluated only under the well-mixed condition.

Development of an equation for the salt intrusion length during infrequent events

A simple equation that can consider is the variability of the governing parameters assuming constant depth, roughness, tidal period and density difference is as follows (see [2] and [17]):

$$L^{HWS} = g[Q, H] \quad (1)$$

The parameters involved in the intrusion length were correlated through dimensional analysis. The most important dimensionless parameters were found to be $Q/A\sqrt{g\underline{h}}$ and H/h (see [14]) where $h = h_0$ is water depth, A is the area of the cross- section, and g is the gravity acceleration. Equation (1) may be reduced in terms of a set of dimensionless parameters as:

$$\frac{L^{HWS}}{\underline{h}} = g\left[\frac{Q}{(A\sqrt{g\underline{h}})}, \frac{H}{(\underline{h})}\right] \quad (2)$$

To include the effects of astronomical phenomena's in pervious formula (2), h can be defined as $h = h_0 + h_{Astronomical\ events}$. A power law form may be expressed as:

$$\frac{L^{HWS}}{\underline{h}} = a\left[\left(\frac{Q}{(A\sqrt{g\underline{h}})}\right)^{b}\left[\frac{H}{(h_0+h_{Astronomical\ events})}\right]^{c}\right] \quad (3)$$

where a is the coefficient and b and c are the exponents of the equation. To develop the relationship between dimensionless parameters, the numerical model (HEC-RAS Model) was used to simulate several conditions with different river flow and tidal ranges. Then, the obtained results were used as the data set of salt-intrusion lengths to develop the empirical formula. The following formula was obtained by nonlinear multivariable regression:

$$\frac{L^{HWS}}{\underline{h}} = 643.32\left[\left(\frac{Q}{(A\sqrt{g\underline{h}})}\right)^{-0.46}\left[\frac{H}{(h_0+h_{Astronomical\ events})}\right]^{0.80}\right] \quad (4)$$

Eq.4 can be used as a rapid assessment tool to assist managers in decision-making processes in the Bouregreg estuary during astronomical events.

KEYWORDS

Estuaries, Infrequent events, Salt intrusion length, Equation development.

REFERENCES

[1] Kurup R and Hamilton D (2002) Flushing of dense, hypoxic water from a cavity of the Swan river estuary, Western Australia. Estuaries 25(5): 908–915.

[2] Etemad-Shahidi A, Afshar A, Alikia H, Moshfeghi H., (2009). Total dissolved solid modeling; Karkheh reservoir case example.Int J Environ Res 3:671-680.

[3]Schubel JR (1992) Managing Freshwater Discharge to the San Francisco Bay/Sacramento–San Joaquin Delta Estuary: The Scientific Basis for an Estuarine standard. Report to the EPA, Sacramento, CA, USA.

[4]An Q, Wu Y, Taylor S and Zhao B (2009) Influence of the three gorges project on saltwater intrusion in the Yangtze River estuary. Environmental Geology 56(8): 1679–1686.

[5]Etemad-Shahidi A, Dorostkar A and Liu WC (2008) Prediction of salinity intrusion in Danshuei estuarine system. Hydrology Research 38(5): 497–505.

[6]Haddout, S., & Maslouhi, A. (2018). One-Dimensional hydraulic analysis of the effect of sea level rise on salinity intrusion in the Sebou estuary, Morocco. Marine Geodesy, 41(3), 270-288.

[7]Rigter, B.P., 1973. Minimum length of salt intrusion in estuaries.Journal of theHydraulic Division, Proceedings of ASCE 99, 1475-1496.

[8] Fischer, H.B., 1974. Discussion of 'Minimum length of salt intrusion in estuaries' by B.P. Rigter, 1973. Journal Hydraul. Div. Proc. 100, 708-712.

[9] Brockway, R., Bowers, D., Hoguane, A., Dove, V., Vassele, V., 2006. A note on salt intrusion in funnel-shaped estuaries: Application to the Incomati estuary, Mozambique. Estuarine, Coastal and Shelf Science, 66(1), 1-5.

[10]Prandle, D., 1982. "Estuarine circulation patterns." Journal of Physical Oceanography 11: 1311-1324.

[11] Savenije, H.H.G. 1986.A one-dimensional model for salinity intrusion in alluvial estuaries. Journal of Hydrology, 85 (1–2), pp.87-109.

[12] Gay, P.S., O''Donnell, J., 2007. A simple advection-dispersion model for the salt distribution in linearly tapered estuaries.Journal of Geophysical Research, 112(C7), C070201.doi:10.1029/2006JC003840.

[13] Monismith, S.G., Kimmerer, W., Burau, J.R., Stacey, M.T., 2002. Structure and flow- induced variability of the subtidal salinity field in northern San Francisco Bay. Journal of Physical Oceanography 32, 3003-3019.

[14] Parsa J, Etemad-Shahidi A., (2011).An empirical model for salinity intrusion in alluvial estuaries. Ocean Dyn 61:1619-1628.

[15]Haddout, S. (2020). A power-law multivariable regression equation for salt intrusion length in the Bouregreg estuary, Morocco. Marine Georesources & Geotechnology, 38(4), 417-422.

[16]Priya, K. L. A., Haddout, S., & Casila, J. C. C. (2022). Implications of turbulent shear on clay floc break-up along the Atlantic estuary (Bouregreg), Morocco. International Journal of Sediment Research, 37(2), 248-257.

[17]Etemad-Shahidi, A., Rohani, M. S., Parsa, J., & Lemckert, C. (2015). Effects of sea level rise on the salinity of Bahmanshir estuary. International journal of environmental science and technology, 12(10), 3329-3340.

Computational Fluid Dynamics Simulation of Aerosol Particle Transport in Stored Product Facilities

Fei Xyza B. Asuncion
Carl and Melinda Helwig Department of Biological and Agricultural Engineering
Kansas State University - Manhattan, Kansas, USA
fxbasuncion@ksu.edu

ABSTRACT

Aerosol insecticides have become widely used as methyl bromide replacements to control stored product insects in flour mills, rice mills, and other food facilities. The effectiveness of aerosol application for insect control requires knowing the spray characteristics of the equipment to be used and understanding factors that influence particle transport, spatial distribution, and deposition. While it is a challenge to assess the relationship of the physical and aerodynamic factors affecting aerosol efficacy, computational fluid dynamics (CFD) is one approach to optimize aerosol application. Through a discrete phase model developed in ANSYS FLUENT 20.1, simulations were conducted to predict the airflow, track pyrethrin droplets of various sizes, and determine their deposition onto Petri dishes located in a controlled chamber. Deposition efficiency was calculated as a measure of aerosol efficacy. Results showed that the predicted deposition increased with increasing droplet size largely due to inertial and gravitational effects. With the proper computational domain and boundary conditions that best represent the actual experimental setup, and selecting the appropriate numerical solution, a CFD model developed in ANSYS can predict the behavior of different factors affecting the air and particle flow. Results of the simulations could be used for determining the optimum operating conditions and improving aerosol application techniques for stored product insect control.

KEYWORDS

Aerosol insecticide, particle deposition, ANSYS FLUENT, computational fluid dynamics (CFD), stored product insect

GIS-Based Mapping of Appropriate Soil Texture-Based Four-Wheel Tractor Power Ratings in the Philippines

Rossana Marie C. Amongo[1, a *], Ronaldo B. Saludes[2,b], Ralph Kristoffer B. Gallegos,[1,c] Patrick Lemuel P. Relativo[2,d] , Adrian Daniel L. Pantano.[1,e] , Ria Salustia d.G. Duminding[1,f], Gherlee Nelle L. Lalap-Borja[1,g], and Julius John Paul A. Cunan[1,h]

[1]1Agribiosystems Machinery and Power Engineering Division, Institute of Agricultural and Biosystems Engineering, College of Engineering and Agro-Industrial Technology,
University of the Philippines Los Baños, College, Los Baños, Laguna, Philippines

[2]Agrometeorology, Bio-structures, and Environment Engineering Division, Institute of Agricultural and Biosystems Engineering, College of Engineering and Agro-Industrial Technology,
University of the Philippines Los Baños, College, Los Baños, Laguna, Philippines

[a]rcamongo@up.edu.ph , [b]rbsaludes@up.edu.ph , [c]rbgallegos@up.edu.ph, [d]pprelativo@up.edu.ph, [e]alpantano@up.edu.ph , [f]rdduminding@up.edu.ph , [g]gllalap@up.edu.ph , [h]jacunan@up.edu.ph

Under-utilization of Agricultural Mechanization Technologies (AMTs) is one of the challenges in the current Philippine agricultural mechanization setting. The National Agri-fisheries Investment Audit Team (NAFIAT), a project spearheaded by the Department of Agriculture-Bureau of Agricultural and Fisheries Engineering (DA-BAFE), reported cases of under-utilized agricultural machines because of mismatches of power ratings with what is required based on the end-user's farm characteristics [1]. Hence, there is a need for the provision of AMTs that fits the three dimensions of technology appropriateness namely technical, environmental, and socio-cultural. For agricultural tractors, some environmental factors that affect machine performance include the slope of land and the soil textural classification, which dictates the draft that the tractor must be able to overcome in order to perform a successful tillage operation. Hence, there is a need to determine which tractor power rating is matched with the farm conditions and configurations, along with the machine's technical specifications and the preference of the end-users. This paper presents the development of a protocol for the appropriateness of tractor power in rice production areas using Geographic Information System (GIS) and machine test data.

The Multiple Criteria Decision Analysis (MCDA) procedure was applied in the appropriateness mapping of agricultural tractors in lowland rice production areas with slope, road proximity, and flood risk of the area as the identified environmental factors. The criteria for each factor shown in Table 1 were determined based on past studies while the relative weights were calculated by applying the Analytical Hierarchy Process (AHP) [2]. Spatial data for slope, road networks, flood risk, and delineated rice areas were generated using the Interferometric Synthetic Aperture Radar (IFSAR), OpenStreetMap, Light Detection and Ranging (LIDAR), and C-band Synthetic Aperture Radar (SAR) images, respectively.

Tractor sizing was done by computing the soil specific draft using Equation 1 for each of the soil textural classification. The computation was based on the test results for four-wheel tractors mounted with a 3-bottom disk plow running for at most 8 kph. Appropriateness mapping of the tractor power was done based on three criteria, marginally appropriate, moderately appropriate, and highly appropriate areas.

Table 1: Criteria considered in the appropriateness of agricultural tractors.

Factor	Weight (%)	Description	Appropriateness scale
Slope	65	< 4 deg	2
		4 - 8 deg	1
		> 8 deg	0
Road Network proximity	15	< 100 m	2
		100-200 m	1
		> 200m	0
Flood hazards	20	Low risk	2
		Moderate risk	1
		High and very high risk	0

$$D_s = S_D \times w \times d\ (kg) \quad (1)$$

Equation 1: Formula for soil specific draft

Where:
D_s is the soil draft, kg
S_D is the specific draft, kg/cm²
w is the effective width of cut of implement, cm
d is the depth of cut of the implement, cm

Results of the tractor power rating computation for each soil textural classification show that sandy and sandy loam soil have the lowest power requirements of 19 kW (25 hp) while dry adobe yielded the highest value of 97 kW (130 hp). The sample tractor appropriateness map of Capiz province, Philippines presented in Figure. 1 shows the appropriate tractor power ratings in rice production areas. Majority of the areas are appropriate for standard light tractors of 25 kW – 37 kW (33hp – 49 hp) and standard medium tractors of 52 kW- 66 kW (70 hp-89 hp).

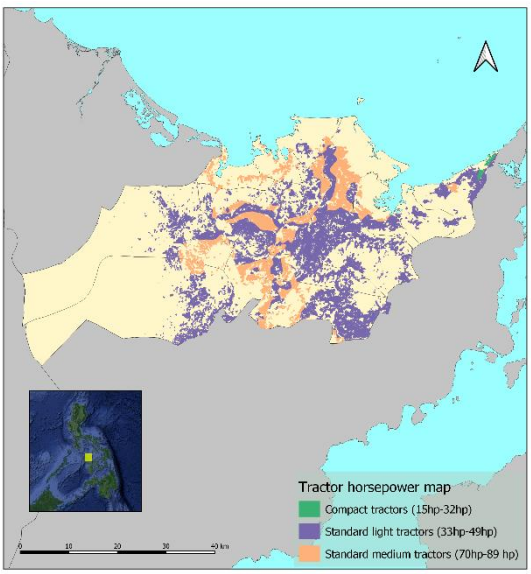

Fig. 1: Tractor power rating map of Capiz province, Philippines.

The results of the study show that GIS and remote sensing are effective tools in the development of protocol for appropriate tractor power ratings in rice production areas based on environmental considerations. Moreover, the results of the study can aid in decision-making and planning process in the selection of appropriate AMTs to achieve sustainability of agricultural mechanization that fits all aspects of technology appropriateness.

KEYWORDS

Four -wheel tractor, Tractor power rating, Soil Texture Classification, GIS and Remote sensing

REFERENCES

[1] Department of Agriculture - Bureau of Agricultural and Fisheries Engineering (DA-BAFE). (2020). (Contributing authors: Resurreccion, A.N., Amongo, R.M.C., Fajardo, A.L., Gavino, R.M., Eusebio, R.E., Panagsagan, J.R., Sibulo II, N.A.M., Tamayo, R.H., Domingo, V.L., Brampio, E., Nevares, D.M., Ditarro, C.D., Adriatico, D.E., Nebres, N., Polido, C.C.P., Rosas, R.M.R., Carpio, N.L., Limbo, M.T.A, Antenor, A.E.A, Dizon, P.J.S., and Marticio, K.I.S.). Nationwide Agri-Fisheries Investment Audit First Phase Consolidated Report.

[2] Saaty, T.L. (1980). The Analytic Hierarchy Process. McGraw-Hill, New York.

Level of Mechanization of the Rice and Corn Production and Post-Production Systems in Region IV

Rossana Marie C. Amongo[1, a *], Maria Victoria L. Larona[2,b], Ralph Kristoffer B. Gallegos[1,c], Mark Keylord S. Onal[1,d], Ronnie C. Valencia[2,e], Kit Ignatius S. Marticio[1,f], Andrea Elaine A. Antenor[1,g], Paul John S. Dizon[1,h], David L. Bondoc[1,i], Renz Kevin R. Ilagan[1,j], Gherlee Nelle L. Borja[1,k], Ria Salustia D. Duminding[1,l]

[1]Agribiosystems Machinery & Power Engineering Division, Institute of Agricultural & Biosystems Engineering,
[2]Center for Agri-Fisheries and Biosystems Mechanization
College of Engineering and Agro-Industrial Technology, University of the Philippines Los Baños,
College, Los Baños, Laguna, Philippines

[a]rcamongo@up.edu.ph, [b]mllarona@up.edu.ph , [c]rbgallegos@up.edu.ph , [d]msonal@up.edu.ph , [e]rcvalencia1@up.edu.ph , [f]ksmarticio@up.edu.ph , [g]aaantenor1@up.edu.ph , [h]psdizon1@up.edu.ph , [i]dlbondoc@up.edu.ph , [j]rrilagan@up.edu.ph, [k]gllalap@up.edu.ph , [l]rdduminding@up.edu.ph

The level of agriculcultural mechanization is considered as one of the bases of agricultural mechanization intervention for the development of the agri-fisheries sector. Various studies have been conducted in determining the level of agricultural mechanization in the past years, however, there have been no standardized procedure in determining the level of mechanization in the Philippines. In 2017, the Department of Agriculture adopted a unified measurement of the level of mechanization in the country through the Modified Agricultural Mechanization Index (MAMI) as stipulated in DA Memo No. 17-076 to 078. Several parameters were considered in the formulation of MAMI as shown in Figure 1. The Southeast Asian Regional Center for Graduate Study and Research in Agriculture (SEARCA) in collaboration with the Philippine Council of Agriculture and Fisheries (PCAF) utilized the MAMI in the conduct of their study on the intensive use of machineries in rice, corn, cassava and coffee production in the selected regions in the Philippines[1]. This paper presents the assessment of the level of agricultural mechanization in Region IV to establish the agricultural mechanization index per province using a standard methodology /protocol.

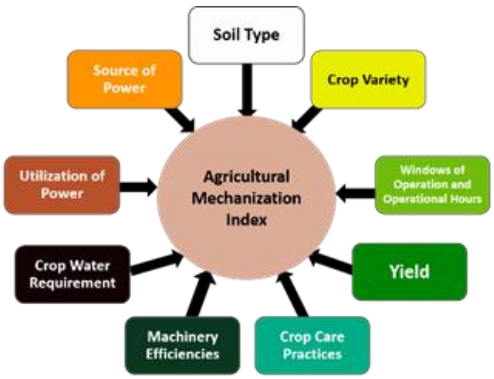

Figure 1. Parameters in the calculation of MAMI

The Modified Agricultural Mechanization Index (MAMI) developed by Amongo et al., (2017)[2], Amongo et al., (2018)[3] was used in determining the level of mechanization in each province of Region IV. The theoretical or ideal AMI for the rice and corn production systems were computed based on the utilization of prevalent agricultural mechanization technologies (AMTs) in the country for the rice and corn farm production operations such as land preparation operations (plowing and harrowing), crop establishment, crop care, harvesting, drying, hauling, and milling operations. The actual agricultural mechanization index was computed using Equation 1. Moreover, survey instruments were developed for the assessment of rice and corn production systems.

$$MAMI = \frac{1}{Window} \times \sum \left(\frac{\left(P_{source} + \left(P_{man} \times n_{operator}\right)\right) \times T}{Area \times t_{source}} \right) \quad (1)$$

Where:
MAMI is the Modified Agricultural Mechanization Index of the crop, ha/hp
P_{source} is the power source (machine/animal/man), hp
P_{man} is the power of man, hp
$n_{operator}$ is the number of operator
t_{source} is the time of operation of power source, h
Window is the window of operation of the whole province, days
Area is the total coverage area, ha
T is the total time to finish the operation in a given area, h

Tables 1 and 2 show the level of mechanization per province and per crop for Regions IV-A and IV-B, respectively. Table 1 indicates that Quezon has the highest level of mechanization for rice production

system with 3.01 hp/ha while Batangas has the highest mechanization index for corn production systems with 2.50 hp/ha. Rizal (1.62 hp/ha) and Cavite (1.40 hp/ha) had the lowest mechanization index in Region IV-A for rice and corn, respectively. Table 2, on the other hand, Mindoro Occidental (3.66 hp/ha) and Mindoro Oriental (5.26 hp/ha) had the highest computed mechanization level for rice and corn production systems in Region IV-B, respectively. Meanwhile, Romblon had the lowest mechanization level in Region IV-B for both rice (1.53 hp/ha) and corn (0.51 hp/ha). Region IV-A had an average agricultural mechanization index of 2.48 hp/ha for rice and 1.93 hp/ha for the corn production system. Region IV-B had an average mechanization level of 2.67 and 2.64 hp/ha for rice and corn production systems, respectively.

Table 1. Level of mechanization per province in Region IV-A.

Province	Level of Mechanization (hp/ha)	
	Rice	Corn
Cavite	2.14	1.40
Laguna	2.87	1.52
Batangas	2.74	2.50
Rizal	1.62	2.12
Quezon	3.01	2.10
Min Value	**1.62**	**1.40**
Max Value	**3.01**	**2.50**
Average Value	**2.48**	**1.93**

Table 2. Level of mechanization per province in Region IV-B.

Province	Level of Mechanization (hp/ha)	
	Rice	Corn
Mindoro Occidental	3.66	3.63
Mindoro Oriental	2.84	5.26
Marinduque	1.75	1.68
Romblon	1.53	0.51
Palawan	3.54	2.14
Min Value	**1.53**	**0.51**
Max Value	**3.66**	**5.26**
Average Value	**2.67**	**2.64**

Tables 3 and 4 show the level of mechanization per farm operation and per crop in Regions IV-A and IV-B, respectively. For Region IV-A, harvesting operation had the widest range of level of mechanization for rice with 0.47-1.79 hp/ha while for the corn production, land preparation has the largest range with 0.62-1.420 hp/ha. Region IV-B had similar trend as Region IV-A where harvesting (0.69-2.42 hp/ha) and land preparation (0.21-3.29 hp/ha) also had the widest range of mechanization index for rice and corn productions systems, respectively. Irrigation and crop care operations had the smallest range of mechanization index in Region IV since most of the farm areas surveyed were rainfed and the application of fertilizers and pesticides was usually done manually.

Table 3. Level of mechanization per farm operation in Region IV-A.

Operation	Level of Mechanization per farm operation (hp/ha)			
	Rice		Corn	
	Range	Ave.	Range	Ave.
Land Preparation	0.86-1.47	1.16	0.62–1.42	1.04
Crop Establishment	0.03-0.08	0.06	0.04–0.24	0.12
Crop Care	0.02-0.04	0.02	0.01–0.02	0.01
Irrigation	0-0.03	0.01	0	0.00
Harvesting	0.47-1.79	1.14	0.05–0.24	0.12
Hauling	0.02-0.1	0.07	0.04–0.15	0.09
Drying	0.01-0.05	0.02	0.05–0.41	0.26
Shelling	-	-	0.11-0.59	0.29

Table 4. Level of mechanization per farm operation Region IV-B.

Operation	Level of Mechanization per farm operation (hp/ha)			
	Rice		Corn	
	Range	Ave.	Range	Ave.
Land Preparation	0.57-1.33	0.85	0.21-3.29	1.25
Crop Establishment	0.03-0.08	0.06	0.05-0.30	0.14
Crop Care	0.01-0.06	0.03	0.01-0.03	0.02
Irrigation	0-0.02	0.01	0-0.02	0.01
Harvesting	0.69-2.42	1.41	0.04-0.69	0.39
Hauling	0.04-1.01	0.29	0.04-1.29	0.56
Drying	0.02-0.04	0.03	0.02-0.15	0.05
Shelling	-	-	0.09-0.52	0.23

The results show that determining the level of mechanization is crucial in identifying the mechanization requirements or gaps in the region. Furthermore, this study can be a useful tool in determining which province/s and farm operation needs to be prioritized for mechanization for an effective and efficient distribution of agricultural machinery in the Region.

KEYWORDS

Level of mechanization, agricultural mechanization, MAMI, mechanization index and Region IV.

REFERENCES

[1] Southeast Asian Regional Center for Graduate Study and Research in Agriculture (SEARCA). (2019). (Contributing authors: Amongo, R.M.C., Del Rosario,

A.C., Larona, M.V.L., Rodulfo, Jr. V.A., Duminding, R.S.DG., Salandanan, A.D., Bondoc, D.L., and De Padua, V.A.N.). Intensive Use of Mechanized Technology in the Agriculture Sector: An Evaluation of the Effects and Implications in Selected Commodity Value Chains. Ed: Landicho, N.M. Project Funded by the Department of Agriculture – Philippine Council for Agriculture and Fisheries (DA-PCAF).

[2] Amongo, R.M.C., M.V.L. Larona, M.K.S. Onal, C.I.L. Ilao, G.N.L. Lalap, L.E. Oguis, and P.B. Melendez. (2017). Determination of Mechanization Index in Selected ASEAN Countries. Technical Paper presented during the 14th International Conference and 67th PSAE Annual National Convention. Legazpi City Convention Center, Legazpi City, Albay. 23-29, April 2017.

[3] Amongo, R.M.C. Onal, M.K.S., Larona, M.V.L., Fajardo, A.L., Ilao, C.I.L., Lalap, G.N.L, Borja, A.A., Deniega, C.G.V., and Sumague, J.V. (2018). Level of Agricultural Mechanization in Oriental Mindoro, Laguna and Quezon, Philippines Using the Modified Agricultural Mechanization Index for Lowland Rice. Philippine Journal of Agricultural and Biosystems Engineering (PJABE), 14, 55-70.

Process Simulation of a Multi-Pressure Ethanol Distillation System Using Aspen Plus ® Software

Eros Paul V. Estante [1,a *], Rex B. Demafelis [1,b], Manolito E. Bambase, Jr.[1, c], Butch G. Bataller[1, d], and Bernadette T. Magadia[1, e]

[1]Department of Chemical Engineering, College of Engineering and Agro-Industrial Technology, University of the Philippines Los Baños, College, Laguna, Philippines 4031

[a]evestante@up.edu.ph, [b]rbdemafelis@up.edu.ph, [c]mebambase@up.edu.ph, [d]bgbattaler@up.edu.ph, [e]btmagadia@up.edu.ph

In a bioethanol plant, energy cost presents significant item in the plant's operating cost. Energy costs, combined with raw material acquisition make up to 85% of the operating cost. Out of all energy costs, 75% is related to steam production [1]. Distillation is more energy consuming than the other process and the product obtained at this process directly affects the performance of the dehydration [2].

Distillation column is expected to operate for more than 30 years. Thus, replacement of an existing column for energy reduction alone is not reasonable due to higher investment cost. The most feasible approach to improve performance is by retrofitting plant's existing distillation columns.

Small changes that require minimum capital investment in the existing distillation set-up can produce great benefits. One of which is changing the feed tray location in the distillation column [3]. In real-life distillation column, the current feed tray may not be positioned to its optimal location. Finding the optimum feed tray location could save the processing plant from large reboiler duties and can also increase the product recovery.

One way to optimize plant process to improve and attain optimum performance of a distillation process is through simulation and control studies. It uses more profound techniques of analysis and synthesis while reducing risk of rework in plant. One of the widely used simulation software for plant processes worldwide is Aspen Plus ® by AspenTech.

In this study, the current bioethanol distillation set-up was simulated using Aspen Plus ® software from the data gathered in the bioethanol plant. Two scenarios were then established: Scenario 1: locating the optimum feed tray location for lowest reboiler duty at the same product recovery and purity and Scenario 2: locating the optimum feed tray location for highest product recovery at the same reboiler duty and product purity. Rigorous simulation in Aspen Plus ® was conducted by varying the feed tray location in the distillation to find the optimum feed tray location from the two scenarios established. Financial assessment of the optimized process from the two scenarios was then compared to the existing distillation set-up.

Figure 1 shows the distillation process overview of the rectifier column of the bioethanol refinery under study.

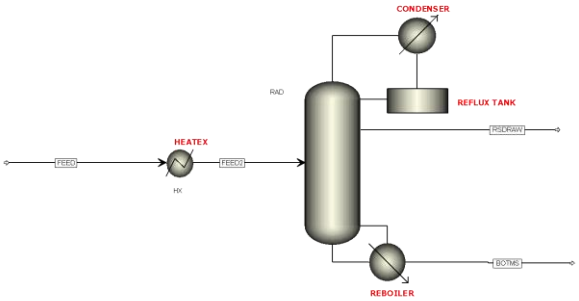

Fig. 1. Rectifier column process

Feed with 10-15 % v/v ethanol from extractive distilling column is preheated from 95 deg C to 110 °C before entering the rectifier column where it is concentrated to 95 % v/v EtOH and is drawn on the RS Draw (Distillate) stream. The bottoms product, known as spent lees is drawn at the bottom of the column.

Table 1 shows the comparative financial analysis for Scenario 1. Optimum feed tray for this set up was located at feed tray 69.

Table 1. Comparative financial analysis for the optimum feed tray location for scenario 1.

	Unit	Plant Data	Optimized Case
Feed Tray Location (from the top)		54	69
Daily Ethanol Production (95%)	m3/day	114.03	114.03
Reboiler Duty	kW	4500.00	4239.39
Decrease in Reboiler	%		5.79%

Duty			
Annual Energy Cost	Php/year	12,512,699.46	11,130,034.63
Energy Cost per Liter (Distillation)	PhP/L	0.32	0.29
Annual Savings due to Decrease in Energy Cost	Php/year	1,382,664.83	
% Increase in Net Income	%	0.06%	

Based on the table above, reduction of reboiler duty about 5.79% resulted to a decrease in energy cost due to consumption of coal from 0.32 PhP/L to 0.29 PhP/L. This resulted to an annual savings of PhP 1,382,664.83 due to decrease in cost of energy production. Increase in net income from this savings is 0.06% from the current distillation process.

Shown in Table 2 is the comparative financial analysis for Scenario 2. The highest product recovery was located at feed tray 60 where 99.9997% of ethanol was recovered from the feed.

Table 2. Comparative financial analysis for the optimum feed tray location for scenario 2.

	UNIT	**PLANT DATA**	**OPTIMIZED CASE SCENARIO**
Feed Tray Location (from the top)		54	60
Daily Ethanol Production (95%)	m3/day	114.03	117.56
Increase in Ethanol Volume		3.10%	
Additional Net Income per Year due to Increase in Ethanol Volume	Php/year	67,872,375.72	
% Increase in Net Income	%	3.00%	

Based on the Table 2, it shows that an increase in product recovery by about 3.10% from the optimized case would result to an increase in annual net income per year of Php 67,872,375.00.

This means optimizing feed tray location for higher product recovery would yield greater financial gain in terms of increase in income due to increase in distillate recovery.

It is recommended to explore other parameters and its effect in locating the optimum tray location such as the treating the feed ethanol concentration, feed rate, and feed condition as variable to further study the dynamics of the distillation column. Other parameters can also be explored in the optimization of the distillation plant such as exploring the effect of operating pressure and pressure drop in the distillation process, and addressing a number of operational problems leading to reduction in energy efficiency and product recovery such as fouling, defective column internals, and the inefficiency of the insulation of the equipment.

KEYWORDS
process simulation, feed tray optimization, distillation, bioethanol

REFERENCES

[1] Budimir, N. J., Jarić, M. S., Jaćimović, B. M., Genić, S. B., & Jaćimović, N. B. (2011). Rectified ethanol production cost analysis. Thermal Science, 15(2), 281–292.

[2] Bastidas, P., Parra, J., Gil, I., & Rodríguez, G. (2012). Alcohol distillation plant simulation: Thermal and hydraulic studies. Procedia Engineering, 42(December 2012), 80–89.

[3] Pendergast, J., Jewell, D., Vickery, D., & Bravo, J. (2018). Save energy in distillation. Chemical Processing, 80(4), 16–21.

Rice Monitoring and Yield Estimation in Dumangas, Iloilo, Philippines Using Satellite Imagery

Kezia Shem G. Brusola[1, a *], Moises A. Dorado[1,b], Marion Lux Y. Castro[1,c], and Pompe C. Sta. Cruz[2,d]
[1]Agrometeorology, Bio-structures and Environment Engineering Division, Institute of Agricultural and Biosystems Engineering, College of Engineering and Agro-Industrial Technology,
University of the Philippines Los Baños, College, Laguna, Philippines
[2]Crop Science Cluster, College of Agriculture and Food Science,
University of the Philippines Los Baños, College, Laguna, Philippines
[a]kgbrusola@up.edu.ph, [b]madorado@up.edu.ph, [c]mycastro@up.edu.ph, [d]pcstacuz@up.edu.ph

Traditional monitoring practices can be costly and tedious. There is a need to set up near-real-time and site-specific agricultural monitoring and yield forecasting techniques for the use of agricultural technicians, officers, and decision-makers in the local government unit in estimating in production. Since there is no yield estimation before the harvest season in Dumangas, spatial information in yield modeling on a barangay level was explored. The output of this study can serve as an essential tool when integrated with the traditional methods used in monitoring.

This study aims to assess the status of the standing rice crops in the area by using SARAI-Enhanced Agricultural Monitoring System (SEAMS) methodology, determine the threshold for Normalized Difference Vegetation Index (NDVI) per crop stage using the Ground Control Points (GCP) and Sentinel 2 data, and conduct rice yield simulation by integrating remotely sensed data into the Agricultural Production Systems Simulator (APSIM).

NDVI is used to monitor crop health. It shows the photosynthetic behavior of the plant and the change through time due to the physiological development of the crop [1]. The value ranges from -1 to 1, where lower than 0.1 depicts water and snow, moderate values from 0.2 to 0.5 show sparse vegetation and senescing plants, and high values above 0.6 are highly vegetative with peak and healthy vegetation [2]. NDVI is significantly correlated to green biomass yield [3]. Different wavelengths have specific effects on the plant pigments. The plant absorbs the visible light spectrum while the leaves' near infrared light (NIR) is reflected [2]. Equation 1 shows the formula of NDVI.

$$NDVI = \frac{NIR - Red}{NIR + Red} \qquad (1)$$

To determine the area with standing crops and growth stage for the 2nd and 3rd cropping of 2020, NDVI was computed monthly using the optical satellite Sentinel 2 and the scenario observed in the field by the agricultural technicians of Dumangas. The method utilized for the analysis was based on the NDVI threshold of greater than or equal to 0.3 for areas with standing crops established by SEAMS, a component of Smarter Approaches to Reinvigorate Agriculture as an Industry in the Philippines or Project SARAI, which maximizes free and open-source satellite technology in developing efficient agricultural monitoring techniques, weather forecasts, and disaster risk management methods.

For the phenology analysis of the 20 GCP during the seasons of interest, the NDVI graph for each point was plotted. The phenological parameters[4] were determined from the graph as seen in Fig. 1. The selection of the values of these parameters depended on the clearest available satellite data and the on-field observation derived from SEAMS Image Capturing Application (SICApp). Analyzing the phenological metrics, the range of NDVI for different growth stages was determined.

APSIM crop simulation model was used for yield modeling. Rice yield data during the 2019 cropping season per barangay was used for testing the validity of APSIM along with the site-specific inputs derived from satellite and the management practices being done in the field.

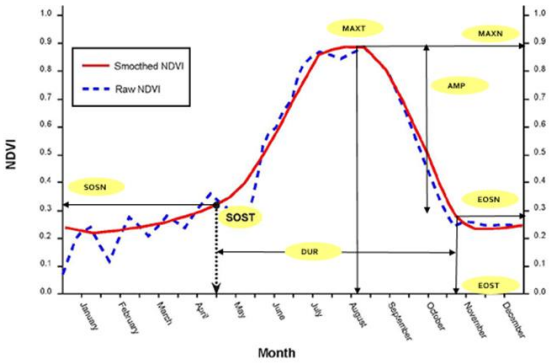

Fig 1. Phenological metrics from NDVI

Based on the NDVI analysis, 2nd cropping, which usually begins in September [5], started in October because of the delayed planting during the previous

season and it was harvested in January 2021. Meanwhile, 3rd cropping lasted from February to April 2021. However, it was noted that three barangays - Bolilao, Nanding Lopez, and Dacutan, did not plant rice during this season because of inadequate irrigation supply as informed by the agricultural technicians. It was beneficial because the satellite can detect vegetation changes even though rice is not planted in the area. Based on the crop duration, the usual variety planted in the area was hybrid with around 85 to 100 days period. The NDVI range for each crop stage was determined as presented in Fig. 2. The seedling stage ranged from 0.163 to 0.309. The vegetative stage varied from 0.35 to 0.682. The reproductive stage had values from 0.535 to 0.671. The maturity or ripening stage went from 0.235 to 0.533. Lastly, harvested areas had observed values from 0.2075 to 0.237. The overlap between the range of vegetative and reproductive stages indicated that the maximum NDVI was observed during the transition of vegetative to reproductive stage, probably in the late vegetative stage[6]. From the results, the methodology established by SEAMS was analyzed to be a functional and easy way of investigating the characteristics of the vegetation in the area as well as its spatial distribution.

For yield modeling, APSIM was promising in predicting rice yield because it included most of the necessary input parameters in its system. The simulation produced good values with high correlation during the 1st cropping of 2019. However, barangays were identified to have consistently low yield predictions throughout the cropping seasons. It was concluded that there might be an inaccuracy in the soil inputs obtained from the satellite. Underestimation and low yields were simulated for the cropping seasons with limited water availability. Further exploration of the model should be done since generalized management practices for each barangay were assumed. It is suggested to include actual planting date, tillage practices, weed management, and pest control in the assumptions to increase the accuracy of the model.

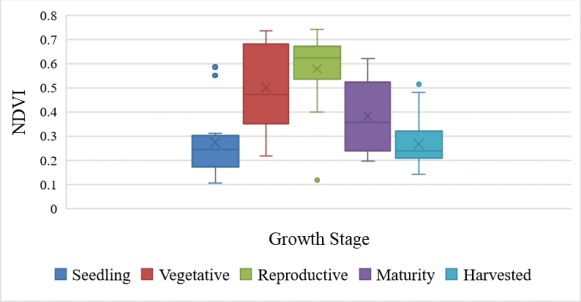

Fig. 2. Range of NDVI per growth stage

The method of identifying the standing crops and growth stage at a community level through satellite data was advantageous because it was easier, efficient, and time-saving. It provided a spatial visualization of the fields planted in the area during a specific time. It was also considered helpful during the pandemic when there were government-imposed restrictions on mobility and we were limited from going outside to conduct interviews and field surveys. In addition, remotely sensed data can be used as inputs for crop models, given a lack of ground observation.

As a recommendation, aside from using the NDVI threshold, other vegetation indices can be utilized and incorporated for a similar study. Unmanned aerial vehicle (UAV), which is a low altitude remote sensing, can also be considered.

KEYWORDS

rice monitoring, NDVI, GIS, remote sensing, yield estimation

REFERENCES

[1] Junges AH, Fontana DC, Anzanello R, Bremm, C. 2017. Normalized difference vegetation index obtained by ground-based remote sensing to characterize vine cycle in Rio Grande do Sul, Brazil. Ciência e Agrotecnologia, 41(5): 543-553

[2] USGS. 2020. NDVI, the foundation for remote sensing phenology. Retrieved November 2, 2020 from https://www.usgs.gov/core-science-systems/eros/phenology/science/ndvi-foundation-remote-sensing-phenology?qt-science_center_objects=0#qt-science_center_objects

[3] Noureldin NA, Aboelghar MA, Saudy HS, Ali AM. 2013. Rice yield forecasting models using satellite imagery in Egypt. The Egyptian Journal of Remote Sensing and Space Sciences 16,125-131.

[4] USGS. 2020. Deriving phenological metrics from NDVI. Retrieved November 23, 2020 from

https://www.usgs.gov/special-topics/remote-sensing-phenology/science/deriving-phenological-metrics-ndvi

[5] Decastillo ED. 2007. Climate field school (CFS) module. Municipality of Dumangas, Iloilo.

[6] Madigan E, Guo Y, Pickering M, Held A, Jia X. 2018. Quantitative monitoring of complete rice growing seasons using Sentinel 2 time series images. IGARSS 2018 - 2018 IEEE International Geoscience and Remote Sensing Symposium.

Adsorption Study of Phosphates in a Fixed bed Utilizing Concrete Cement Wastes

Liza Bautista-Patacsil[1, a *], Marc Angelo V. Diongco [2,b], and Czarina Jean N. Masicat [2,c]
[1]Department of Engineering Science, College of Engineering and Agro-Industrial Technology, University of the Philippines Los Baños, College, Los Baños, Laguna 4031 Philippines
[2]Department of Chemical Engineering, MITL, Malayan Colleges Laguna, Pulo Diezmo Rd., Cabuyao City, Laguna 4025 Philippines
[a] lbpatacsil@up.edu.ph, [b]mvdiongco@gmail.com, [c]masicat.czarina@gmail.com

Pursuant to the Philippine Clean Water Act of 2004 (RA 9275) and Executive Order 192, a stricter Water Quality Guidelines (WQG) and General Effluent Standards (GES), DAO 2016-08 was promulgated. Nutrients like nitrate and phosphate have been included to the pollutants to be monitored. Studies have shown that conventional Sewage Treatment Plant (STP) exhibits low removal of nutrients[1,2], hence, additional treatment system is deemed necessary. Several reported treatments for phosphate usually employ sorption. Chemical sorption process is too costly, and the increase sludge production as a by-product of the process is another concern, while biological treatment systems entail rigorous monitoring and in-house operating expertise[2]. Adsorption process for phosphate removal then becomes a viable option.

As the construction industries continue to prosper, the trimmings from the manufacture of hollow blocks piled up. The concrete cement contains silica that can adsorb phosphates. Also, there are other desirable contents present in concrete such as aluminum, iron and calcium that can bind with phosphates. Thus, utilizing these wastes can be a solution to a cost-efficient phosphate removal for a small-scale system. Hence, this study evaluated the adsorptive capacity of concrete cement wastes as a retrofit system for the removal of phosphates using fixed bed reactor.

The reported average phosphorus content in the effluent for year 2010 and 2011 in the Philippines is 3.8 ppm[3]. Other industries have reported to have phosphate level in the effluent in the range of 4–6 ppm. Such values exceeded the allowable discharge for Class C waters, which is 0.5 ppm, in accordance with Department of Energy and Natural Resources Administrative Order (DAO 2016-08). Hence, this study employed a synthetic influent with initial phosphate concentrations of 2 and 4 ppm for the adsorption tests. Concrete cement wastes with a nominal size of 4 cm diameter were used. Adsorption capacity, and sorption kinetics were determined through batch experiments. Preliminary experiments revealed the sorption equilibrium to be at 64h. So, this is the sorption time used for all batch experiments.

Figure 1 shows the graph of the adsorption capacity vs time for the 2 initial phosphate concentrations. It was observed that the higher the initial phosphate concentration, the larger is its adsorption capacity. This is due to more P molecules available and possible utilization of all active sites available for adsorption at higher concentration[4]. Also, higher solute concentrations would encourage other mechanisms such as higher boundary concentrations leading to double layer adsorption and possible complex formation [5]. The occurrence of desorption at 4 h for 5-ppm phosphate can be explained by possible competition to the available sorption sites. However, based on the % phosphate removal as shown in Figure 2, the 2-ppm initial phosphate concentration still gave a higher % phosphate removal. The 2-ppm and 5-ppm initial phosphate concentrations in influent yielded 70.42% and 59.82% removal, respectively. Since the same amount of concrete wastes were used for both samples, these results suggest that for higher phosphate concentrations in the influent, the effluent standards for phosphate can be achieved by utilizing large number of concrete wastes as adsorbent.

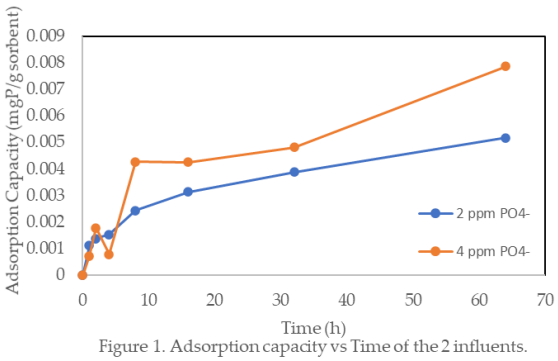

Figure 1. Adsorption capacity vs Time of the 2 influents.

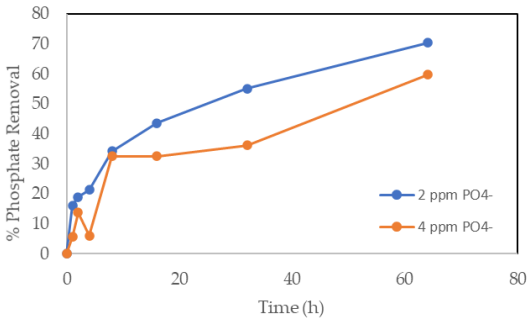

Figure 2. % Phosphate Removal vs Time of the 2 influents.

Table 1 shows the rate constants as well as the degree of linearity obtained for both pseudo-first order and pseudo-second order kinetic models.

Table 1. Rate constants of pseudo-first order and pseudo-second order kinetic models

PO_4^{-} (mg/L)	Pseudo-first order model		Pseudo-second order model		
	k_1 (h^{-1})	R^2	k_2 ($g \cdot mg^{-1}\ h$)	R^2	
2	0.0399	0.9471	0.00057	0.9715	
4	0.0293	0.7244	0.00038	0.7455	

The linear equation for pseudo first-order is:

$$ln\ (q_e - q_t) = ln\ ln\ q_e\ - k_1 t \quad (1)$$

where q_e ($mg \cdot g^{-1}$) is the amount of adsorbate adsorbed at equilibrium, q_t ($mg \cdot g^{-1}$) is the amount of adsorbate adsorbed at time t, and k_1 (h^{-1}) is the rate constant. On the other hand, the pseudo-second order equation is express in its linearized form as:

$$\frac{t}{q_t} = \frac{1}{k_2 q_e} + \frac{1}{q_e} t \quad (2)$$

where k_2 ($g \cdot mg^{-1}$ min) is the equilibrium rate constant. From the results obtained as shown in Table 1, the sorption kinetics of reaction follows the pseudo-second order kinetic model.

Continuous sorption using a fixed bed reactor was conducted to evaluate further the adsorption capacity of the concrete cement wastes. The fixed bed was

rated at HRT of 48h and a loading rate of $10L \cdot d^{-1}$. nples of effluent were taken at different tank depths 18 and 27 cm) at 2h interval to evaluate the effect of height for phosphate removal. It was observed that during the first 4 h, the % removal reached around 93 % for all samples taken at different depth and slowly decreased with time. At higher bed height, the % removal was lower. The decrease of adsorption capacity can be justified by the reason that all binding sites were not accessible to adsorbate molecules in higher bed height (due to overlap of active sites), and as a result, some of these particles were not effectively used[6]. The results obtained from this study suggest that concrete cement wastes can be an alternative adsorbent material for the removal of phosphate in wastewater.

KEYWORDS

Adsorption, phosphates removal, concrete cement wastes, fixed bed reactor

REFERENCES

[1] El-Bestawy E, Hussein H, Baghdadi H and El-Saka M F. 2005, Comparison between biological and chemical treatment of wastewater containing nitrogen and phosphorus. J. Ind. Micro & Biotech, Vol 32, Issue 5, pp.195-203.

[2] Bunce J T, Ndam E, Ofiteru I D, Moore A, Graham D W. 2018. A review of phosphorus removal technologies and their applicability to small-scale domestic wastewater treatment systems. Front. Environ. Sci. Vol. 6, Article 8.

[3] Mogol G, Sandoval TS, Rivera Jr M. Wastewater production, treatment and use in the Philippines. Accessed on Feb. 14, 2022 from https://www.ais.unwater.org/ais/pluginfile.php /501/mod_page/content/87/reports_philippines.pdf .

[4] Ragheb, S. M. (2013). Phosphate removal from aqueous solution using slag and fly ash. *HBRC Journal*, *9*(3), 270–275.

[5] Deng, Y, & Wheatley, A. (2018). Mechanisms of phosphorus removal by recycled crushed concrete. *Int'l J on Env Res and Public Health*, 15, 357.

[6] Marzbali, MH, Esmaieli, M. 2017. Fixed bed adsorption of tetracycline on a mesoporous activated carbon: Experimental study and neuro-fuzzy modeling. *J. of App. Res. and Tech., 15(5), 454–463.*

Prediction of Energy Expenditure in Construction Sites Using Artificial Neural Network

Catherine Mae E. Bautista[1,a *], John Kenneth P. Punongbayan[1,b*], Diana Marie R. De Silva[1,c*], Stephanie Caridad D.R. Landicho[1,d*], and Josefa Angelie D. Revilla[1,e*]
[1]Department of Industrial Engineering, Pili Dr, Los Baños, 4031 Laguna, Philippines
[a]cebautista@up.edu.ph, [b]jppunongbayan@up.edu.ph, [c]drdesilva1@up.edu.ph, [d]sdlandicho@up.edu.ph, and [e]jdrevilla@up.edu.ph

Over-exertion or under-exertion of energy has been a proven factor in developing health and safety hazards; hence, the necessity of understanding the required energy expenditure in a workplace. To date, in the Philippines, there are still limited to no studies that determine the energy expenditure in local construction sites despite the workers' exposure to various ergonomic stresses, repetitive tasks, and excessive force demands [1]. Several international regression-based energy expenditure formulas are available; however, these serve only as general guidelines and do not ensure a sound calculation for work involving heavy loads such as the construction industry [2].

This energy expenditure, in general, is often perceived to be challenging to assess, especially in the Philippine construction industry. This delimited assessment is because of the little laboratory calorimetric testing in the country and as well as the expensive, and work-interfering process of the evaluation[3]. Internationally, the standard practice is regression analysis which can be compared to another reliable emerging predicting tool— the artificial neural network. With this, the study aims to predict the energy expenditure in the local construction sites of the Philippines, particularly in Manila, using an artificial neural network (ANN).

METHODOLOGY

The study's methodology was generally subdivided into two main parts: the artificial neural network analysis and the validity test.

Both methods used the same data gathered from the 68 construction workers. These data were obtained using portable devices such as a Fitbit Alta HR, anemometer, hand-to-foot body fat scale, a laser measuring tool, and a heart rate monitoring device.

Artificial Neural Network Analysis

The learning technique used in the ANN model was the feedforward architecture and backpropagation learning based on Levenberg-Marquardt (LM) algorithm. With a single hidden layer and a varying number of neurons from 1-30, the final ANN model was determined through a series of trials.

The input variables of the ANN model, on the other hand, were categorized into four different sets and as shown in Figure 1.

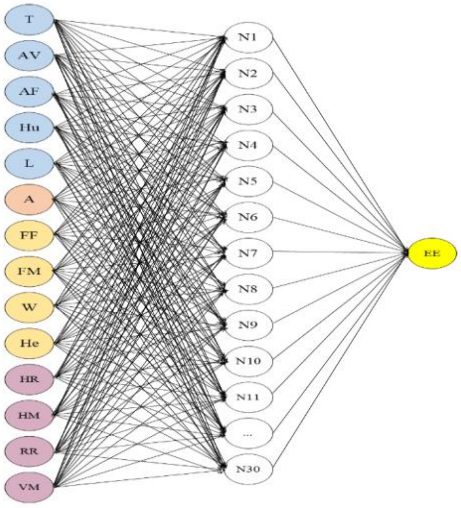

Fig. 1. The architecture of the ANN model

Represented by different colors, the input variables of the ANN model were categorized into environmental factors (blue), demographic data (pink), anthropometric measurements (orange), and respiratory variables (purple). Each set consists of the following variables, as shown in Table 1.

Table 1. Input variables of ANN model

Set	Description	Input Variables	Unit
A	All Variables	-	-
B	Environment Factors	Temperature Air Velocity Air Flow Humidity Light	°C m/s Cubefeet/min %RH Lux

C	Demo-graphic Data	Age	Years
D	Anthro-pometric Measure-ments	Fat-free Mass Fat Mass Weight Height	Kilograms Kilograms Kilograms Meters
E	Respi-ratory Variables	HR Rest HR Max Respiratory Rate VO_2Max	(1/min) (1/min) (1/min) (ml/min*kg)

Using the MATLAB version R2021b as the neural network toolkit, the set that generated the highest coefficient of determination was considered the best performing model.

Validity Test

Through the Minitab 18 software, a chi-square test of association was done to categorical variables. A frequency distribution table was made through Microsoft Excel to comply with the assumptions of the chi-square test. Thereafter, correlation analysis and multiple linear regression analysis were done for the validity test of the study. The predictive model generated from both methods was compared to the Metabolic Equivalents (METs) values under the 2011 Adult Compendium of Physical Activities to develop the methods' root mean squared error (RMSE).

SUMMARY OF FINDINGS

Figure 2 shows that Set E, which are the respiratory variables, obtained the highest R^2 value (85.47%).

The set consists of only four variables: the resting heart rate, maximum heart rate, resting respiratory rate, and maximal oxygen consumption (VO_2Max). Therefore, the hidden neurons of the model were only limited to at most nine neurons since the number of neurons must be the doubled value of the input variables plus one [4].

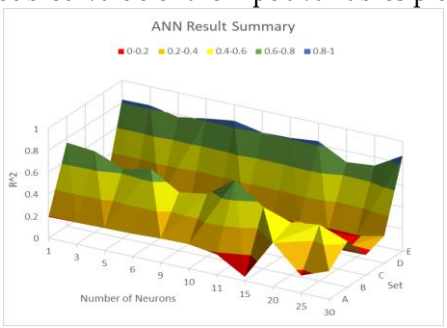

Fig. 2. Summary of ANN results

The regression analysis, on the other hand, resulted in the final equation as shown:

$$EE = -11.76 + 0.2106T + 0.09933HR_{max} \quad (1)$$

with only temperature and maximum heart rate as the correlated variables and a R^2 value of 62.30%.

The entire validity test resulted in a root mean squared error (RMSE) of ±1.67 for the ANN approach and a ±1.76 RMSE for the regression analysis.

CONCLUSION AND RECOMMENDATIONS

Based on the ANN training trials and validity tests, it can be concluded that ANN provides a more accurate prediction than the conventional regression analysis based on the higher coefficient of determination and lower root mean squared error. With this, the final developed ANN predictive model is a 4-9-1 (input variables-neurons-output variable) feed-forward neural network with resting heart rate, maximum heart rate, resting respiratory rate, and maximal oxygen consumption as the input variables.

The developed predictive model serves as an effective alternative to the currently known expensive and time-consuming energy expenditure assessment. Furthermore, the new approach offers increased accuracy and accessibility to health and safety management practitioners in the construction industry. However, a cross-validation test is highly suggested to give a more profound understanding regarding the model's performance in terms of different physical activity types beyond the construction industry.

KEYWORDS

energy expenditure, construction industry, artificial neural network, regression model, metabolic equivalents

REFERENCES

[1] Maiti, R. 2008. Workload assessment in building construction related activities in India. Applied Ergonomics. 39(6): 754–765.

[2] World Health Organization. 1985. Energy and protein requirements. Report of a joint FAO/WHO/UNU Expert Consultation. World Health Organization Technical Report Series. 724: 1–206.

[3] Hwang, S., Seo, J., Ryu, J., & Lee, S. 2016. Challenges and Opportunities of Understanding Construction Workers' Physical Demands through Field Energy Expenditure Measurements Using a Wearable Activity Tracker. Construction Research Congress. 2039–2049.

[4] Hecht-Nielsen, R. 1998. A theory of cerebral neocortex. Institute for Neural Computation. 1459–1464

Determinants of Household Evacuation Mode Choice Behavior in a Rural Community

Maria Elaine A. Gonzales[1, a *], Ma Bernadeth B. Lim[1,b], Harvey S. Maunahan[1,c], and Crisaulo M. Reynoso[1,d]

[1]Department of Civil Engineering, University of the Philippines Los Baños

[a] magonzales5@up.edu.ph, [b]mblim4@up.edu.ph, [c]hsmaunahan@up.edu.ph, [d]cmreynoso@up.edu.ph

Agricultural areas in provinces are not exempted to the impacts of typhoons. To ensure more effective evacuation of elements at risk, it is important to understand evacuation behaviors. One important behavioral aspect is the mode choice when traveling away from an area at risk of hazard. This study aims to determine the factors affecting the evacuation mode choice of households in an agricultural community.

The lowland barangays of Tagumpay and San Isidro in Bay, Laguna were examined. A survey was conducted among 434 households affected by Typhoon Ulysses (Internationally Named Vamco) in 2020. Representatives from each household were interviewed to know their socio-demographic characteristics and experiences during the typhoon. Potential factors that were identified based on findings in the past literatures (e.g. 1,2,3,4,5) were obtained through the survey. After data preparation, the factors were subjected to backward stepwise selection to eliminate insignificant variables and reduce the complexity of the models. A multinomial and a binomial logistic regression model were used to examine the factors.

Logit model is a type of discrete choice model that is used to construct mode choice models. Discrete choice models describe users' mode choice in an array of comprehensive and mutually exclusive alternatives. Established mode choice models are governed by the utility maximization hypothesis, an economic concept surrounding the decision-making process of consumer. Further, three alternative mode choices are considered in the study: private vehicles, government vehicles, and public utility vehicles. The probability of using a mode relative to the probability of using the reference mode is shown in Eq. 1. The variable $P_{mode\,i}$ is the probability of choosing a specific mode and $P_{ref\ mode}$ is the probability of choosing own vehicle. β_o is the model intercept, β_k is the coefficient of the k^{th} variable and x_k is the independent variables.

$$ln\ ln\left(\frac{P_{mode\,i}}{P_{ref\ mode}}\right) = \beta_o + \beta_1 x_1 + \beta_x x_2 + \cdots + \beta_k x_k \quad (1)$$

For the binary logit model, the probability of using a personal vehicle and other modes is represented by Eq. 2. The variable $P_{mode\,i}$ is the probability of choosing personal vehicle or other modes. β_o is the model intercept, β_k is the coefficient of the k^{th} variable and x_k is the independent variable.

$$P_{mode\,i} = \frac{e^{(\beta_o+\beta_1 x_1+\beta_x x_2+\cdots+\beta_k x_k)}}{1+e^{(\beta_o+\beta_1 x_1+\beta_x x_2+\cdots+\beta_k x_k)}} \quad (2)$$

The -2Log-likelihood (-2LL) value was computed to quantify goodness-of-fit. For each model, the likelihood ratio (LR) Chi-square test was performed to show its validity. The LR value of the model and critical value were compared in the interest of rejecting the null hypothesis that the final model containing the determinants performs the same as the null model. Further, McFadden's pseudo-R^2 was used to verify if the data and analysis are useful in making a conclusion on determinants affecting evacuation mode choice by measuring the effect size. A higher value of R^2 signifies a better fit than the other model.

The precision of each model was then calculated using Eq.3 where TP is the number of true positives and FP is the number of false positives.

$$Precision = \frac{TP}{TP+FP} \quad (3)$$

Results show that the determinants for evacuation mode choice include age (AGE) and gender of household head (GEN), presence of children (PCHILD), and vehicle ownership (VEH), occupation (OCCU) and hose ownership (HOWN) as shown in Tables 1 and 2. It is interesting that vehicle ownership remains a significant factor in evacuation mode choice behavior for an agricultural community.

Table 1. Parameter estimates of Model 1

VARIABLES	GOVERNMENT VEHICLE			PUBLIC VEHICLE		
	β	Sig.	OR	β	Sig.	OR
Intercept	5.742	<0.001		5.035	<0.001	

Characteristics of the head of the household and socio-demographic characteristics of the household						
AGE	-	-	-	-0.463	0.005	0.630
GEN	-	-	-	0.943	0.009	2.568
OCCU	0.645	0.009	1.906	-	-	-
HOWN	-	-	-	-1.278	0.057	0.279
PCHILD	-1.048	0.015	0.351	-0.857	0.019	0.424
VEH	-4.733	<0.001	0.009	-5.289	<.001	0.005
Evacuation-related variables						
DDEC	-0.810	0.016	0.445	-	-	-
ECOST	-1.063	0.022	0.345	-	-	-

Table 2. Parameter estimates of Model 2

VARIABLES	β	Sig.	OR
Intercept	6.476	<0.001	
Characteristics of the head of the household and socio-demographic characteristics of the household			
AGE	-0.422	.007	.656
GEN	.816	.015	2.261
PCHILD	-0.793	.025	.453
VEH	-5.156	<.001	.006
-2LL at zero	360.866		
-2LL at convergence	233.891		
Likelihood Ratio χ^2	126.974		
Degrees of Freedom	5		

In both models, it is revealed that households are more likely to take their own vehicle instead of relying on government-assigned vehicles or using public vehicle. The presence of children also positively influences the decision to use their own vehicle. Considering convenience and safety, it is rational that the household head is more likely to use their own vehicle for evacuation because relying on government-assigned vehicle or public transportation poses risks to the small children. In the same way, female household heads are more likely to utilize public transportation than their own vehicle. Lastly, older household heads prefer using their own vehicle rather than using other modes of transportation. This can also be explained by the evacuees' tendency to choose the mode choice that will provide the highest level of convenience.

Model 1 presents unique predictors for choosing their personal vehicle instead of other modes. If the head of the household works in a private sector or as a government employee, they are more likely to use a government vehicle compared to their own vehicle. Households evacuating to a house of a friend or family is less likely to use a government-provided vehicle. Houses of family/friends might be out of the way of the provided vehicle's route to evacuation centers. Model 1 suggests that if there are expenses expected to be incurred when evacuating, households are less likely to use a government-assigned vehicle. This may be because government vehicles in both barangays assist evacuees to schools used as evacuation centers. Evacuating to a friend or a relative's house means that aside from having free lodging and free food, they are more comfortable in a familiar shelter. Lastly, residents who have ownership of their houses are less likely to use public vehicles.

At 0.05 level of significance, the final models show significant improvement in fit compared to the baseline models. Hence, the validity of the final models is supported. Using the McFadden pseudo R-square, 29.8% of the variation that is observed in the mode of evacuation (own vehicle, government vehicle, and public transportation) can be explained by the determinants of Model 1. Meanwhile, 35.1% of the variation that is observed in the evacuation mode (either own vehicle or others) can be explained by the determinants of Model 2. Model 1 has an AUC score of 0.816 and Model 2 has 0.874 which both show excellent discrimination.

For internal validation, the results of the LR test contradicts with its overall accuracy of 80.7%, which is relatively higher compared to the accuracy of Model 1 of 68.5%. Model 2 has a high accuracy rate according to other statistical measures but is considered invalid after performing the LR test. The precision of the multinomial logit model (61.4%) is higher than the precision of Model 2 (58.3%). In this case, the value of precision attests that although Model 2 has a high AUC, it also has a high false positive rate. The 20-80 distribution of Model 2 is considered as moderately imbalanced. This imbalance may have contributed to the invalidity of the model.

Ultimately, the developed models can help the selected rural barangays in strengthening evacuation management and strategies by predicting mode choice.

KEYWORDS

Typhoon; Evacuation modeling; Evacuation behavior; Logistic regression; Mode choice

REFERENCES

[1] Bian R, Wilmot CG, Gudishala R, Baker E J. 2019. Modeling household-level hurricane evacuation mode and destination type joint choice using data from multiple post-storm behavioral surveys. Transportation Research Part C: Emerging Technologies, 99, 130-143. doi: 10.1016/j.trc.2019.01.009

[2] Lim HR, Jr, Lim MBB, Piantanakulchai M. 2016. Determinants of household flood evacuation mode choice in a developing country. Natural Hazards, 84, 507-532. doi: 10.1007/s11069-016-2436-4

[3] Sadri AM, Ukkusuri SV, Murray-Tuite P, Gladwin H. 2014. Analysis of hurricane evacuee mode choice behavior. Transportation Research Part C: Emerging Technologies, 48, 37–46. doi:10.1016/j.trc.2014.08.008

[4] Luathep P, Suwansunthon A, Sutthiphan S, Taneerananon P. 2013. Flood evacuation behavior analysis in urban areas. Journal of the Eastern Asia Society for Transportation studies, 10, 178-195. doi: 10.11175/easts.10.178

[5] Sugiarto S, Lulusi Isya M, Taufik, Haiqal M. 2019. Characterizing mode choice behaviors of the evacuees during emergency evacuation using a Logistic regression model. IOP Conference Series: Materials Science and Engineering, 523. doi: 10.1088/1757-899X/523/1/012032

Effects of Various Grip Exertion Levels and Forearm Postures on Hand-Arm Transmitted Vibration

Josefa Angelie D. Revilla[1, a *], Satoshi Muraki[2,b], and Ping Yeap Loh[2,c]
[1]Department of Industrial Engineering, University of the Philippines Los Baños, Laguna, Philippines
[2]Faculty of Design, Kyushu University, Fukuoka, Japan
[a] jdrevilla@up.edu.ph, [b] muraki@design.kyushu-u.ac.jp, [c] py-loh@design.kyushu-u.ac.jp

BACKGROUND AND OBJECTIVE

The Philippines is a tropical country where agriculture is one of the primary sources of livelihood. Approximately 25 to 35% of the labor force is under the agricultural sector [1]. With this, mechanization has become prevalent to improve the efficiency of farming and other related operations. One of the common agricultural equipment is the hand tractor (Fig. 1). This is a hand-guided engine-powered equipment used to cultivate small and medium-sized farmland.

Fig. 1. Local hand tractor used for farming [2]

A typical hand tractor has a 2,400 to 3,600 RPM engine that generates and transmits vibration. Previous studies have investigated the amount of engine vibration being transmitted to the hand-arm system of the operators [2, 3]. It was found that during plowing and harrowing, engine vibration is 21.74 m/s^2 and 19.46 m/s^2 while transmitted vibrations to the hand and elbow are 17.02 m/s^2 and 14.67 m/s^2 for plowing and 16.15 m/s^2 and 13.56 m/s^2 for harrowing [2]. These values exceeded the exposure limit value or the allowable safe value of 5 m/s^2. Various interventions such as installation of handle grips and grip straps, inclusion of engine mounts, and modification of the handlebar structure were proposed to reduce this amount [4, 5, 6]. The series of research significantly reduced transmitted vibrations, but they were not able to consider the physiological effects of transmitted vibrations to humans.

Hence, this report focused on addressing the identified research gap. The amount of transmitted vibration does not only depend on the characteristics of vibration magnitude of the source. Instead, it is also influenced by biomechanical factors such as grip force and forearm posture applied by the operators [7, 8, 9].

METHODOLOGY

The experiments were conducted in a controlled laboratory set-up [10, 11, 12]. The experiments focused on determining the effects of various grip force levels and two forearm postures on the amount of hand-arm transmitted vibrations and forearm muscle loading. The main task is to hold the vibrating handlebar for a few minutes using the desired grip force and forearm posture. Transmitted vibrations and forearm muscle activities were recorded and measured during each task performance.

Vibration source

A fabricated handlebar structure was attached to a vibration table that served as the source of vibration (Fig. 2).

Fig. 2. Vibration source and handlebar structures

The vibration source has a nominal frequency of 60 Hz or 3,600 RPM, which implies that the resonant frequencies appear in multiples of the nominal frequency (Fig. 3).

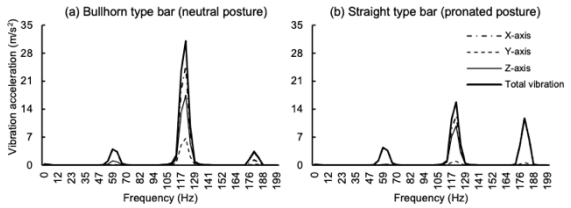

Fig. 3. Frequency spectra of the vibration value at baseline with peak accelerations within multiples of the nominal frequency

Transmitted vibrations

The calculated total vibration accelerations on the tip of the handles are 13.0 m/s² and 10.5 m/s². This was computed using Eq. 1.

$$AT_i = \sqrt{Ax_i^2 + Ay_i^2 + Az_i^2} \quad (1)$$

where *ATi* is the total vibration acceleration, *Axi*, *Ayi*, and *Azi* are the vibration acceleration measured along the x-, y-, and z-axes on measurement location *i*. Similarly, the vibration acceleration at the hand and wrist of the participants were recorded and calculated. The amount of transmitted vibration to the hand and wrist were computed using Eq. 2. A triaxial accelerometer (Pico Technology, Japan) was used to measure the vibration at each location.

$$Tr_i = \frac{AT_i}{AT_{baseline}} \quad (2)$$

where *Trhandle*, *Trwrist*, and *Trelbow* are the percentages of transmitted vibration to the handle, wrist, and elbow.

Forearm muscle activities

On the other hand, forearm muscle activities were recorded and measured using the BA-U410m surface bipolar active electromyography (EMG) electrodes (Nihon Santeku, Japan). The EMG signals were amplified using a BA1104m bio-instrumentation amplifier (Nihon Santeku, Japan) before being transmitted to the ML880 PowerLab 16/30 (ADInstruments, New Zealand) at a sampling rate of 1 kHz. The signals were filtered, calculated, and analyzed in LabChart 7.3.8 (ADInstruments, New Zealand). Four forearm muscles, associated with hand grip, were considered. These are the extensor carpi radialis (ECR), finger flexors (FF), flexor carpi ulnaris (FCU), and flexor carpi radialis (FCR). The main muscle that was used to monitor grip exertion level was the ECR. The other three forearm muscles were used to investigate the muscle loading of the forearm during the different combinations of grip force levels and postures. A high forearm muscle loading denotes high physical workload. The placement of the accelerometers and surface EMG is shown in Fig. 4.

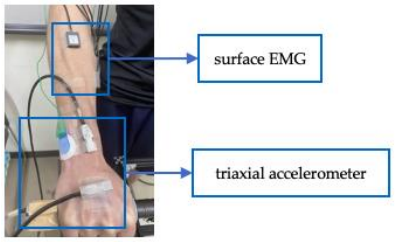

Fig. 4. Placement of triaxial accelerometers and surface electromyography

Experiment protocol

In the experiments, the participants were asked to hold the handlebar at the desired grip level. They were instructed to sustain the same level of grip for a few minutes while vibration and muscle activations are being recorded. A visual feedback of the participant's grip exertion level was presented in a computer monitor to assist them in sustaining the required grip level throughout the task performance. The experimental set-up is roughly demonstrated in Fig. 5.

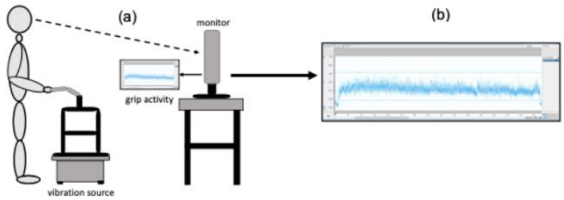

Fig. 5. Illustration of the experimental set-up: (a) schematic diagram of the task performance and (b) a sample visual feedback to monitor grip exertion

Mild grip is set at 10% of the participant's maximum grip strength. Moderate and hard grips are 30% and 50% of the maximum grip strength. The maximum grip strength (in kgf) was taken prior to the start of the experiment using a T.K.K.5710B dynamometer (Takei, Japan). It was connected to a TSA-110 strain amplifier (Takei, Japan) that shows the real-time force exertion. This served as the basis for the mild, moderate, and hard grip percentages. On the other hand, a bullhorn-type handlebar was used to simulate a neutral forearm posture and a straight handlebar was used to impose a pronated forearm posture

(Fig. 4). The handlebars were interchanged depending on the condition to be performed.

Measurement variables

There are six conditions, which were performed in different sets of experiments but with roughly the same controlled environment and protocol, that were compared. These are: (i) mild grip in neutral, (ii) mild grip in pronated, (iii) moderate grip in neutral, (iv) moderate grip in pronated, (v) hard grip in neutral, and (vi) hard grip in pronated. The independent variables are grip force levels and forearm postures while the dependent variables are hand-arm transmitted vibrations and forearm muscle activities (Table 1). Note that the same vibration magnitude was used across all the experiments.

Table 1. Description of the variables

Variable Name	Variable Type	Description
Grip force levels	Independent	Denoted by mild, moderate, and hard grip
Forearm postures	Independent	Denoted by neutral or normal posture and pronated or unnatural posture
Transmitted vibrations	Dependent	Measured on the handle, hand, and wrist using the triaxial accelerometers
Forearm muscle activities	Dependent	Measured the activities of the ECR, FF, FCU, and FCR using surface EMG and LabChart

Statistical analysis

The SPSS Statistics 25.0 (IBM, USA) was used for all the statistical analyses. The data were checked for normality via Shapiro-Wilk test. Outliers were removed to satisfy normality. Repeated measures ANOVA was used to determine the influence of grip force level and forearm posture on transmitted vibrations and forearm muscle loading. Bonferroni correction served as the post-hoc analysis for multiple pairwise comparisons.

SUMMARY OF THE FINDINGS

The diagram in Fig. 6 shows the summary of the results. In the figure, WTV and HTV are wrist and hand transmitted vibrations that were calculated during the different conditions. On the other hand, the forearm muscle activities were also determined. Both transmitted vibrations and forearm muscle loadings increase with grip exertion, specifically hard grip resulted to significantly higher transmitted vibrations and muscle loadings ($p < 0.01$) than mild grip. On the other hand, forearm posture did not influence transmitted vibrations and muscle loadings. Finally, there were no interaction effects found.

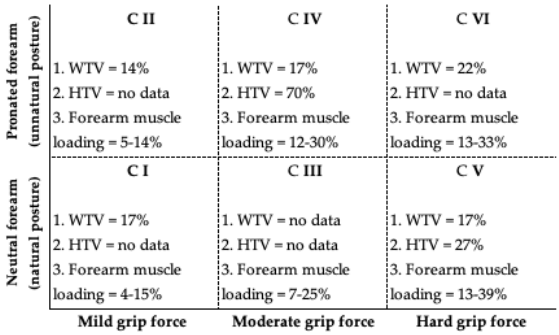

Fig. 6. Summary of relevant findings

CONCLUSION AND RECOMMENDATION

The series of experiments confirmed that the amount of transmitted vibration is influenced by force exertion. Similarly, forearm muscle loadings increase with grip force level. Although muscle activations were not directly influenced by change in posture, the unnatural position of the forearm muscles during pronation caused discomfort to the participants, specifically when it is in concurrent with strong grip force.

Hence, it is suggested that when a task requires extreme force, the arm must be in its natural or neutral posture to mitigate the negative impacts of vibration exposure. On the other hand, when the task requires mild force, either the normal or awkward posture may be applied but only under a short-term exposure (less than 5 mins). Extended exposure to vibration, regardless of the amount of exerted force or applied posture, can lead to serious illnesses such as the hand-arm vibration syndrome that can impair basic hand functions. Thus, this must be avoided.

KEYWORDS
grip force, forearm posture, muscle activity, transmitted vibration

REFERENCES

[1] Food and Agriculture Organization (FAO) of the United Nations. 2019. Philippines at a glance. Retrieved from http://www.fao.org/philippines/fao-in- philippines/philippines-at-a-glance/en/

[2] Revilla JA, Yap MA, Layaoen HD, Ramos MJ. 2015. Baseline measurement and analysis of hand-arm transmitted vibration for an ergonomically designed two- wheel tractor. Philippine Agricultural Scientist. 98(2): 166-173.

[3] Layaoen HD, Yap MA, Palomar R, Pesigan C. 2015. Optimal handle grip and engine mount combination for minimized hand vibration from gasoline hand tractors. Philippine Agricultural Scientist. 98(2): 157-165.

[4] Yap MA, Layaoen HD, Revilla JA, Ani A, Blanco FM. 2016. Effectiveness of substitute vibration dampers in reducing hand-arm vibration of a gasoline-fueled hand tractor. Philippine Agricultural Scientist. 99(2): 191-201.

[5] Binarao JK, Layaoen HD, Revilla JA, Ani A, Caroche ML. 2017. Effectiveness of commercially available vibration dampeners in reducing hand-arm vibrations on diesel-powered and gasoline-powered hand tractor. Philippine Agricultural Scientist. 100: 133-142.

[6] Mojica JM, Yap MA, Layaoen HD, Amongo RM, Ani A, Revilla JA. 2016. Design and fabrication of an ergonomic handlebar structure of a hand tractor for vibration suppression. Philippine Agricultural Scientist. 99(1): 58-67.

[7] Burström L. 1994a. The influence of biodynamic factors on the absorption of vibration energy in the human hand and arm. Nagoya Journal of Medical Science. 57(3–4): 159-167.

[8] Carlsöö S. 1982. The effect of vibration on the skeleton, joints and muscles. A review of the literature. Applied Ergonomics. 13(4): 251-258.

[9] Burström L. 1994b. The influence of individual factors on the absorption of vibration energy in the hand and arm. Journal of Low Frequency Noise, Vibration and Active Control. 13(4): 115-122.

[10] Revilla JA, Loh PY, Muraki S. 2019. Exploratory study on the impacts of handle vibration on the hand and forearm. Industrial Engineering & Management Systems. 18(4): 591-599.

[11] Revilla JA, Muraki S, Loh, PY. 2020. Early effects of short-term exposure to mid- range vibration frequency on the hand and forearm. Journal of the Philippine Institute of Industrial Engineers. 17(2): 1–8.

[12] Revilla JA, Loh PY, Muraki S. 2021. Effects of two grip force levels and forearm postures on hand-arm transmitted vibration and physiological responses. Human Factors and Ergonomics in Manufacturing & Service Industries. 31(6): 679-692.

Efficiency Evaluation of the JXYS and ZQVR Ergonomic Keyboard Layouts

Eliza B. Cuevas[1,a *], Kathleen L. Baldoz[1,b*], Maria Liezel P. Caroche[1,c*],
Allen Lemuel G. Lemence[1,d*], and Josefa Angelie D. Revilla[1,e*]
[1]Department of Industrial Engineering, Pili Dr, Los Baños, 4031 Laguna, Philippines
[a]ebcuevas1@up.edu.ph, [b]kblee2@up.edu.ph, [c]mpcaroche@up.edu.ph ,
[d]aglemence1@up.edu.ph, and [e]jdrevilla@up.edu.ph

Physical keyboards are one of the technological tools that enable people to communicate during work, academic, and leisure activities. Research has shown that the universal keyboard, known as the QWERTY keyboard, was not ergonomically designed primarily because it promotes the same hand and finger usage, increasing the risk of repetitive strain injuries[1, 2, 3]. Alternative keyboard layouts have been developed across the world to accommodate certain languages while also providing ergonomic benefits.

In the Philippines, there have been studies on the theoretical efficiency of ergonomic keyboard layouts for Philippine languages but there are few to no studies on the physical testing of the developed layouts; hence, the need for experimental research on the real-world benefits of these keyboards. Two previously developed ergonomic keyboard layouts called "JXYS" and "ZQVR" were made for the English, Tagalog, and Taglish languages[4] (Fig. 1 and 2). The goal of this study is to measure the efficiency in adapting to these keyboard layouts and to determine the keyboard layouts' physical, cognitive, and perceptual demands.

J	X	Y	S	D	M	T	B	C	F	*	*
H	U	O	N	E	I	A	G	K	*	*	
Z	Q	V	R	W	P	L	*	*	*		

Fig. 1. JXYS letter keyboard layout [4]

Z	Q	V	R	W	P	L	B	C	F	*	*
H	U	O	N	E	I	A	G	K	*	*	
J	X	Y	S	D	M	T	*	*	*		

Fig. 2. ZQVR letter keyboard layout [4]

Methodology

A four-day experiment was conducted on fifteen college students with average typing proficiency. For three days, they were exposed to the JXYS and ZQVR keyboards. Physical testing of the keyboards was done on days two and four of the experimentation period to account for the one-day and three-day exposure to the two keyboards. Preliminary results reveal that the Tagalog language can represent the Taglish language, hence the experiment will only employ the English and Tagalog languages. During the physical test, each participant performed five trials for each language and layout pair namely QWERTY-English, QWERTY-Tagalog, JXYS-English, JXYS-Tagalog, ZQVR-English, and ZQVR-Tagalog. Shown in Figures 3 and 4 are the physical keyboard used during the experimentation period. These keyboard layouts were run by a user interface.

Fig. 3. JXYS physical keyboard prototype

Fig. 4. ZQVR physical keyboard prototype

Non-parametric tests were used since the gathered data appeared to violate normality assumptions. The experiment data was subjected to a Kruskal Wallis H test to compare the performance of participants utilizing the JXYS and ZQVR keyboards to the QWERTY keyboard. The Wilcoxon Signed-Rank test was used to assess if there was a significant improvement in the participants' performance after a one-day and three-day exposure to the JXYS and ZQVR keyboards. The Mann-Whitney test was performed to see if there were significant differences in subjective evaluation scores between the JXYS and ZQVR keyboards.

Kruskal Wallis H Test

Upon doing statistical analyses for eight hypotheses for the typing speed (characters per minute) and completion

time (seconds) which accounts for the 1-day and 3-day exposure to the keyboard layouts, they all resulted in a p-value of 0.000 which indicates that both JXYS and ZQVR keyboard layout still cannot be at par with typing speed and completion time using a QWERTY layout in both the English and Tagalog language. This was following the claim that new keyboard layouts require a long time before a user can acclimatize [5].

However, in typing accuracy (error percentage), all four hypotheses (p-value of 0.414, 0.492, 0.378, and 0.374) show that there was no significant difference across the keyboard layouts in both English and Tagalog languages during the one-day and three-day exposure to the keyboards. This indicates that errors remain the same across all keyboards.

Wilcoxon Signed-Rank Test

This statistical test was utilized to compare the JXYS and ZQVR keyboards in terms of typing accuracy, speed, and completion time between a one-day and three-day exposure to the keyboards.

According to the statistical results, end-user performance changes significantly after one and three days of exposure to the JXYS and ZQVR keyboard layouts. It shows that when end-users utilize keyboard layouts in both English and Tagalog, their typing accuracy, speed, and completion time improve by 23.55% to 42.52%. However, utilizing the JXYS keyboard in Tagalog and the ZQVR keyboard in English did not enhance typing accuracy significantly, with p-values of 0.431 and 0.208, respectively.

Subjective Rating Assessment

The survey was adopted from the study of Anderson [3] and this was modified to get a more accurate result. In this assessment, the participants were asked to rate the physical, cognitive, and perceptual demands of the JXYS and ZQVR keyboards based on their user experience.

Results of the Mann-Whitney test show that the scores of the JXYS and ZQVR keyboards as a function of physical, cognitive, and perceptual demands in both English and Tagalog languages do not have any significant difference having p-values > 0.268. This indicates that the JXYS and ZQVR keyboards have the same demands for the end-users.

To further support the physical demand scores, video analysis of the typing test will be conducted. This will show real data on the finger and hand alternation when using the JXYS and ZQVR keyboard layouts.

Conclusion and Recommendation

End-users who utilized the JXYS and ZQVR keyboards did not perform at the same level when using the universal keyboard layout. Thus, further familiarization with the new keyboard layouts is necessary to achieve the same degree of expertise as the QWERTY keyboard. Further analysis on user safety, typing accuracy, typing speed, and usability will still be conducted to choose the best keyboard layout.

The findings of this study can help design a more ergonomic keyboard layout for users of English, Tagalog, and Taglish by considering new letter placements that will improve the typing speed and completion time while reducing physical, cognitive, and perceptual demands.

KEYWORDS

keyboard, keyboard layout, efficiency, QWERTY, ergonomic

REFERENCES

[1] Hiraga Y, Ono Y, Yamada H. 1980. An analysis of the standard English keyboard. In Proceedings of the 8th conference on Computational linguistics (COLING '80). Association for Computational Linguistics, USA, 242–248. doi:10.3115/990174.990218

[2] Fagarasanu M, Kumar S. 2003. Carpal tunnel syndrome due to keyboarding and mouse tasks: A Review. International Journal of Industrial Ergonomics, 31(2), 119-136. doi:10.1016/s0169-8141(02)00180-4

[3] Anderson A, Mirka G, Joines S, Kaber D. 2009. Analysis of Alternative Keyboards Using Learning Curves. Human factors. 51. 35-45. doi:10.1177/0018720808329844.

[4] San Juan A. 2021. Development of an Ergonomically-Programmed Keyboard Layout for English, Tagalog, and Taglish Languages using Python Software.

[5] Baker, N. (2013). The effectiveness of alternative keyboards at reducing musculoskeletal symptoms at work: A Review. Digital Human Modeling and Applications in Health, Safety, Ergonomics, and Risk Management. Human Body Modeling and Ergonomics, 189-195. doi:10.1007/978-3-642-39182-8_2

Classification of grains using near-infrared hyperspectral imaging and multivariate analysis

Princess Tiffany Dantes-Mendoza[1, a *]
[1]Department of Grain Science and Industry, Kansas State University, Manhattan, Kansas, USA
aptiffany@ksu.edu

ABSTRACT

Recent demand for high quality, gluten-free and safe foods has prompted the development of non-destructive, rapid and accurate testing methods for quantitative and qualitative evaluation of food and grains. One of the major issues in the grain industry is the commingling of gluten-free grains (such as oat) with non-gluten ones. Near-infrared hyperspectral imaging has been successfully used in the food industry for classification, detection of contaminants and prediction of quality attributes.

In this study, near-infrared hyperspectral imaging (900 – 1700 nm) was used to classify different types of grains (barley, oat, and wheat). Background subtraction, wavelength reduction, selection of region of interest, and spectral pre-processing with standard normal variate were applied on the hyperspectral data. Spectral data were extracted a) object-wise (from mean spectra of 675 seeds), and b) pixel-wise (from each pixel of three seeds). Classification models were developed using partial least squares discrimination analysis. Processing and analysis of hyperspectral data were performed in MATLAB and HYPER-tools.

Mean reflectance spectra of oat and barley seeds in this study were almost similar and were relatively higher than those of wheat seeds (Fig. 1).

Classification accuracy for model fitting and validation were 0.99 and 0.98 for object-wise and pixel-wise approaches, respectively. Both approaches provided good prediction classification of new grain samples. Results show that near-infrared hyperspectral imaging has the potential to be used in screening and identification of grains for an efficient and accurate non-destructive quality control.

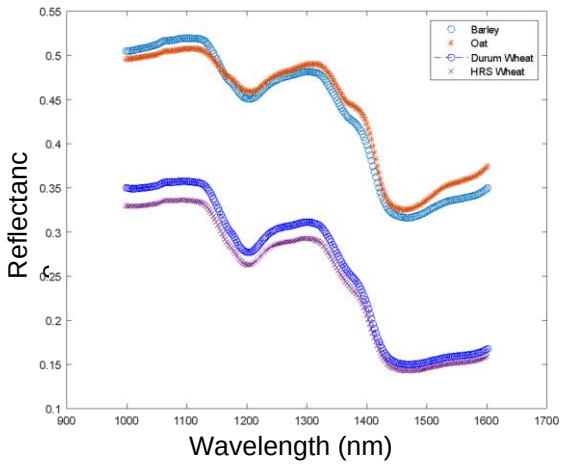

Fig. 1. Mean reflectance spectra of 270 barley, 245 oat, 100 Durum wheat, and 60 hard red spring wheat seeds.

KEYWORDS

near-infrared, grains, classification, hyperspectral imaging, chemometrics

Rapid identification of the geographical origin and quality of paddy rice using near-infrared spectroscopy

Joanne P. Foliente[1, a], Fidelina T. Flores[1, b], Mary Jane L. Quindoy[1, c], and Kevin F. Yaptenco[1, d]
[1]Agricultural, Food and Bioprocess Engineering Division, Institute of Agricultural and Biosystems Engineering, College of Engineering and Agro-Industrial Technology, University of the Philippines Los Baños, 4031 College, Laguna, Philippines
[a] jpfoliente@up.edu.ph, [b] ftflores@up.edu.ph, [c] mlquindoymar@up.edu.ph, [d] kfyaptenco@up.edu.ph

In today's market, returned paddy seeds undergo seed quality assessment (vigor rate and germination rate) to determine if seed quality is still acceptable. Returning of seeds to the main facility and testing process (5-7 days) takes a lot of time. An estimated cost of Php 900,000.00 per year are spent for logistics that covers land/sea transportation, inventory, and labor for seed testing.

Rice is the main staple food in the Philippines. It is only planted twice a year during the months of June-July and November-December. The low yield and high demand drive the market price to rise. Paddy seed adulteration has been a pertinent issue as it does not benefit both farmers and consumers. There is a need to establish a rapid method that save time, logistics cost and identify geographical origin, which is essential for assessing the quality of paddy seed.

Near infrared spectroscopy (NIRS) is a rapid and non-destructive analysis used for seed identification and seed quality parameters. Several studies have shown the potential of NIR in predicting seed quality parameters. However, these studies used different varieties, storage period, varietal, geographical, range of spectral wavelength and data acquisition [1,2,3,4].

This study will focus on the potential application of this principle and technology on the available seed being sold to local market.

The study aims to develop calibration models using NIRS to predict seed quality parameters (geographical origin, age, vigor rate, germination, and seed class) and identify significant wavelength. The NIR system set-up is composed of Ocean Optics Inc. spectrometer-NIR QUEST 512 with wavelength range 900-1,700 nm in reflectance mode. The light source used is Ocean Optics HL-2000 with tungsten-halogen lamp that covers wavelengths from 360 to 2,400 nm. The system was calibrated using a standard reference white Labsphere Spectralon disc. Data acquisition analysis followed preprocessing techniques and multivariate analysis [5]. Standard laboratory test for gemination and vigor was conducted simultaneously.

This study used one variety that is planted and grown at different locations (India, Philippines), harvest year (year 1: March 2019-October 2019 and year 2: July 2020-November 2021) and seed class (low, moderate, high, very high). There are 145 seed lots which were scanned five times generating 725 spectral data.

The reflectance spectral data were subjected to pre-processing technique, principal component analysis (PCA) and partial least square regression (PLSR) to predict seed quality parameters. Performance of the models were evaluated through coefficient of determination R^2 and Root Mean Square Error (RMSE). Samples were allocated to training (calibration and validation) and independent testing (prediction set). The training sets were divided into a 4:1 ratio for calibration and validation set.

The model with the highest prediction performance based on R^2 is for year harvest with 0.722 (RMSE= 0.088), next is germination with 0.496 (RMSE= 3.001), vigor with 0.480 (RMSE=3.969), seed class with 0.364 (RMSE=0.251) and location 0.304 (RMSE=0.296).

Significant wavelength identified using loadings were in the range of 1117.8 nm, 1299.3 nm, 1405.4 nm, and 1618.8 nm. These wavelengths correspond to the following bonds: N-H, O-H, C-H. These bonds are affected by variation in seed composition (water and lipids, fatty acids, starch) which changes with time [6,7,8]. NIR prediction models developed could predict paddy seed quality parameters (geographical location, year harvested, vigor, germination, and seed class).

The model for year of harvest had the highest performance (R2=0.722), followed by germination

(R2=0.496) and vigor(R2=0.480). However, the performance of these models can still be improved by strengthening spectral library by adding another geographical location and year of harvest.
NIR spectroscopy is an effective method of a rapid and non-destructive monitoring of seed authenticity and viability.

KEYWORDS
NIR, germination rate, seed vigor, seed classification, geographical location

REFERENCES

[1] Li, Y., Jiang D. Liu Y. Ding W, Ding Q, Zha L. 2014. Testing of Germination Rate of Hybrid Rice Seeds Based on Near-Infrared Reflectance Spectroscopy. Spectroscopy and Spectral Analysis. 34(6): 1528-1531

[2] Li, X., He, Y., Wu, C. 2008. Non-destructive discrimination of paddy seeds of different storage age based on vis-NIR spectroscopy. J Stored Prod Res. 44:264-268

[3] Peijin, T., Lim, J.K., Wei, T., Untzizu E., Zhang H., Jang Y., Cao W. 2021. Rapid identification of the variety and geographical origin of Wuyou No. 4 rice by fourier transfrom near-infrared spectroscopy coupled with chemometrics. Journal of Cereal Science 102. 103322. 1-7

[4] Fhardi M., Tigabu M., Pietryzkowski M., Danusevicius D., Oden P.C. 2017. Application of near infrared spectroscopy for authentication of *Picea abies* seed provenance, New Forests. 48: 629-642

[5] Flores, F.T., Foliente, J.P., Yaptenco K.F., Armstrong, P.R. 2020. Non-Destructive Prediction of Paddy Seed Quality Using Near Infrared Spectroscopy. Philippine Journal of Agricultural and Biosystems Engineering 16 (2), 65-74

[6] Wang, Y., Peng, Y., Zhuang, Q., & Zhao, X. (2020). Feasibility analysis of NIR for detecting sweet corn seeds vigor. Journal of Cereal Science, 93(102977), 1-7

[7] Hao, Y., Geng, P., Wu, W., Wrn, Q., & Rao, M. (2019). Identification of rice varieties and transgenic characteristics based on near-infrared diffuse

reflectance 125 spectroscopy and chemometrics. Molecules, 24(24), 1-11

[8] Juliano B.O. (1985) Polysaccharides, proteins, and lipids of rice. Juliano BO (ed.), In Rice Chemistry and Technology. pp. 59–174, American Association of Cereal Chemists, USA.

COVID-19 Pandemic Activity Travel Patterns of the Commuters in Quezon City, Philippines

Joseph Amiel R. Rempillo[1,a] *, Ma. Bernadeth B. Lim[1,b] , Judie Ann A. Ramos[1,c] and Kale Ashley P. Carurucan[1,d]
[1]Department of Civil Engineering, University of the Philippines Los Baños, Philippines
[a] jrrempillo1@up.edu.ph, [b] mblim4@up.edu.ph, [c] jaramos3@up.edu.ph, [d] kpcarurucan@up.edu.ph

Several community quarantine measures and mobility restrictions have been implemented by the government to slow the spread of the virus which include the shutting down of the public transportation system. Due to these measures and restrictions, the daily routine of the people drastically changed especially in their travel behavior. The study aims to assess the changes on the travel behavior and identify the factors affecting the transport mode choice of the commuters in Barangay Pinyahan, Quezon City.

Data was gathered through online surveys and house to house distribution of printed survey questionnaires to the prospective respondents that can participate in the study. The population of Barangay Pinyahan is 27,653 based on the 2015 Census [1]. With a 95% level of confidence and margin of error of 5%, the minimum sample size for the study is 379. A total of 411 responses were gathered and used for analysis.

The survey questionnaire used in the study was divided into different parts which includes (1) data protection consent; (2) sociodemographic profile in terms of sex, age, educational attainment, employment status, monthly income and vehicle ownership; (3) travel behavior before and the pandemic in terms of mode choice, travel purpose and destination, trip frequency and schedule; (5) preferred transport mode after the pandemic; and (6) risk perception of COVID-19 pandemic.

To determine the distribution of the respondents, the frequency and percentage distribution of each category were computed and tabulated. To determine the relationship between the transport mode choice and the demographic profile of the respondents, travel pattern and risk perception on COVID-19 and their strength of association, Chi Square Test of Independence and Likelihood Ratio were performed and p-values and Cramer's V were determined. For this study, a 95% confidence interval is selected and if the p-value is less than or equal to 0.05, the result is said to be statistically significant. Table 1 shows the interpretation of association of the estimated values of Cramer's V.

Table 1. Interpretation of Association of the Estimated Cramer's V Values.

ESTIMATED VALUE	INTERPRETATION OF ASSOCIATION
0.00 - 0.10	Negligible
0.10 - 0.20	Weak
0.20 - 0.40	Moderate
0.40 - 0.60	Relatively Strong
0.60 - 0.80	Strong
0.80 - 1.00	Very Strong

Source: Lee, 2016 [2]

Lastly, to determine the significant relationship between the transport mode choice (1) before and during the pandemic, (2) during and after the pandemic and (3) before and after the pandemic, the McNemar-Bowker Test was used.

The gathered data show that the majority of the respondents in this study are male with 52.3% (215), those with ages 21-29 years old with 35.5% (146), college undergraduates with 38% (156), employed before and during the pandemic with 69.8% (287) and 60.8% (250), respectively and with monthly income of P20,001 to P30,000 before and during the pandemic with 38.4% (158) and 35% (144), respectively. It can be observed that 50.3% (206) of the respondents do not own any motorized vehicle and that the most owned motorized vehicle is motorcycle which has a percentage of 21.7% (89). Data also showed that before and during the pandemic, the main purpose of travelling is work with 66.2% (272) and 40.9% (168), mostly travel 5 times per week with 53.8% (221) and 26.5% (109) and around 6AM to 7AM with 28.5% (117) and 20.2% (83).

The transport mode choices before, during and after the pandemic is shown and visualized in Fig. 1.

Fig. 1. Transport Mode Choices Before, During and After the Pandemic.

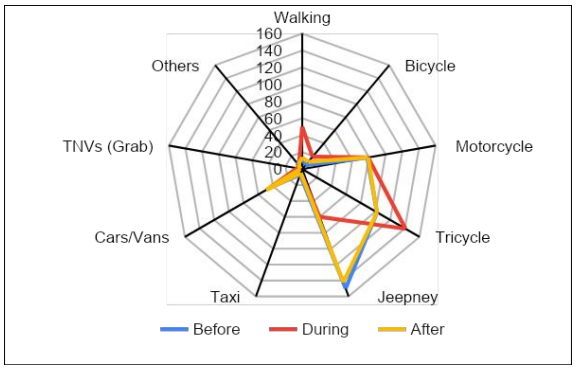

The selection of mode of transportation of the respondents (1) before vs. during the pandemic, (2) during vs. after the pandemic and (3) before vs. after the pandemic were cross-tabulated to determine the marginal homogeneity between the two using McNemar-Bowker Test. Table 2 shows the results of the statistical analysis.

Table 2. Results of McNemar-Bowker Test.

	Before vs During the Pandemic	During vs After the Pandemic	Before vs After the Pandemic
Test Statistic	102.302	99.238	11.016
p-value	< 0.001	< 0.001	0.528
Statistically significant?	Yes	Yes	No

The differences in transport mode preference before vs during the pandemic and during vs after pandemic are found to be statistically significant. However, the differences in mode choice before vs after the pandemic are not significant which indicates that no significant behavioral change is expected after the pandemic as they just wanted to return to normalcy.

For the relationship between the all the variables and the transport mode choice of the respondents, all of the variables had a significant relationship with the respondents' selection of transport mode before, during and after the pandemic. However, for the risk perceptions, all of the statements had a weak association with the mode choice which means that they are not significant factors influencing the selection of mode choice of the respondents. Table 3 shows the summary of the results of the statistical analyses.

Table 3. Relationship between the Variables.

Variables	Chi Square	Likelihood Ratio	p-value	Cramer's V
Sex				
Before the pandemic	0.6008	48.9421	<0.0001	0.3273
During the pandemic	46.3151	48.7149	<0.0001	0.3357
After the pandemic	45.1281	48.2578	<0.0001	0.3357
Age Group				
Before the pandemic	87.4089	88.2894	<0.0001	0.2663
During the pandemic	112.9256	117.8124	<0.0001	0.3026
After the pandemic	121.8151	121.6965	<0.0001	0.3143
Educational Attainment				
Before the pandemic	100.0609	94.741	<0.0001	0.2207
During the pandemic	98.6351	94.741	<0.0001	0.2191
After the pandemic	110.5556	108.1407	<0.0001	0.2319
Vehicle Ownership				
Before the pandemic	799.1737	565.0099	<0.0001	0.5693
During the pandemic	951.6884	647.6129	<0.0001	0.6212
After the pandemic	890.2277	624/7538	<0.0001	0.6008
Employment Status				
Before the pandemic	133.1598	121.6949	<0.0001	0.4025
During the pandemic	201.5698	157.9138	<0.0001	0.4952
Monthly Income				
Before the pandemic	195.9297	183.8392	<0.0001	0.3452
During the pandemic	204.4433	187.1926	<0.0001	0.3526
Travel Purpose				
Before the pandemic	153.8843	140.139	<0.0001	0.2736
During the pandemic	234.8141	187.4311	<0.0001	0.3086
Travel Destination				
Before the pandemic	293.8756	284.4878	<0.0001	0.4882
During the pandemic	284.8842	280.5499	<0.0001	0.4807
Trip Frequency				
Before the pandemic	139.9706	144.0664	<0.0001	0.2382
During the pandemic	222.5512	208.4653	<0.0001	0.3004
Trip Schedule				
Before the pandemic	192.9908	170.2802	<0.0001	0.4882
During the pandemic	212.6295	209.4511	<0.0001	0.4807

It is recommended to conduct the same study after the pandemic and have an assessment and comparison on the changes on travel behavior since the study only focuses on the changes on the travel behavior before and during the pandemic. It is also recommended to consider other travel characteristics influencing the selection of mode of transportation aside from travel purpose, travel destination, trip frequency and trip schedule.

Hydrophobic Anti-Corrosion Coatings for Steel Plates using Nanosilica Modified with Hexamethyldisilazane

Marish S. Madlangbayan[1, a *], Engelbert K. Peralta[1,b], Milagros M. Peralta[2,c], Carl Jerome N. Centeno[1,d], Paolo Miguel W. Abuan[1,e], Alvin Karlo G. Tapia[2,f], Rossana Marie C. Amongo[1,g], Francis M. Mulimbayan[1,h], Aidrean P. Opaco[1,i], and Maris Asuncion L. Bayhon[1,j]

[1]College of Engineering and Agro-Industrial Technology, Univ. of the Philippines Los Baños, Philippines

[2]College of Arts and Sciences Univ. of the Philippines Los Baños, Philippines

[a]msmadlangbayan@up.edu.ph, [b]ekperalta@up.edu.ph, [c]mmperalta@up.edu.ph, [d]cncenteno@up.edu.ph, [e]pwabuan1@up.edu.ph, [f]agtapia@up.edu.ph, [g]rcamongo@up.edu.ph, [h]fmmulimbayan@up.edu.ph, [i]apopaco@up.edu.ph, [j]mlbayhon@up.edu.ph

The utilization of chromate and lead-based corrosion inhibitors for metal parts in the construction industry is becoming a prime environmental and health concern. It was found that 61% of the commercially available enamel-based paints contain lead compounds ranging from 10,000 ppm to 156,000 ppm which exceeded the 90-ppm threshold value [1]. Thus, there is a need to develop non-toxic formulations as an alternative to the current corrosion inhibitors in the market. This study was conducted to develop a hydrophobic anti-corrosion coating using rice hull ash (RHA) nanosilica modified with hexamethyldisilazane (HMDS). The RHA nanosilica (Figure 1) was prepared using the sol-gel method which yielded an amorphous nanosilica with a polydispersity index (PDI) of 0.366 ± 0.1443 and a hydrodynamic diameter of 17.815 ± 0.7894 nm.

Fig. 1. Synthesized Nanosilica

The RHA Nanosilica was then used to formulate a silicate-based and silicate conversion coating that were applied to stainless steel (7mm x 7mm) samples using Successive Ionic Layer Adsorption and Reaction (SILAR) and Dip Coating methods, respectively. The silicate surface was then modified using HMDS to achieve a hydrophobic coating. The cured samples were subjected to contact angle test for hydrophobicity and electrochemical impedance spectroscopy (EIS) analysis at the frequency range of 0.005 Hz to 100 KHz. The cell setup for the EIS is shown in Figure 2.

Fig. 2. Cell Setup for EIS

Hydrophobicity test results (Figure 3) show a water contact angle (WCA) of 134^0 using ImageJ which confirmed the successful surface modification of the nanosilica surface [2].

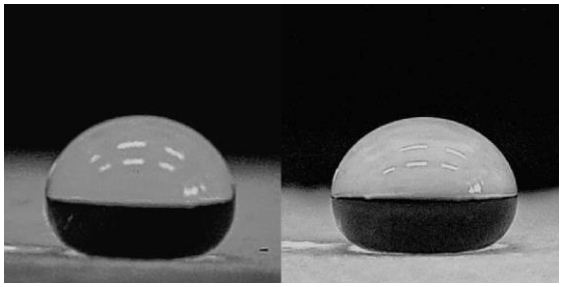

Fig. 3. Water Contact Angle

The EIS analysis showed a total impedance of 2.37×10^5 Ω and 1.94×10^6 Ω for the silicate-based and conversion coating, respectively. The Bode plots of the bare and coated stainless steel are shown in Figure 4.

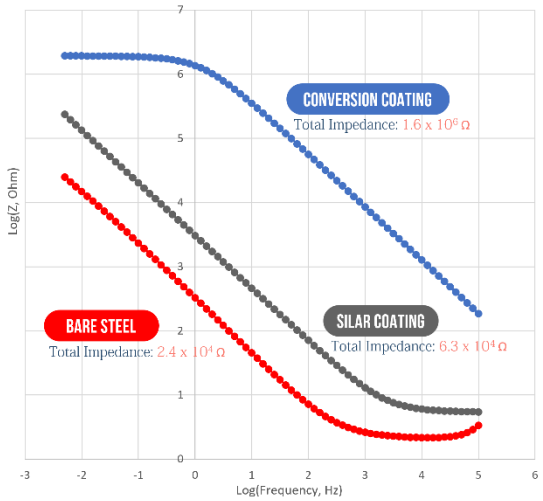

Fig. 4. Bode Plot

Based on the Bode plots generated using EIS (Figure 4), it was found out that the optimum formulation using the dip coating method exhibited the highest impedance readings among the coatings being developed. Both the WCA and EIS analysis results indicate that the HMDS-modified nanosilica coatings yielded an improved corrosion protection for stainless steel plates when compared to the performance of bare stainless steel.

KEYWORDS
Conversion Coating, Electrochemical Impedance Spectroscopy, Nanosilica, Rice Hull Ash, SILAR

REFERENCES

[1] ECOWASTE COALITION AND THE EUROPEAN UNION (2013) "Lead in New Enamel Household Paints in the Philippines National Report" by the Eco Waste Coalition and The European Union 2013

[2] CALDONA EB, SIBAEN JW, TACTAY CB, MENDIOLA SLD, ABANCE CB, AÑES MP, ... & DE GUZMAN, MMS. (2019). Preparation of spray-coated surfaces from green-formulated superhydrophobic coatings. SN Applied Sciences, 1(12), 1-9.

Cradle-to-Grave Life Cycle Assessment of a Pedestrian Bridge in University of the Philippines-Los Baños, Laguna, Philippines

Adrian Carlo A. Fajardo[1,a*], Maricel A. Eneria[1,b], Resmond L. Reaño[2,c], Emel Ken D. Benito[1,d], Andre C. Cruz[1,e]
[1]Department of Civil Engineering, University of the Philippines Los Baños, Philippines
[2]Department of Engineering Science, University of the Philippines Los Baños, Philippines
[a]aafajardo1@up.edu.ph, [b]maeneria@up.edu.ph, [c]rlreano@up.edu.ph, [d]edbenito@up.edu.ph, [e]accruz4@up.edu.ph

The amount of emissions from the construction industry is considered to be one of the major concerns in environmental pollution. These emissions associated with building a structure need to be assessed, to aid planning and policy-making in reducing the environmental and public health impacts. This study aimed to conduct a cradle-to-grave life cycle assessment (LCA) of a destroyed pipe and pedestrian bridge constructed in 1968 at the University of the Philippines-Los Baños, Laguna, Philippines, and damaged by a typhoon in 2006. Refer to Fig. 1 for the location of the bridge, marked with an "X". Fig. 2 shows the bridge after being damaged by the typhoon.

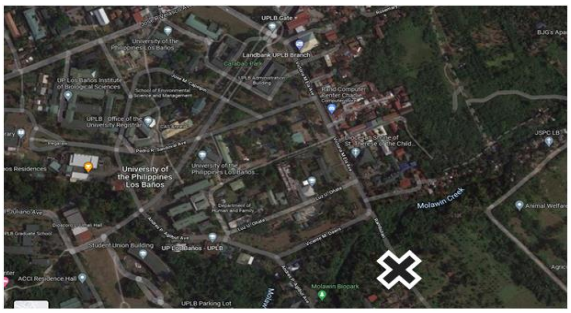

Fig . 1. Location of the bridge.

Fig. 2. The damaged bridge after the typhoon[1].

The data for the maintenance and demolition phase of the bridge was not available. The bridge is 1.2-m wide and 64-m long, made of reinforced and prestressed concrete materials. LCA was conducted using OpenLCA v.1.10 software with Ecoinvent 3.6 database, following ISO 14040 and ISO 14044 procedure, and CML 2001 methodology. Impact categories considered were abiotic depletion potential (ADP), acidification potential (AP), global warming potential (GWP), human toxicity potential (HTP), photochemical oxidation potential (POP), and terrestrial ecotoxicity potential (TEP).

Fig. 3 shows the contribution of emissions per life cycle stage, from the result of LCA. Manufacturing phase was found to be the highest contributor of sulphur dioxide (SO_2), phosphate (PO_4^{3-}), carbon dioxide (CO_2), 1,4-dichlorobenzene (DCB), antimony, and ethylene among all the life cycle stages, followed by the construction phase. The material transportation and structure demolition phase, however, were estimated to produce almost negligible environmental impacts.

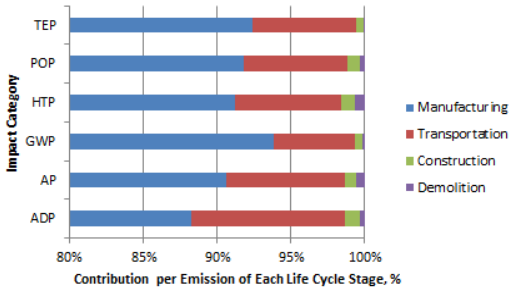

Fig. 3. Contribution of life cycle stages in each impact category

Additional results from LCA shown in Fig. 4 indicated that the prestressed concrete contributed the most in all impact categories considered, amounting to 50 to 80% of the total pollutants emitted. This material is preceded by lightweight concrete under all categories.

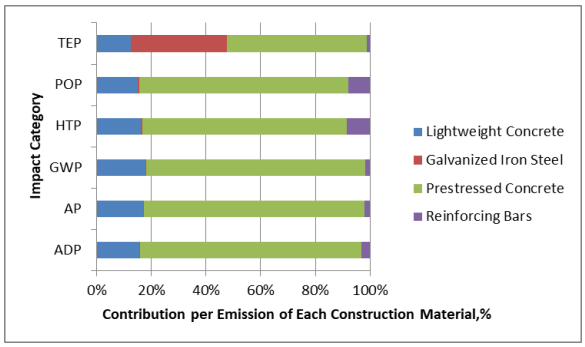

Fig. 4. Contribution of each building material in each impact category

A sensitivity analysis was done by varying the transportation distances to simulate the amount of emissions that can cause potential impacts to the environment. The analysis showed that the transportation of prestressed concrete released the highest amount of emissions in all impact categories, as observed on the steepness of the graphs of emission versus distance.

To reduce excessive emissions in the building of bridges, this paper recommends the use of scrap steels instead of the natural iron ores being mined and processed to manufacture reinforcing bars. Binders made from industrial by-products, such as blended cements containing fly ash, silica fume, slag, rice husk ash [2], or natural pozzolanic materials can also be used as substitute for Portland cement in prestressed and reinforced concrete members [3,4]. Prefabricated steels can also be used as replacement for prestressed concrete [5]. These claims can be tested by conducting LCA for future studies.

KEYWORDS

LCA, construction, pollution, sustainability, emissions

REFERENCES

[1] Carrillo, G. 2006 September 29. Aftermath ng milenyo part II. Retrieved from https://gccarrillo.wordpress.com/2006/10/07/what-happened-to-the-hanging-bridge-and-other-questions/ on August 19, 2021.

[2] Harvey, LD. 2021. Iron and steel recycling: review, conceptual model, irreducible mining requirements, and energy implications. Elsevier renewable and sustainable energy reviews, 138: 110553.

[3] Raghav M, Park T, Yang, HM, Lee, SY, Karthick, S, Lee, HS. 2021. Review of the effects of supplementary cementitious materials and chemical additives on the physical, mechanical, and durability of hydraulic concrete. Materials, 14: 7270.

[4] Jativa, A, Ruales, E, Etxeberria, M. 2021. Volcanic ash as a sustainable binder material: An extensive review. Materials, 14: 1302.

[5] Premiere Substructures. 2018. Substructures: Why prefabricated steel is the best alternative to precast concrete. Retrieved from https://www.premiersubstructures.com/prefabricated-steel/substructures-why-prefabricated-steel-is-the-best-alternative-to-precast-concrete/#:~:text=Prefabricated%20steel%20can%20be%20a,involved%20when%20constructing%20below%20ground on February 16, 2022.

Natural Fiber Reinforced Concrete: A Review on Mix Designs and Mechanical Properties

Gil S. Beltran
Polytechnic University of the Philippines, Manila, Philippines
Technological University of the Philippines-Cavite, Cavite, Philippines
gil_beltran@tup.edu.ph

ABSTRACT

Sustainable community and development are one of the key areas of concern in pursuit of the mandate given to various agencies of the government. Development of new engineering materials for construction and other allied disciplines are emerging to provide the demands of the industry and at the same time to improve the use of these materials by introducing new developments and methodologies. In this paper, 10 naturally occurring fibers that are used in the study of fiber reinforced concrete (FRC) are randomly chosen and evaluated based on their mix design considerations and the outcome of the mechanical test. Jute, abaca, coconut, pineapple leaf, bamboo, sisal, banana, flax, oil palm, and hemp are the selected natural fibers added to produce the reinforced concrete. They are compared and analyzed in terms of the matrix composition; the proportioning used and the water-cement ratio as a controlling factor in the mix design. These individual articles are further compared in the amount and length of fiber used in the mixture and how treatment affected the behavior of the matrix. The size of the specimen and the specification standards used in the study to evaluate the mechanical properties of the FRC are also given comparison. Based on the derived findings, the traditional matrix component of cement, sand, and gravel is the generally favored composition of the concrete but the use of larger and longer prismatic sections with steel reinforcement is becoming an option to simulate the actual behavior of the fiber in real construction. The range of fiber length that is commonly adopted and being considered in the research is from 10 to 50 mm. In terms of the effect of the fibers in the behaviors and flexural capacities when mixed with concrete, almost all the natural fibers contributed to a significant contribution to strengthening the inert capacity of concrete and improving the deflection resistance of the composite. However, in almost all these articles, they discovered that there is a small to no positive contribution to the compressive strength and split tensile resistance of the FRC.

KEYWORDS
natural fibers, fiber reinforced concrete,

A Cradle-to-Grave Life Cycle Assessment of a University Building

Miguel Carlo S. Alviar[1a], Maricel A. Eneria[1b], Resmond L. Reaño[2c], Ma. Hazel T. Castillo[1d], Richard Dean F. Morales[1e]

[1]Department of Civil Engineering, College of Engineering and Agro-Industrial Technology, University of the Philippines, Los Baños, College, Los Baños, Laguna, 4031, Philippines

[2]Department of Engineering Science, College of Engineering and Agro-Industrial Technology, University of the Philippines, Los Baños, College, Los Baños, Laguna, 4031, Philippines

[a]msalviar@up.edu.ph, [b]maeneria@up.edu.ph, [c]rlreano@up.edu.ph , [d]mtcastillo5@up.edu.ph, [e]rfmorales@up.edu.ph

Emissions brought by the activities and processes in the construction industry have created inevitable harm to the environment [1]. Life cycle assessment (LCA) methodology can provide vital information on the embodied emissions of the building and its impact during its life cycle. The LCA study will be beneficial for future improvements of the building and possible implementations of more advanced building technologies to mitigate adverse environmental impact to future projects. This study will aid in supplementing a more environment-oriented decision done by investors, shareholders, and owners of the buildings.

In this study, a life cycle assessment was performed on a university building (Fig. 1) using inventory data based on the Philippine construction sector, while the environmental impact was assessed using the CML2001 selected impact categories namely, global warming potential (GWP), ozone depletion potential (ODP), acidification potential (AP), eutrophication potential (EP), photochemical oxidation (PO), terrestrial ecotoxicity (TE), and abiotic depletion potential (ADP).

Fig. 1. The Rural Economic Development and Renewable Energy Center building located at University of the Philippines Los Baños

An LCA study is composed of four phases namely, the goal and scope definition phase, the inventory analysis phase, the impact assessment phase, and the interpretation phase[2]. Fig. 2 represents the necessary steps conducted in accomplishing the goals and scope of the LCA study.

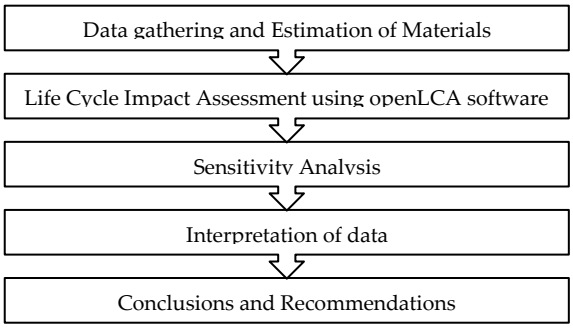

Fig. 2. Framework of the study

Construction material estimations were performed based on the detailed engineering plans provided by the planning office of the university. Materials such as concrete, steel, wood, glass, and paint were the only considered materials for quantifications. The functional unit used in the study is 1m² floor area. Fig. 3 shows the life cycle inventory system boundary used in the study.

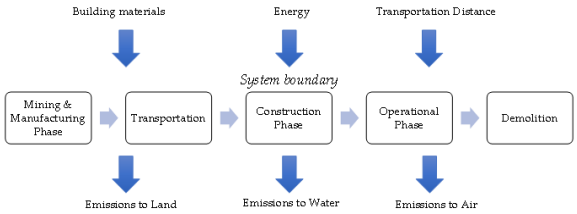

Fig. 3. The LCI System boundary.

Results showed that steel (combining the reinforcing steel and structural steel) followed by concrete contributed the greatest in the environmental impacts of the building (Fig. 4). For the impact categories of building's life stages, Fig. 5 shows that in abiotic depletion potential, the construction phase is prominent; while in acidification potential and global warming potential, the operation phase is the greatest contributor. However, for eutrophication, ozone layer depletion, photochemical oxidation, and terrestrial

ecotoxicity, the manufacturing phase dominates the other phases.

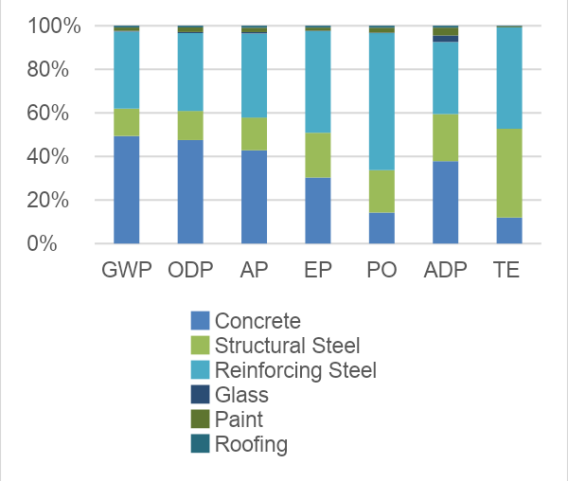

Fig. 4. Results in each impact category of the building materials used in the university office building

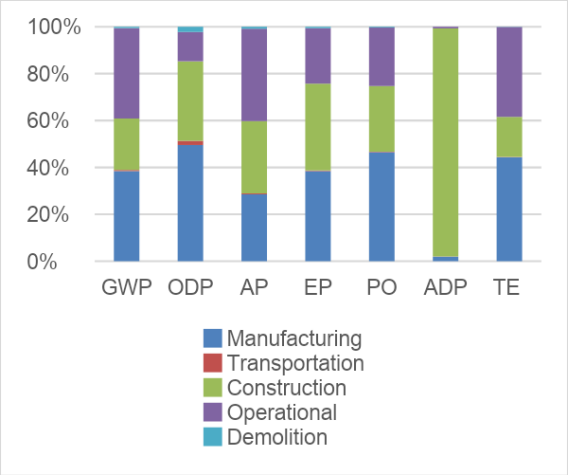

Fig. 5. Results in each impact category of the life stages of the university office building

Steel produces emissions more than 3000gms/kg of carbon monoxide which contribute to the PO and ODP [3]. The steel making industry is a major contributor to environmental problems such as climate change, photochemical smog, and ozone depletion[4]. Through the sensitivity analysis, the study was able to show the effectiveness of using recycled structural steel and reinforcing steel in mitigating the adverse effects of building construction as shown in Fig. 6.

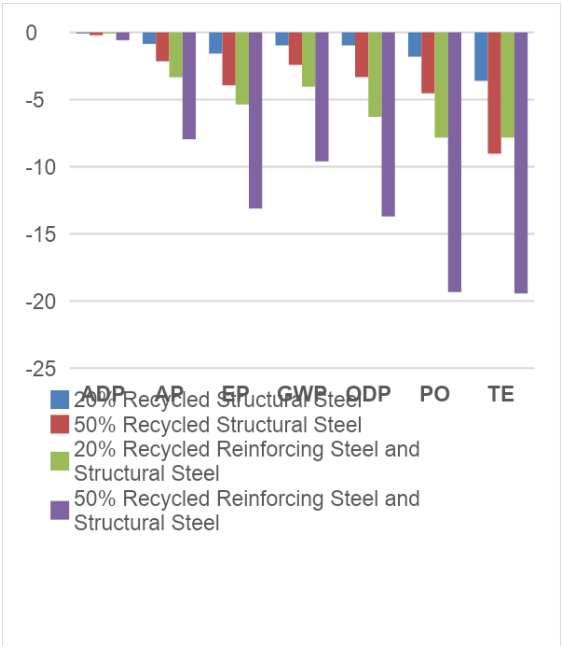

Fig. 6. Percentage difference of the environmental impacts of the building by varying the amount of recycled steel.

It can be observed that incorporating recycled steel in the university office building has caused a decrease in the initial percentages of all the selected impact categories.

The tools in LCA can effectively support the design criteria of new buildings, and aid in deciding the renovation strategy of a building [5]. Moreover, in effectively lessening the impacts brought by these conventional building materials, environmental-friendly alternatives should be introduced in the structure, not only for steel, but also for other building materials [3]. For instance, the use of recycled materials in a building, without compromising the structural integrity of the building, can help lessen the required material that needs to be manufactured. Hence, the production of unwanted emissions to land, water, and air can be mitigated.

KEYWORDS

Embodied emissions, life cycle assessment, building, steel, construction

REFERENCES

[1] Zolfagharian, S., Nourbakhsh, M., Irizarry, J., Ressang, A., & Gheisari, M. (2012). Environmental Impacts Assessment on Construction Sites. Construction Research Congress 2012.

[2] International Organization for Standardization. (2006). ISO 14040: Environmental management life cycle assessment principles and framework. Geneva, Switzerland.

[3] Lomite, H., Kare, S. (2009). Impact of Construction Material on Environment. Unpublished master's thesis – Civil Engineering. University College of Borås. Borås, Sweden

[4] Al-Zboon, K. K., & Forton, O. T. (2019). Indoor Air Quality in Steel Making Industries. Environmental Management and Sustainable Development, 8(1), 147.

[5] Giorgi, S., Lavagna, M., Campioli, A. (2019). LCA and LCC as decision-making tools for a sustainable circular building process. IOP Conference Series: Earth and Environmental Science, 296(1), 012027

Use of Pineapple Core Sugar Extract as Set Retarder in Cement Paste

Rondel A. Dela Cruz[1, a*], Richelle G. Zafra[2, b], Judie Ann A. Ramos[2, c], and Marish S. Madlangbayan[2, d]
[1]Teravera Corporation, Lipa-Alaminos Road, San Agustin, Alaminos, Laguna, Philippines
[2]Department of Civil Engineering, College of Engineering and Agro-Industrial Technology, University of the Philippines Los Baños, College, Laguna, Philippines
[a]rondeldelacruz@teravera.ph, [b]rgzafra@up.edu.ph, [c]jaaramos3@up.edu.ph, [d]msmadlangbayan@up.edu.ph

The performance of concrete highly depends on its plastic consistency before casting [1]. With the possible dangers of hot weather conditions and long-distance deliveries on the consistency of concrete, set retardation becomes essential.

Pineapple core is a bio-waste that contains sucrose, glucose and fructose which have set-retarding capacities [2]. In this study, pineapple core sugar extract was used as a set retarder in cement paste. Ethanol was added to the homogenized pineapple core as a solvent for the extraction of sugars from the material. Sugars from the core were separated from ethanol and water through the use of Biobase Rotary Evaporator. The sugar extract was then analyzed through Phenol-Sulfuric Method, and was proven to have a significant amount of total sugars—104mg sucrose/mL.

Varying percentages of the mass of cement—0% (control), 0.2%, 0.4%, 0.6% and 0.8%—of the extract were used to determine the behavior of the setting time as the extract percentage changes. A 27.5%-consistency was ensured in all the treatments. The delay in setting time of Type IP Portland cement was investigated having five cement paste groups with three replications per group. Vicat Needle Apparatus was used to determine the initial and final setting time of cement paste in accordance with ASTM C191, Standard Test Methods for Time of Setting of Hydraulic Cement by Vicat Needle [3].

Table 1. Setting time of cement paste at increasing pineapple core sugar crude extract

DOSAGE	SETTING TIME (min)	
	Initial	Final
0.0%	113.3	171.7
0.2%	153.3	248.3
0.4%	183.3	303.3
0.6%	218.3	335.0
0.8%	248.3	423.3

One-way Analysis of Variance, along with Dunnett's Test as the post-hoc test, verified that for both initial and final setting time, there is a significant difference between the control and the treatments.

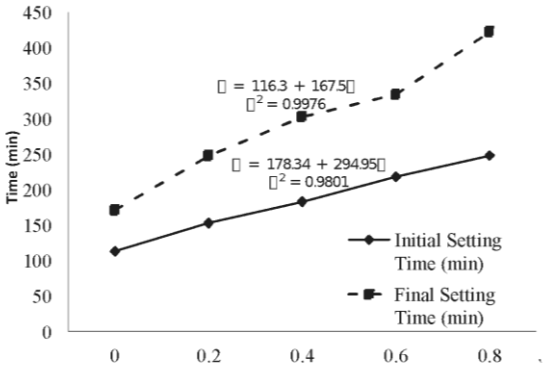

Fig. 1. Effect of the admixture on initial and final setting time of cement

As the extract percentage increases, the initial and final setting time also increase even up to 219% and 247% of the setting time at 0% dosage, respectively. Accordingly, the presence of pineapple core extract on the cement paste effectively retards both the initial and final setting time. The higher the admixture dosage means the greater retardation of setting time.

KEYWORDS
Pineapple core, sugar extract, set retarder, cement paste

REFERENCES

[1] AÏTCIN, P.-C. (2016). Retarders. In Science and Technology of Concrete Admixtures. Retrieved February 12, 2020 from http://doi.org/10.1016/B978-0-08-1006931.00018-7

[2] SITI ROHA, A. M., ZAINAL, S., NORIHAM, A., & NADZIRAH, K. Z. (2013). Determination of sugar content in pineapple waste variety N36. International Food Research Journal, 20(4), 1941-1943. Retrieved January 23, 2020 from http://www.ifrj.upm.edu.my

[3] ASTM C191-19. Standard Test Methods for Time of Setting of Hydraulic Cement by Vicat Needle, ASTM International, West Conshohocken, PA, 2019, www.astm.org

Characterization of harmonic distortion on office-academic buildings

Robert Christian Labalan[1, a*], Kim Jay R. Rosano[1,b*], Rodolfo A. Aguirre[1,c], Elvin D. Dulce[1,d]
[1]Department of Electrical Engineering, College of Engineering and Agro-Industrial Technology,
University of Philippines in Los Baños (UPLB), 4031, College, Laguna, Philippines
[a]rdlabalan1@up.edu.ph, [b]krrosano@up.edu.ph, [c]raaguirre@up.edu.ph, [d]eddulce@up.edu.ph

ABSTRACT
Distortions in the voltage and current waveforms introduced by system non-linearities and irregularities cause power quality issues in the system. These distortions can cause a number of negative effects in the system such as power loss, communication interference, resonant conditions, decreased shelf life, and even overcurrent in the neutral wire, hence the importance of identifying the presence and magnitude of harmonics. In this paper, characterization of harmonic distortion on office-academic buildings is performed. Using Fluke 435-II, power quality analysis was performed on 230V, 500kVA, 60Hz systems through harmonic distortion metrics. For comparison, the buildings were selected primarily on the characteristics of their usage, with heavy loading in the morning, and very light load at night. The results of the study showed different behavior between the voltage and current harmonics if compared to the behavior of the load. Total Harmonic Distortion (THD) on the system voltage is minimal but consistent despite the movement of the load throughout the day. At less than 1.8% THD, the voltage experiences minimal waveform distortion at the system point of connection. Current THD, on the other hand, has higher waveform distortion that reaches more than 40% THD. There is also a significant distortion in the current waveform at night when the system loading is low. Interestingly, the system load complemented the harmonic distortion at heavy loading as the harmonic distortion at those times consistently went down. Overall, harmonic distortion evaluation on both systems showed distortions external to the system. The results of this study could help in characterizing the system load and understanding flow of harmonic distortions in an electrical system.

KEYWORDS
Harmonics, Load behavior, Power Quality, THD

Probabilistic Modelling of Vehicular Accidents by Collision Type in Metro Manila, Philippines

Gracelou Marie B. Tapang[1, a], Ma. Bernadeth B. Lim[1,b], Judie Ann A. Ramos[1,c*], and Jedidiah Joel C. Aguirre[1,d]

[1] Department of Civil Engineering, University of the Philippines Los Baños, Philippines

[a] gbtapang@up.edu.ph, [b] mblim4@up.edu.ph, [c] jaramos3@up.edu.ph, [d] jcaguirre@up.edu.ph

Road safety is recognized by the World Health Organization (WHO) as a global issue. In the Philippines, it is in the National Capital Region, the second most populated region, that a high number of motorists contribute to traffic congestion with high probability of road crash occurrence. The road crash occurrence must be minimized especially along the major roads of Metro Manila due to its alarming crash count.

There are different factors to consider as to why a road crash occurs. Rear-end collisions frequently happen due to insufficient vehicle spacing while trucks are involved in a single-vehicle collision, in addition to weather-related factors[1,2]. On the other hand, sideswipe collisions are mostly associated with lane-changing vehicles[3].

This study first identifies the road crash locations by heat maps. Also this study attempts to test logistic regression's applicability to estimate collision type outcomes (rear-end and sideswipe) to multilane urban roads with high-speed limit. Similarly, this study attempts to improve previous research by expanding collision type choices and additional crash-site explanatory variables. The study provides insights into ways to improve and develop road safety and road design.

METHODOLOGY

This study examined the relationship between crash occurrences in EDSA, C-5 Road and Commonwealth Avenue and road characteristics according to collision type. A total of 5,197 road crash incidents for the years 2017 to 2019 were identified and considered. This was further specified to designated areas with counts of 3,486, 1,088, and 623 samples in EDSA, C-5 Road, and Commonwealth Avenue, respectively. The crash data which includes the location, coordinates, light condition, and type of crash was obtained from the database "Data for Road Incident Visualization Evaluation and Reporting (DRIVER)", while road characteristics were obtained by manual observations using the Google Earth Pro.

The crash risk factors selected for this study were limited to light condition (LC), bound direction (BD), lane width (LW), number of lanes (NL), presence of median barriers (B), road signs, pedestrian crossing (PC), U-turn (UT) and right turn (RT), type of land use (LU), and lane position (LP). These variables determined the likelihood of crash occurrence by type such as side swipe, rear end, single vehicle, angle, and head on using logistic regression analysis. The statistical analysis along with all the computations involved to generate the models was done in a statistical program called SPSS. The odds ratio (Eq. 1) which describes the likelihood of events[10], where O is the odds ratio P_R is the probability that the crash is rear-end.

$$O = \frac{P_R}{1-P_R} \qquad (1)$$

The logarithmic of the determined odds ratio is the logit transformation (Eq. 2) of the probability of the present event (rear-end event), where, Y_R is the logit transformation that the collision is rear end, β_0 is the model constant, $\beta_n\chi_n$ is the unknown parameters with the explanatory variables. Mathematically, the logit transformation of the probability of the absent event (sideswipe event) is the negative of the equation.

$$Y_R = \beta_o + \sum \quad \beta_n\chi_n \qquad (2)$$

The parameters were estimated using the maximum likelihood estimation (MLE) and the probability of an event is represented by Equation 3 and Equation 4, where z is the logit transformation that the collision is rear-end P_S is the probability that the crash is side swipe.

$$P_R = \frac{e^z}{1+e^z} \qquad (3)$$

$$P_S = 1 - P_R = \frac{1}{1+e^z} \qquad (4)$$

The best model was determined using the backward stepwise method. Models with the most significant variables were compared accordingly with the pseudo-R^2 values. The model in comparison with higher R^2value implies a better model[11]. Moreover, model validity was in accordance with the model significance from the model fitting information with a null hypothesis that the model performs better with intercept only[4]. From the SPSS[5], area under the curve (AUC) as a measure was used for the goodness of fit and accuracy evaluation of the model. To validate the results of the models, the Mean Square Error (MSE) was used.

RESULTS AND DISCUSSIONS

In addition to the heat maps, findings in this study include several significant correlations between variables for all the train sets considered. However, the values were all less than 0.7 and all variables were still considered in the modelling except for the presence of median barrier for EDSA and Commonwealth Avenue, and presence of pedestrian crossing in EDSA due to collinearity. The following provides a summary of the findings in this study.

Heatmaps. Fig. 1 shows the generated heat maps for (a) EDSA, (b) C-5 Road, and (c) Commonwealth Avenue, which are the locations of the greatest number of collisions in NCR.

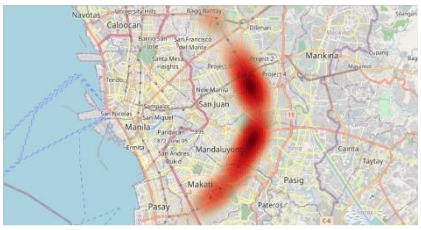

(a)

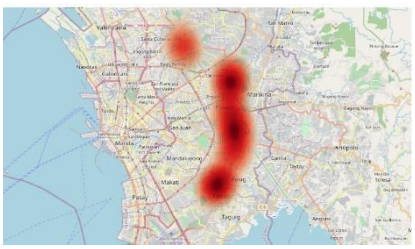

(b)

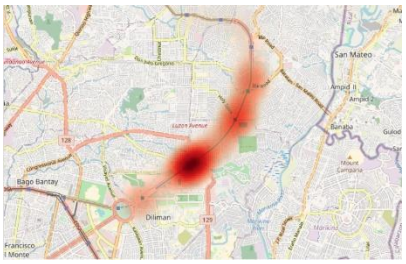

(c)

Fig. 1. Heatmaps for (a) EDSA, (b) C-5 Road, and (c) Commonwealth Avenue.

Logit Models. The model with (R^2 = 0.238-0.318) was selected as the final logistic regression model for EDSA. The model includes the presence of u-turn, lane position with innermost as the base, light condition (Day), bound direction (South), lane width, presence of road sign, and along with the model constant. The overall accuracy of the model is 69.9% while the overall AUC is 0.765.

The model, with (R^2 = 0.158 -0.218) was selected as the best model for C-5 road. Significant variables include lane position base innermost, Light condition (Day), number of lanes, presence of U-turn. The overall accuracy is 67% and the overall AUC is 0.712. Similar results from the EDSA model were found from the model fitting information.

Similarly, eight models were tested for selection, and the model with (R^2 = 0.117-0.182) was chosen as the final model for this highway. Significant variables were limited to lane position, light condition (Day), and number of lanes. The overall accuracy is 78.4% and overall AUC is 0.738. Same conclusion was drawn from the other models for the model fitting information.

Validation of Logistic Regression Model Results. The generated models were applied to its respective test set. The EDSA model, C-5 Road model and Commonwealth Avenue Model correctly identified 341 side swipe and 389 rear end, 179 side swipe and 32 rear end, 142 side swipe, respectively. The overall correct prediction was 69.9% (MSE = 0.3), 64.5% (MSE = 0.35), and 75.9% (MSE = 0.24), respectively. The relatively high accuracy and relatively low MSE, the results were acceptable.

CONCLUSIONS

The validity of the model results was tested by applying the built models to its respective test set and obtained very low percentage difference from the

train set and low MSE. Hence, the results were acceptable and the corresponding logit models for the three roads can be used for forecasting future crashes considering rear-end and sideswipe collisions.

RECOMMENDATIONS

This study is limited with the use of data from DRIVERS. It is recommended to acquire raw data from a government agency for counterchecking. Also, in future studies, consideration of other road geometry, road characteristics, road users' behavior, and actual traffic count is recommended for the improvement of the study. The discarded categories may be further investigated by specifically focusing on these occurrences. In line with this, the inclusion of road crashes in arterial intersections together with the segments may also be examined. The generated logistic models for the three roads may be further examined through external validation and assessment of model transferability by using data from other locations. Lastly, the study may be improved by considering other discrete outcome models.

KEYWORDS

Correlation analysis, logistic regression, vehicular accidents, internal validation

REFERENCES

[1] Dimitriou L, Stylianou K, Abdel-Aty MA. 2018. Assessing rear-end crash potential in urban locations based on vehicle-by-vehicle interactions, geometric characteristics and operational conditions. Accident Analysis & Prevention, 118, 221–235. DOI: https://doi.org/10.1016/j.aap.2018.02.024

[2] Naik B, Tung LW, Zhao S, Khattak AJ. 2016. Weather impacts on single-vehicle truck crash injury severity. Journal of Safety Research, 58, 57–65. DOI: https://doi.org/10.1016/j.jsr.2016.06.005

[3] Intini P, Berloco N, Fonzone A, Fountas G, Ranieri V. 2020. The influence of traffic, geometric and context variables on urban crash types: A grouped random parameter multinomial logit approach. Analytic Methods in Accident Research, 28, 100141. DOI: https://doi.org/10.1016/j.amar.2020.100141

[4] IBM. (2014). Information Criteria. Retrieved from https://www.ibm.com/docs/en/spss-statistics/23.0.0?topic=effect-information-criteria last 15 February 2022.

[5] LAERD STATISTICS. (2018). How to perform a Binomial Logistic Regression in SPSS Statistics. Retrieved from https://statistics.laerd.com/spss-tutorials/binomial-logistic-regression-using-spss-statistics.php last 15 February 2022.

AC Conductivity of Gel Phantom with Varying Degree of Defect

Arvin Lester C. Jusi[1, a *], Alvin Karlo G. Tapia[1,b], John Lorenzo M. Reyes[2,c], Ravtor A. Lebosada[2,d], Viktor Joshua L. Belizario[2,e], Melvin C. Ilang-Ilang[2,f], Rock Christian V. Tomas[2,g], and John Paolo A. Ramoso[2,h]

[1]Institute of Mathematical Sciences and Physics, University of the Philippines Los Baños, College, Laguna, 4031 Philippines

[2]Department of Electrical Engineering, University of the Philippines Los Baños, College, Laguna, 4031 Philippines

[a]acjusi@up.edu.ph, [b]agtapia@up.edu.ph, [c]jmreyes20@up.edu.ph, [d]ralebosada@up.edu.ph, [e]vlbelizario@up.edu.ph, [f]mcilangilang3@up.edu.ph, [g]rvtomas@up.edu.ph, [h]jaramoso@up.edu.ph

Gel phantoms are useful materials in medical diagnostics and impact testing. Depending on the preparations, the gel phantom can model various tissues by its bulk, microscopic, or molecular components. As a result, damages made to a gel phantom due to impact are similar to those observed in real tissues[1]. Therefore, impact testing on gel phantoms can provide suggestive settings for actual medical diagnostics, bioengineering, and industrial use. These applications require the production of high-quality gel phantoms to meet certain standards, such as consistency (i.e. monitoring the factors that may affect the gel's consistency)[2]. During actual preparation and synthesis, gels are likely to be damaged or have internal defects[3]. As a model material, it would be useful to characterize and differentiate these defects. Since the bulk, microscopic, and molecular components of gel phantoms have responses under an AC electric field, AC Impedance Spectroscopy is an effective technique to measure these defects.

A wide variety of methods for preparation of gel phantoms suited for impact testing applications already exist[2]. In this study, a commercially-available gel powder (Knox® Unflavored gelatin) was used to create gel phantoms. It was turned into a solution by mixing 28.3 g of the gelatin powder was to 220 mL of hot water. The solution was allowed to settle at a temperature of 4-8°C. After two hours, the solution was subjected to a hot water bath until it was liquified once again. After the solution had melted, it was allowed to cool down to room temperature. Then after 30 minutes, the solution was allowed to finally settle under a temperature of 4-8°C for 12 hours. This method yielded a robust gel that has a very slow dehydration. Cylindrical samples with a diameter of 1.8 cm were cut from the gel using a ring. The defects were formed by piercing a needle through the samples and the degree of defect was varied by increasing the number of piercings in the samples (see Fig. 1).

The AC conductivities of the gel samples with different degrees of defects were derived from the AC impedance (see Fig. 2). The conductivities at 20 Hz (leftmost part of the plot) follow an increasing trend as the degree of defects increases. This is due to water leakage in the pierced regions, which promotes conduction of charged species. At the higher frequency region, the conductivities exhibit a plateau which is due to the mechanisms of space charge relaxation[4] that is related to the charge distribution in the gel. However, Fig. 2 also shows that higher defects lead to lower conductivities at higher frequencies. The localization of charges due to the defect-induced barriers at higher frequencies may account for this phenomenon.

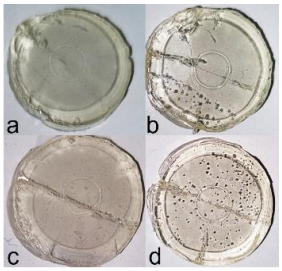

Fig. 1. Photos of gel samples with a) no defect, b) 1st degree defect, c) 2nd degree defect, and d) 3rd degree defect

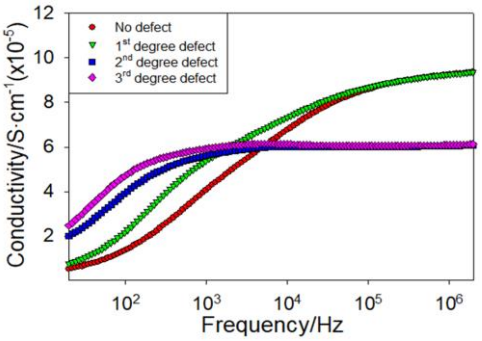

Fig. 2. AC Conductivities of the Gel samples with and without defects

KEYWORDS

Gel Phantom, Defect, AC Impedance, Equivalent Circuit

REFERENCES

[1] Jin Y, Mai R, Wu C, Han R, Li B. 2018. Comparison of ballistic impact effects between biological tissue and gelatin. Journal of the Mechanical Behavior of Biomedical Materials. 78: 292-297.

[2] Carr DJ, Stevenson T, Mahoney PF. 2018. The use of gelatine in wound ballistics research. SPC International Journal of Legal Medicine. 132: 1659-1664.

[3] Bertasa M, Dodero A, Alloisio M, Vicini S, Riedo C, Sansonetti A, Scalarone D, Castellano M. 2020. Agar gel strength: A correlation study between chemical composition and rheological properties. European Polymer Journal. 123: 109442.

[4] Bandara TMWJ, Mellander BE. 2011. Evaluation of Mobility, Diffusion Coefficient and Density of Charge Carriers in Ionic Liquids and Novel Electrolytes Based on a New Model for Dielectric Response. Ionic Liquids: Theory, Properties, New Approaches, IntechOpen. 383-406.

Gas Transmission Rates of Mango (*Mangifera indica* L. 'Carabao') Peel with Chitosan-Nanosilica Coating

Ma. Camille G. Acabal[1,a*], Kevin F. Yaptenco[2,b], Jessie C. Elauria[3,c] and Elda B. Esguerra[4,d]

[1,2,3] Institute of Agricultural and Biosystems Engineering, College of Engineering and Agro-Industrial Technology, University of the Philippines Los Baños, Laguna 4031, Philippines

[4] Postharvest Horticulture Training and Research Center, College of Agriculture and Food Science, University of the Philippines Los Baños, Laguna 4031, Philippines

[a] mgacabal@up.edu.ph, [b] kfyaptenco@up.edu.ph, [c] jcelauria@up.edu.ph, [d] elda_esguerra@yahoo.com

Fruit coating is a form of modified atmosphere packaging (MAP) that involves the modification of atmospheric condition inside the fruit to prevent or minimize deterioration[1]. The basis for selecting the appropriate coating formulation for a fruit depends on the permeability of the coating material and the rate of gas exchange between the fruit and the environment[2,3]. One way of determining the gas exchange is by direct measurement of gas transmission rates of fruit peels and coating materials[2]. However, gas transmission rates of coating materials and coated produce cannot be compared because the measurement of barrier properties of coatings is carried out using different techniques in a range of environmental conditions that are very different during the storage of coated produce[1,4]. Hence, for optimization of surface coating for fruits and vegetables, direct measurement of gas transmission rates of coated commodity under controlled environmental conditions should be employed. This study aimed to determine the oxygen (O_2) and carbon dioxide (CO_2) transmission rates of mango peel as affected by chitosan (CS) and nanosilica (NS) composite fruit coatings under different storage temperatures using the exponential decay method.

The fruit coatings were prepared by dissolving CS powder (0.75%, 1%, 1.5%, 2%, w/v) in an aqueous solution of glacial acetic acid (0.25%, v/v) and stirred (800 rpm at 60°C) for two hours. NS-in-fluid dispersion (0.06%, w/v) was prepared by stirring (800 rpm at 30°C) the solution for 30 minutes before sonicating for 5 hours. 1.5% and 2% CS were mixed with 0.06% NS to obtain CS-NS solutions. The solutions were amended with Tween 80 (0.1%, v/v) and 1 M NaOH. The coatings were 0.75% CS, 0.75% CS+0.03% NS, 1% CS, and 1% CS+0.03% NS.

The peels were obtained from green and mature mango fruits[2], and the outer surface was dipped in the coating for one minute. O_2 and CO_2 transmission rates of the peel samples at three storage temperatures were estimated using Moyl's Exponential Decay Method[2,5] and are presented in Table 1 and Table 2.

Table 1. Gas transmission rates (mL $cm^{-2}h^{-1}$) *of peels under three storage temperatures over 15 trials*

Temperature (°C)	O_2	Co_2	Source
15	1.68[b]	3.29[a]	Experimental
20	2.16[a]	3.80[a]	
25	2.39[a]	3.71[a]	
14	1.11	3.51	[2]
27	1.43	3.76	

Means within group in a column followed by a common letter a differ with each other at Tukey's Honest Significance Difference at 5% level.

The mean (n=15) gas transmission rates of uncoated mango peel are close to the published data where the average O_2 and CO_2 transmission rates of mature mango with peel color index 1 (green) were higher at 27°C than at 14°C[2]. Gas transmission rates are increasing with increasing temperature. High temperature increases the energy level of permeating molecules, thereby increasing the permeability values [3,4].

In all temperature regimes, gas transmission rates are higher in peels coated with 0.75% than 1% CS. The measured thickness of 1% CS was 3.65 μm and 2.55 μm for 0.75% CS which means that the effective path for diffusion is longer when peels are coated with higher concentrations of CS[6]. The incorporation of 0.03% NS decreased the O_2 transmission rate by 10% to 20% and CO_2 transmission rate by 5% to 14%. The presence of the ordered dispersed silicate layers forces the gas traveling through the film to follow a tortuous or maze-like path [7].

Table 2. Gas transmission rates (mL $cm^{-2}h^{-1}$) *of coated peels under three temperatures over 6 trials*

Treatment	15°C		20°C		25°C	
	O_2	CO_2	O_2	CO_2	O_2	CO_2
0.75% CS	0.8[a]	3.0[a]	0.94[a]	3.16[a]	1.14[a]	3.24[a]
0.75% CS + 0.03% NS	0.66[b]	2.85[a]	0.83[a]	2.91[a]	0.99[a]	3.04[a]
1% CS	0.45[c]	1.68[b]	0.53[b]	1.92[b]	0.60[b]	2.02[b]
1% CS+ 0.03% NS	0.41[c]	1.59[b]	0.45[b]	1.67[b]	0.53[b]	1.74[b]

Means within group in a column followed by a common letter do not differ with each other at Tukey's Honest Significance Difference (HSD) at 5% level.

O_2 transmission rate of coated peels is reduced to over half of the value of the uncoated peel as seen in Fig. 1. Coatings exert their effect on the peel permeance to gases by blocking the lenticels and improving the coverage of cracks in the cuticle[1].

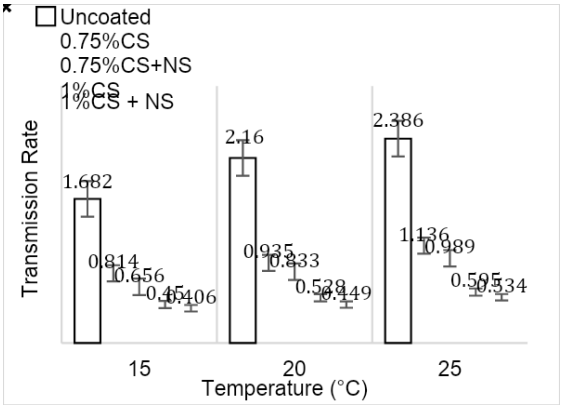

Fig. 1. O_2 transmission rate of coated and uncoated mango peel at different storage temperatures

The gas transmission rates of the peel coated with CS-NS can be further used in determining the compatibility of a formulated CS-NS composite as a coating for mango fruits to extend postharvest life. This could be done by comparing the oxygen transmission rates of the coated peel with the O_2 consumption of the fruit during respiration at a given temperature and relative humidity. This could also be done to other coating materials such as polysaccharides like starch and alginate, and to other fruits to prevent injuries related to exposure to gas concentrations during storage[2].

KEYWORDS

Gas exchange, fruit coating, modified atmosphere packaging, peel permeance

REFERENCES

[1] Aramante C, Banks N, Ganesh S. 2001. Relationship between character of skin cover of coated pears and permeance to water vapor and gases. Postharvest Biology and Technology. 21: 291-301.

[2] Flores FT, Yaptenco KF, Serrano EP. 2019. Determination of oxygen and carbon dioxide gas transmission rates of mango (*Mangifera indica* L. cv 'Carabao') peel using exponential decay method and respiration mass balance. Philippine Journal of Agricultural and Biosystems Engineering, 15, 63-74.

[3] Gennadios A, Weller C, Testin RF. 1993. Temperature effect on oxygen permeability of edible protein-based films. Journal of Food Science. 58: 212-214.

[4] Hong SI, Krochta JM. 2006. Oxygen barrier performance of whey-protein-coated plastic films as affected by temperature, relative humidity, base film and protein type. Journal of Food Engineering. 77: 739-745.

[5] Moyls L, Hocking R, Beveridge T, Timbers G. 1992. Exponential decay method for determining gas transmission rate of films. In Transactions of the American Society of Agricultural Engineers. 35: 1259-1265.

[6] Dang KM, Yoksan R. 2016. Morphological characteristics and barrier properties of thermoplastic starch/chitosan blown film. Carbohydrate Polymers. 150: 40-47.

[7] Ray SS, Okamoto VM. 2003. Polymer/ layered silicate nanocomposites: a review from preparation to processing. Progress in Polymer Science. 28: 1539-164

Poster Presentations

Food Systems, Bio Process Engineering, Agricultural and Fisheries Mechanization

Development of a Manually Operated Checkrow Seeder for Rice Production Systems	Mark Angelo F. Ranches, Rossana Marie C. Amongo, Ralph Kristoffer B. Gallegos, Erwin P. Quilloy, and Patricia Ann J. Sanchez

Land and Water Resources Engineering, Biomass and Biofuels - Renewable Energy

Integration of Life Cycle Analyiss and System Dynamics for Carbon Footprint Assessment of Bioelectricity Production from Rice Straw	R.L. Reano, V.A.N de Padua
Micro-Hydropower Generator Feasibility Study with Inflow Variations Consideration	Melvin A. Jaurigue, Kim Jay R. Rosano, Gabriela Monica M. Gonzales, Krystynne D. Ureta
A P-graph Approach for Planning Sustainable Rice Straw Management Networks	Maria Victoria Migo-Sumagang, Michael Angelo B. Promentilla
Bi-variate and CM Plotting of the Sediment Dynamic Process in the Sebou Estuary (Moroccan Atlantic Coast)	S. Haddout, K.L. Priya, Joan Cecilia C. Casila, A.M. Hoguane

Environmental Engineering and Waste Management

GIS-based Mapping of Appropriate Soil Texture-Based Four-Wheel Tractor Power Ratings in the Philippines	Rossana Marie C. Amongo, Ronaldo B. Saludes, Ralph Kristoffer B. Gallegos, Patrick Lemuel P. Relativo, Adrian Daniel L. Pantano, Ria Salustia DG Duminging, Gherlee Nelle L. Lalap-Borja, Julius John Paul A. Cunan

Materials Engineering, Electrical Engineering, Infrastructure and Civil Engineering

Cradle-to-Grave Life Cycle Assessment of a Pedestrian Bridge in University of the Philippines Los Banos, Laguna, Philippines	Adrian Carlo A. Fajardo, Maricel A. Eneria, Resmond L. Reano, Emel Ken D. Benito, Andre C. Cruz
Natural Fiber Reinforced Concrete: A Review on Mix Designs and Mechanical Properties	Gil S. Beltran
A Cradle-to-Grave Life Cycle Assessment of a University Building	Miguel Carlo S. Alviar, Maricel A. Eneria, Resmond L. Reano, Ma. Hazel T. Castillo, Richard Dean F. Morales
Characterization of Harmonic Distortion on Office-Academic Buildings	Robert Christian D. Labalan, Kim Jay R. Rosano

iCEAT 2022

23 February 2022 (Day 1)

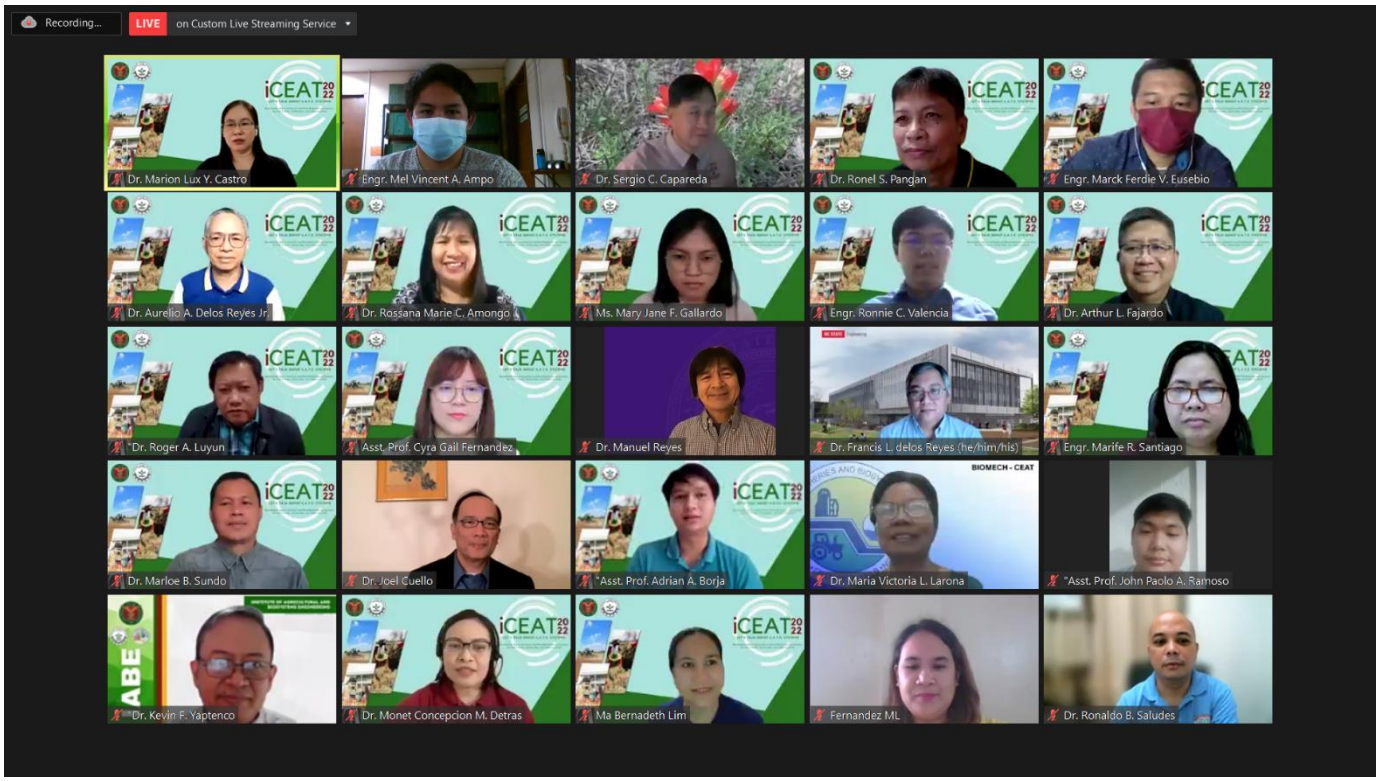

24 February 2022 (Day 2)

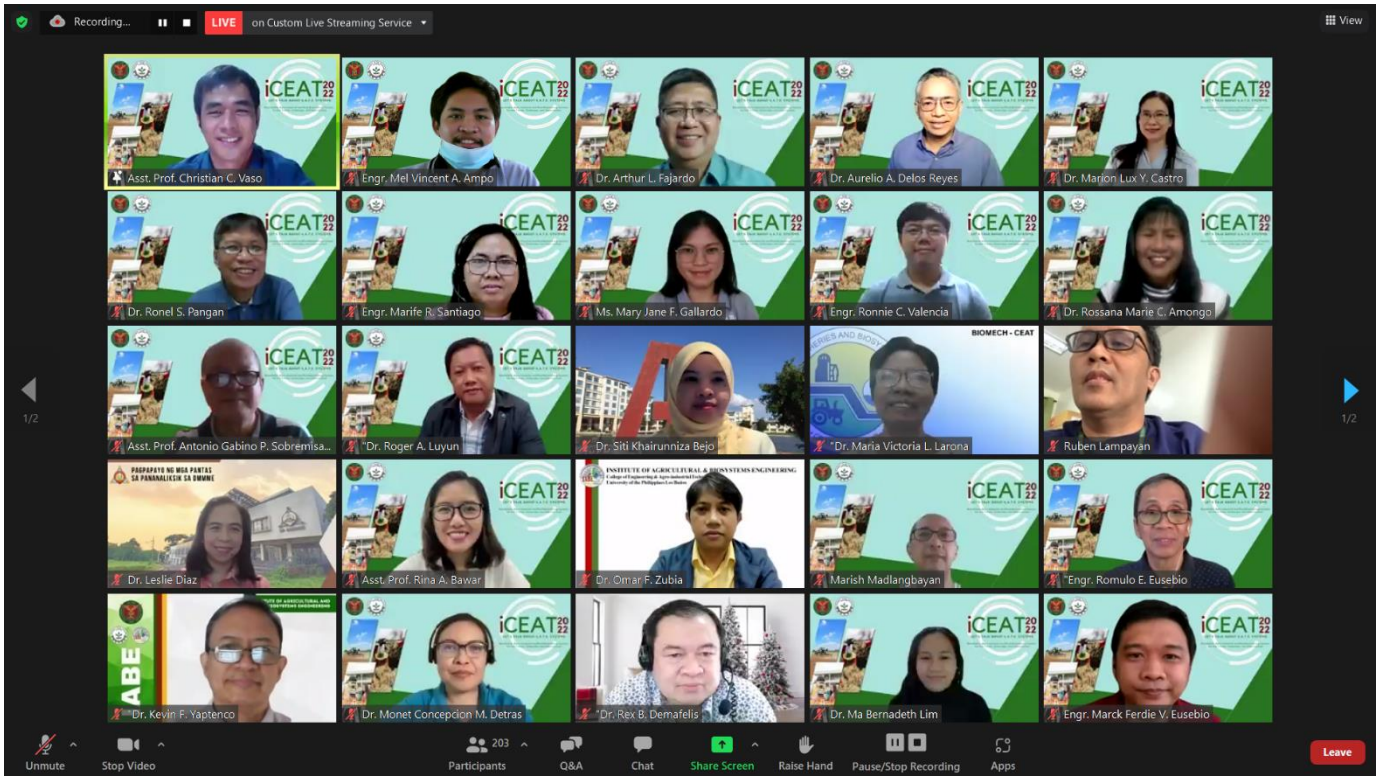


Recording...
View
Asst. Prof. Christian C. Vaso
Engr. Mel Vincent A. Ampo
Dr. Josefa Angelie D. Revilla
Sam Mangaoang
Dr. Ronel S. Pangan
Engr. Ronnie C. Valencia
Dr. Arthur L. Fajardo
*Dr. Butch G. Bataller
UPLB_Cyra Fernandez
*Dr. Roger A. Luyun
Mute
Engr. Marife R. Santiago
Dr. Marion Lux Y. Castro
Toni-An Mae Salcedo
Dr. Ma Bernadeth Lim
*Asst. Prof. Keynty Boy V. Magtoto
Asst. Prof. Jedidiah Joel C. Aguirre
Mary Cris Aleguen
Maria Victoria Castillo
*Dr. Ralph Kristoffer B. Gallegos
Esperidion Suñaz
Dr. Rossana Marie C. Amongo
*Dr. Maria Victoria L. Larona
Dr. Rowena B. Carpio
Foliente J
Asst. Prof. Antonio Gabino P. Sobremisa...
1/3
1/3
Mute
Stop Video
Participants
103
Q&A
Chat
Share Screen
Raise Hand
Pause/Stop Recording
Apps
Leave

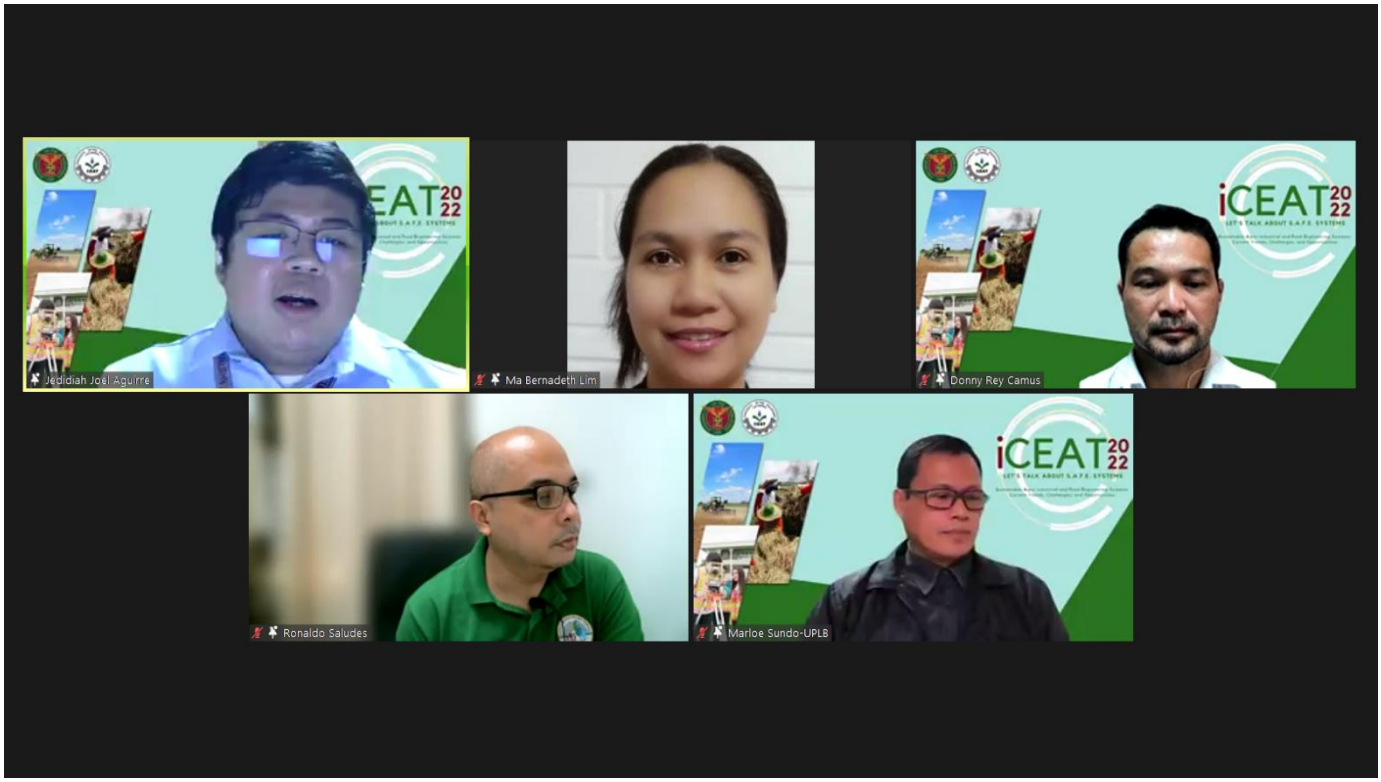
Jedidiah Joel Aguirre
Ma Bernadeth Lim
Donny Rey Camus
Ronaldo Saludes
Marloe Sundo-UPLB

iCEAT 2022 Steering and Working Committees

STEERING COMMITTEE:

Chair:	Dr. Rossana Marie C. Amongo
Co-chair:	Dr. Ronel S. Pangan, BIOMECH
Members:	Dr. Arthur L. Fajardo, AMTEC Dr. Monet Concepcion M. Detras, DChE Dr. Roger A. Luyun, Jr., IABE Asst. Prof. Jedidiah Joel C. Aguirre, DCE Asst. Prof. Roderick L. Catriz, DEE Dr. Josefa Angelie D. Revilla, DIE Asst. Prof. Christian C. Vaso, DES Dr. Ralph Kristoffer B. Gallegos, DME Dr. Marion Lux Y. Castro, DO

ORGANIZING COMMITTEE:

Chair:	Dr. Arthur L. Fajardo, AMTEC
Co-chair:	Dr. Ronel S. Pangan, BIOMECH
Members:	Dr. Kevin F. Yaptenco, AFBED-IABE Asst. Prof. Keynty Boy V. Magtoto, ABSEED-IABE Asst. Prof. Mary Louise P. Pascual, AFBED-IABE Dr. Ruben M. Lampayan; , LWRED-IABE Asst. Prof. Adrian A. Borja, AMPED-IABE Dr. Rex B. Demafelis, DChE Dr. Ramon Christian P. Eusebio, DChE Dr. Ma. Bernadeth B. Lim, DCE Asst. Prof. Emel Ken D. Benito, DCE Asst. Prof. John Paolo A. Ramoso, DEE Asst. Prof. Kim Jay R. Rosano, DEE Dr. Diana Marie R. De Silva, DIE Asst. Prof. Maria Liezel P. Caroche, DIE Dr. Ralph Kristoffer B. Gallegos, DME Engr. Frederic James V. Espiritu, DME Dr. Jey-R S. Ventura, DES Asst. Prof. Claire L. Garing, DES Engr. Romulo E. Eusebio, AMTEC Engr. Fatima Joy J. Raytana, AMTEC Dr. Maria Victoria L. Larona, BIOMECH Dr. Jose D. de Ramos, BIOMECH

INVITATION AND PROGRAM COMMITTEE:

Chair:	Dr. Marion Lux Y. Castro, Associate Dean's Office
Co- Chair:	Dr. Rubenito M. Lampayan, LWRED-IABE
Members:	Dr. Rossana Marie C. Amongo, Dean's Office Dr. Roger A. Luyun, Jr., IABE Asst. Prof. Keynty Boy V. Magtoto, ABSEED-IABE Engr. Romulo E. Eusebio, AMTEC Dr. Rex B. Demafelis, DChE Dr. Butch G. Bataller, DChE Asst. Prof. Jedidiah Joel C. Aguirre, DCE Asst. Prof. Glenson R. Panghulan, DCE Engr. Kyrstynne D. Ureta, DEE Engr. Marc Joseph S. Villanueva, DIE

REGISTRATION COMMITTEE:

Chair:	Dr. Ronel S. Pangan, BIOMECH
Co-Chair:	Asst. Prof. Roderick L. Catriz, DEE
Members:	Engr. Marife R. Santiago, BIOMECH Dr. Jose D. de Ramos, BIOMECH Engr. Ronnie C. Valencia, BIOMECH Engr. Marck Ferdie V. Eusebio, BIOMECH

TECHNICAL PAPER PRESENTATION COMMITTEE:

Chair:	Dr. Kevin F. Yaptenco, AFBED-IABE
Co-chair:	Dr. Jey-R S. Ventura, DES
Members:	Asst. Prof. Adrian A. Borja, AMPED-IABE Asst. Prof. Keynty Boy V. Magtoto, ABSEED-IABE Asst. Prof. Mary Louise P. Pascual, AFBED-IABE Dr. Rubenito M. Lampayan, LWRED-IABE Dr. Rex B. Demafelis, DChE Dr. Ramon Christian P. Eusebio, DChE Dr. Ma. Bernadeth B. Lim, DCE Asst. Prof. Emel Ken D. Benito, DCE Asst. Prof. John Paolo A. Ramoso, DEE Asst. Prof. Kim Jay R. Rosano, DEE Dr. Diana Marie R. De Silva, DIE Asst. Prof. Maria Liezel P. Caroche, DIE Asst. Prof. Claire L. Garing, DES Dr. Ralph Kristoffer B. Gallegos, DME Engr. Frederic James V. Espiritu, DME Dr. Ronel S. Pangan, BIOMECH Dr. Maria Victoria L. Larona, BIOMECH Dr. Jose D. de Ramos, BIOMECH

Dr. Arthur L. Fajardo, AMTEC
Engr. Romulo E. Eusebio, AMTEC
Engr. Fatima Joy J. Raytana, AMTEC

AWARDS COMMITTEE:

Chair: Dr. Josefa Angelie D. Revilla, DIE

Co-Chair: Dr. Ma Bernadeth B. Lim, DCE

Members: Dr. Roger A. Luyun, Jr.
Asst. Prof. Stephanie Caridad DR. Landicho

FINANCE COMMITTEE:

Chair: Dr. Arthur L. Fajardo, AMTEC

Co-Chair: Asst. Prof. Mary Louise P. Pascual, AFBED-IABE

Members: Engr. Frederic James V. Espiritu, DME
Engr. Fatima Joy J. Raytana, BIOMECH
Ms. Marivic L. Mendoza, DO

TECHNICAL AND LOGISTICS COMMITTEE:

Chair: Dr. Ronel S. Pangan, BIOMECH

Co-chair: Asst. Prof. John Paolo A. Ramoso, DEE

Members: Engr. Marife R. Santiago, BIOMECH
Dr. Jose D. deRamos, BIOMECH
Engr. Ronnie C. Valencia, BIOMECH
Engr. Marck Ferdie V. Eusebio, BIOMECH

SOCIAL MEDIA ENGAGEMENT COMMITTEE

Chair: Dr. Diana Marie R. De Silva, DIE

Co-chair: Asst. Prof. Kim Jay R. Rosano, DEE

Members: Ms. Mary Jane F. Gallardo, DO
Asst. Prof. Adrian A. Borja, AMPED-IABE
Asst. Prof. Emel Ken D. Benito, DCE
Asst. Prof. Maria Liezel P. Caroche, DIE
Asst. Prof. Claire L. Garing, DES
Asst. Prof. Allen Lemuel G. Lemence, DIE

DOCUMENTATION COMMITTEE

Chair:	Dr. Monet Concepcion M. Detras, DChE
Co-Chair:	Asst. Prof. Christian C. Vaso, DES
Members:	Asst. Prof. Rina A. Bawar, AFBED-IABE Dr. Jewel A. Capunitan, DChE Dr. Rowena B. Carpio, DChE Asst. Prof. Al Kaxier G. Ancheta, DES Asst. Prof. Jimyl A. Cruz, DES Engr. Ruen Ray R. Sazon, DChE Asst. Mart Merwin C. Magboo, DChE Ms. Mary Jane F. Gallardo, DO

ACADEMIC PUBLICATIONS COMMITTEE:

Chair:	Dr. Maria Victoria L. Larona, BIOMECH
Co-Chair:	Dr. Joan Cecilia C. Casila, LWRED-IABE
Member:	Dr. Ramon Christian P. Eusebio, DChE